CASSIOPE
FAI Characterization Report

Document No: ePOP – 4771

Revision A – June 2008

Prepared by:

Leroy Cogger	*Date*

Prepared by:

Andrew Howarth	*Date*

Concurred by:

Greg Enno	*Date*

Approved by

Andrew Yau	*Date*

Table of Contents

A. Introduction

The purpose of this report is to assemble in one place the results of the tests and analyses that have been undertaken to facilitate the scientific utilization of the Fast Auroral Imager (FAI). Most of the material included in this report is based on measurements that have been made since the completion of the instrument assembly by Routes AstroEngineering (Ottawa) in June 2006. The flight model (FM) was tested at the Facility for Optical Calibration at Low Light Level, University of New Hampshire for the periods August 1 to October, 2006 and December 17, 2006 to January 17, 2007. Prior to that, functional tests were conducted at Routes AstroEngineering for the months of June and July, 2006, and from December 8 to December 16, 2006. Between late January 2007 and delivery to Bristol Aerospace Limited the instrument was located at the University of Calgary. Various tests and modifications have been implemented at all three locations.

The facility at the University of New Hampshire (UNH) was utilized to obtain an absolute calibration of FAI and to measure a variety of optical characteristics. The key component is a calibrated integrating sphere developed by SphereOptics to provide a uniform light source with a diameter of 20 cm. It is situated on an optical table in a dark, clean room ideal for the calibration of space instruments. Other useful devices include a collimator that was built to support the FAI testing, and a rotation table. A photo of part of the facility is shown below. The test procedures were designed at the University of Calgary and carried out by UNH personnel under the supervision of Dr. Marc Lessard.

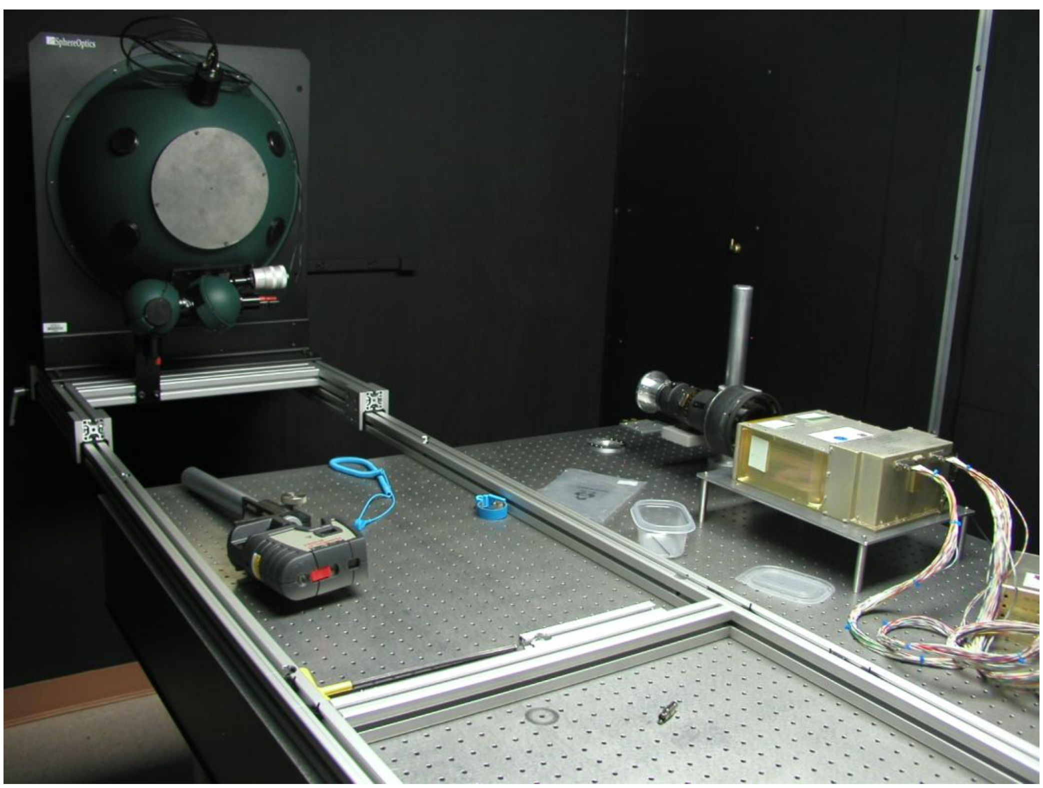

Analysis results from the various tests are included in this report only if the tests were definitive or if they are useful for comparison purposes. The Appendices contain background and technical information that is included here mostly to preserve it in one document. This report does not provide a description of the instrument, the flight software, or the analysis software because its sole purpose is to serve as a characterization document. Characterization is essential preparation for the operation of an instrument, the data processing, and the scientific analysis. What follows is an overview of the numerous topics that comprise the characteristics of the Fast Auroral Imager. The imager consists of two cameras: the SI camera is sensitive to the near infrared region (NIR) from 650 to 1000 nm, and the SV camera is designed to image the OI 630 nm auroral emission.

B. Characterization overview

1. Image orientation and registration

a. Image registration on the CCD

As a useful reference, a sketch of the e2v 67 CCD is given below. The imaging area (top section) contains eight masked dark current rows at the very top and six masked dark current columns on each side. There are also six offset elements on each end of the horizontal transfer register that are read out with each row and appear like offset columns in the data. The central imaging area is 256 by 256 pixels. The position of Mode 4 (no binning) is illustrated. Mode 4 data frames are 256 rows by 280 columns. Each frame contains the 256 by 256 pixel image plus all the dark current and offset columns. This deliberate modification to the earlier size was implemented to better monitor the CCD during operations. The dark current columns will provide an additional indicator of the CCD temperature and mean dark current although caution will need to be taken due to the possibility of charge leakage from the image area into the adjacent masked dark columns. There is also known to be small gradients in the offset across the CCD, and the best way to deal with these gradients is through the measurement of the offset on both sides of the CCD.

In Mode 3 (2 by 2 binning) the image size is 128 by 128 pixels with 3 dark columns and 3 offset columns on either side, making the total size 140 columns by 128 rows. In mode 2 (4 by 4 binning) the image size is 64 by 64 pixels with 1 dark column, 1 offset column and one mixed dark/offset column on either side, making the total size 70 columns by 64 rows.

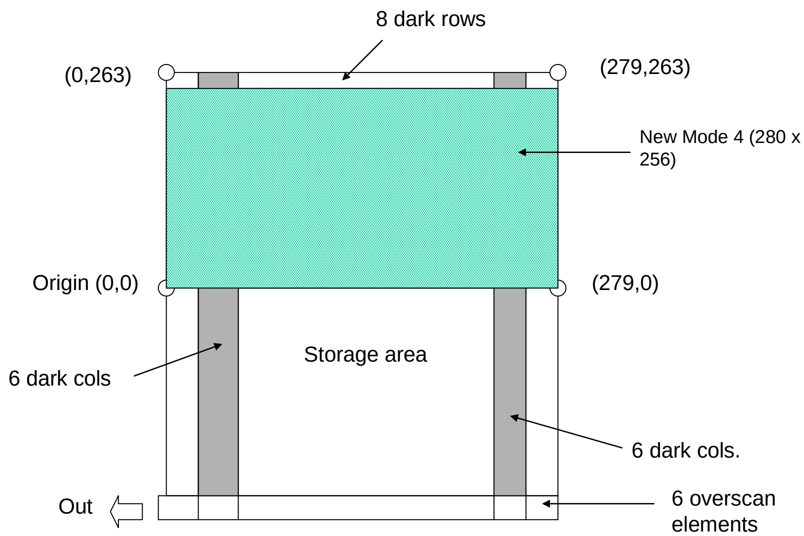

Mode 4 after Nov/06: 280 cols, 256 rows

b. Electronic signal offset

The 6 over-scan elements on each side of the horizontal transport register of the CCD do not accumulate dark current but are read out to provide the magnitude of the electronic offset of the preamplifier. The purpose of this offset is to ensure that the signal level remains positive. For these cameras the level is about 4400 data numbers (DN) from a range of 2^{16}, but was found to vary from image to image by small but significant amounts that needed to be taken into account. It was noted that the offset could vary with the Mode as well as the signal level in the imaging area. After considerable effort to fix this unexpected problem by software and hardware adjustments, it was decided to change the image format to ensure that the over-scan elements would be read with each image. The flight instrument has a total of 12 columns of data that can be used to determine the electronic offset.

c. Camera field of view in relation to the CCD

The location of the field of view (FOV) of each camera on its CCD was determined by using the integrating sphere to fill the FOV with light. The images below were taken on January 10, 2007 for SI and January 12, 2007 for SV. The size of the FOV was found from the best circle fit to the image, and the centre of the circle gave the location of the optical axis of the system. The resulting parameters are given in the following table.

Camera	FOV radius in pixels	Centre CCD column	Centre CCD row
SI	128	142	126
SV	128	140	128

It is obvious that there is some light scattering as well as some distortion of the light pattern on the CCD that increases the uncertainty in the measurement. The numbers in the table should be considered accurate with an uncertainty of +/- 2 pixels (52 microns).
The halo effect is more pronounced for the SV camera. For the SI camera, the width of the halo varies between 5 and 10 pixels and the width of the SV halo varies between 11 and 16 pixels. A likely cause of this effect is a slight mismatch between the size of the input end of the optical fibre taper and the size of the FOV on the taper.

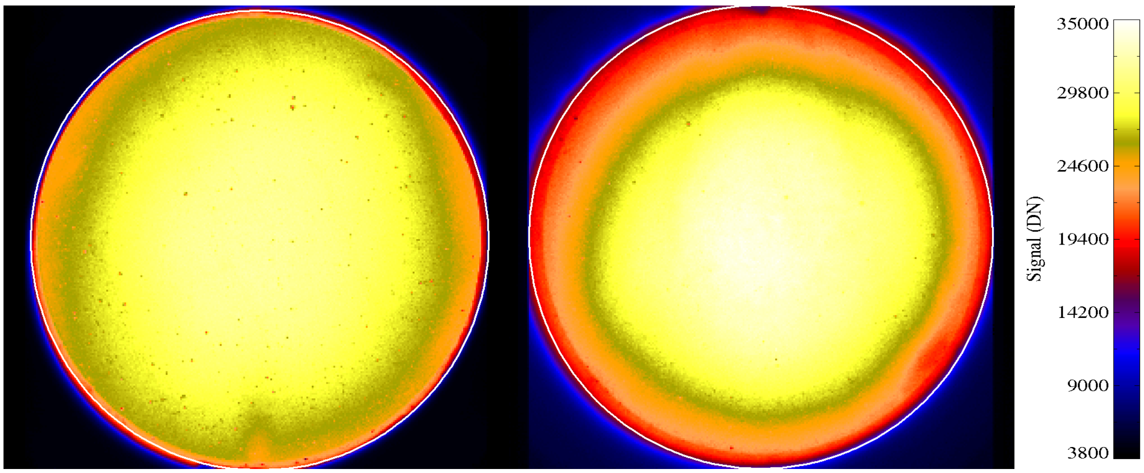

SI Camera SV Camera

d. Co-alignment of the cameras

Co-alignment and registration of the 2 cameras with respect to each other is also important, but could not be determined in the laboratory. Mechanical alignment was addressed by Routes in the design of the instrument. The table below gives the expected alignment numbers presented by Routes at the Critical Design Review. Complete measurements will be carried out during the commissioning phase by observing the same star field with both cameras. In addition to the relationship of the images in the two cameras, the direction of the optical axes with respect to the spacecraft coordinates will be refined.

Alignment at Routes

Alignment	Optical	Mechanical Mounting	Total (RMS)	Requirement
FAI-SI to FAI-SV	±0.23°	±0.09°	±0.26° (2.4 pixels)	5 pixels
FAI Camera to S/C	±0.23°	±0.05° ±0.11°	±0.24° ±0.25°	±0.5° in Y ±0.5° in Z

Measurements at Routes during mechanical assembly in June 2006 showed that the rotation of the CCD rows/columns with respect to the camera base is not more than 0.5 degrees. The positioning difference was measured to be less than 5 pixels in both rows and columns.

e. Orientation of displayed CCD images

For operations in space it is necessary to know the relationship between the image displayed on a monitor and the world external to the camera. This was done by imaging the letter L as shown in the photograph below and then re-orienting it in the IDL display software to appear right side up on the monitor. The process involves both an inversion and a rotation. The physical CCD columns become rows on the monitor, and this will be the default mode for science analysis. However, when it is necessary to refer to the CCD itself, a flag is set to display the CCD columns vertically on the monitor as shown in the CCD sketch above.

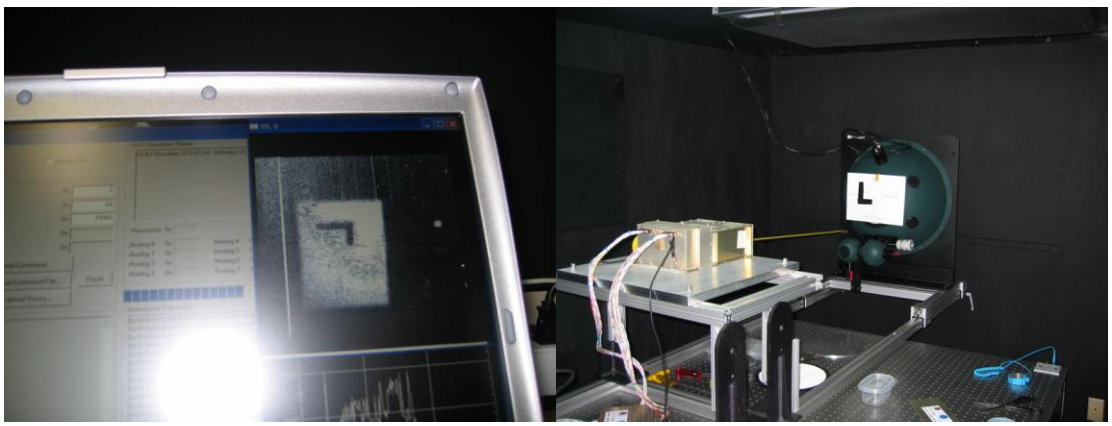

2. Absolute calibration of the FAI instrument

Due to necessary post-assembly changes to the flight model (FM) electronics, it was also necessary to repeat the measurements of the calibrated integrating sphere that were carried out in September 2006 at UNH. The report on the new measurements follows.

Measurements of the integrating sphere at UNH on January 10 and 12, 2007 form the basis for the FAI calibration. Images of the sphere were acquired for intensities that covered the range from weak to near saturation of the 16-bit analog-to-digital converter (ADC). Three images were recorded at each radiance setting. All images were corrected for electronic offset and dark current using the average of three dark current images taken before the series of measurements. The stability of these 'dark current plus offset' measurements was confirmed by repeating the dark current measurements after the series with the sphere. The CCD temperature was kept constant at 4.7 degrees C.

The plot below is for the SI camera. Average data numbers (DN/pixel) from the central 20 by 20 pixel area accumulated in an exposure time of 0.1 s are plotted against the radiance of the integrating sphere in units of nW/cm^2-sr. The radiance is the integrated spectral radiance between 650 nm and 1000 nm. A linear fit to the data is shown.

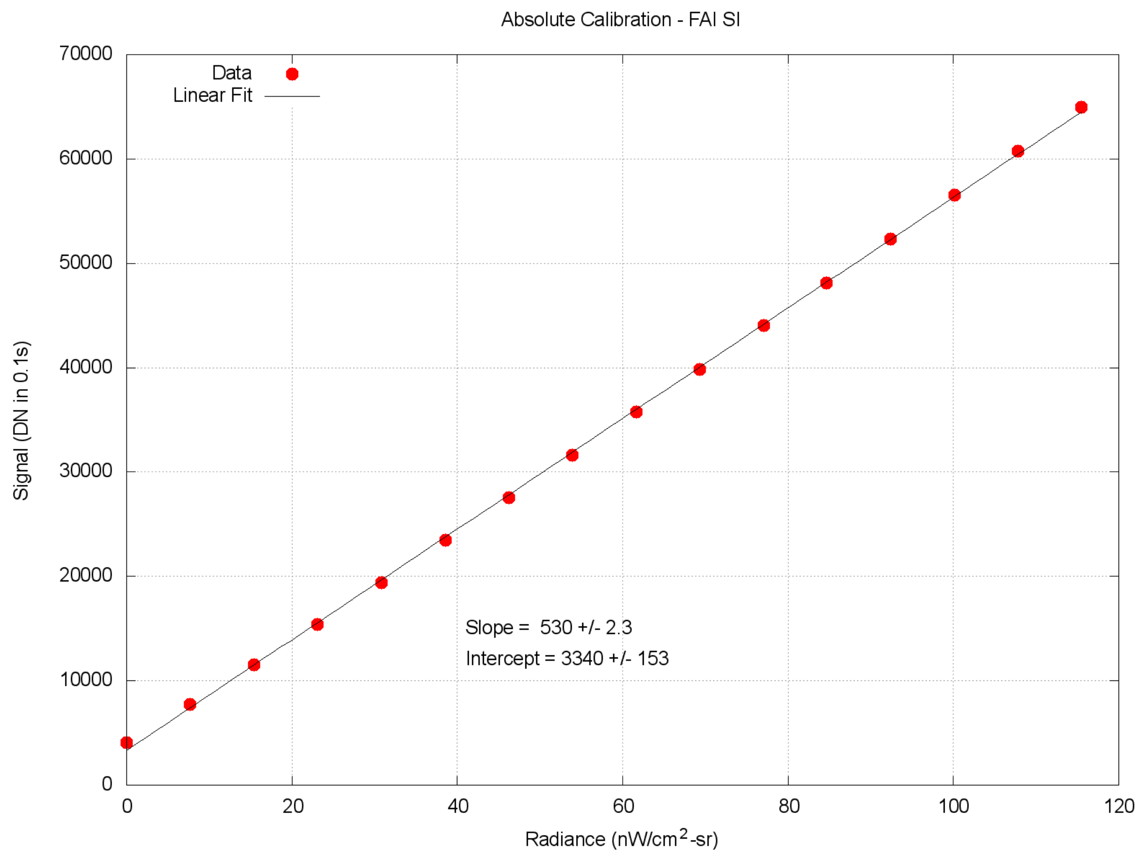

The next plot is for the SV camera. Average data numbers (DN/pixel) from the central 20 by 20 pixel area accumulated in an exposure time of 0.5 s are plotted against the spectral radiance of the integrating sphere in units of nW/cm^2-sr-nm. A linear fit to the data is shown in the figure.

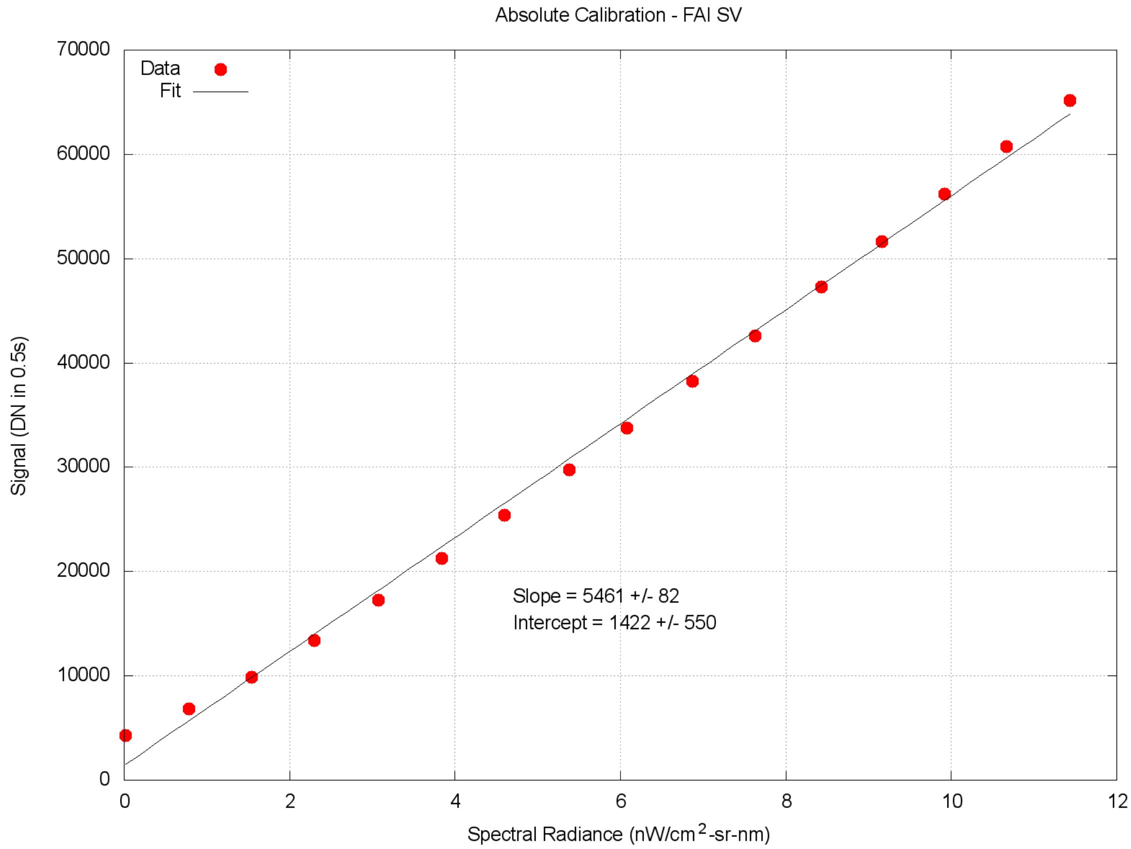

a. Calibration of SI

From the plot of the measurements, the slope of the linear fit to the data points is k = 5300 DN/s per nW/cm^2-sr. Because the rayleigh is the standard unit for aurora and airglow, we must convert the radiance in nW/cm^2-sr to rayleigh units, as follows.

First, multiply the radiance by 4π to convert to omnidirectional radiance.

Second, convert from watts to photons/s, by dividing the number of watts by the energy of a single photon. In this case, an effective or average photon energy can be used. This was found by dividing the sum of the products of spectral radiance and wavelength over the range 650 to 1000 nm by the sum of the spectral radiances in the table provided by SphereOptics. The result is an effective wavelength of 868 nm with a corresponding photon energy of 1.43 eV. This energy in joules is 1.43 eV times 1.6 x 10^{-19} J/eV = 2.29 x 10^{-19} J.

1 nW/cm^2-sr = 10^{-9} x 4π /2.29 x 10^{-19} = 5.49 x 10^{10} photons/cm^2-s

Third, by definition, 1 rayleigh = 10^6 photons/cm^2-s, and therefore

1 nW/cm^2-s = 5.49 x 10^{10} photons/cm^2-s = 5.49 x 10^4 R.

Returning to the slope, k = 5300/5.49 x 10^4 = 0.0965 DN/s per rayleigh

This is the responsivity of the camera in units of DN/R·s. Here we call the calibration constant the reciprocal of the responsivity, i.e. 10.4 R/DN/s

b. Calibration of SV

The bandwidth of the 630 nm interference filter was measured by the manufacturer. Its half-width for a 14-degree cone (f/4) of incident light is 2.0 nm. The effective bandwidth is the width of the rectangle that has the same height as the peak transmission of the filter, and it has been calculated as 2.15 nm from the manufacturer's curve. One reason for caution is that the SV calibration plot shows a slight curvature whose origin is not understood. The approximation to a straight line will be used to demonstrate the procedure.

The process is the same as for the SI camera except that the spectral radiance is used.

The energy of a 630 nm photon is 1.97 eV = 3.15 x 10^{-19} J.

Here 1 nW/cm^2-sr-nm = 10^{-9} x 4π x 2.15 /3.15 x 10^{-19} photons/cm^2-s
= 8.59 x 10^{10} photons/cm^2-s

Since 1 R = 10^6 photons/cm^2-s, 1 nW/cm^2-sr-nm at 630 nm with a 2.15 nm bandpass is 8.59 x 10^4 R. This is the required conversion to rayleigh units.

A linear fit to the measurement data gives a slope of 1.09 x 10^4 DN/s per nW/cm^2-sr-nm

= 1.09 x 10^4/8.59 x 10^4 DN/s/R
= 0.127 DN/s/R. This is the responsivity given in units DN/R·s.

Here we define the calibration constant as the reciprocal of the responsivity:

Calibration constant for FAI SI = 10.4R/DN/s +/-uncertainty
Calibration constant for FAI SV = 7.88 R/DN/s +/-uncertainty

The uncertainties in the calibration constants are discussed below.

A comparison of the two sets of measurements (September 2006 and January 2007) shows that the absolute calibration has not changed significantly due to the electronic modifications. **The values in the following table are based on a linear fit to the data although it is clear that the best fit, especially for the SV camera, is achieved with a quadratic function; i.e. the calibration factor is a function of the input signal.**

Date	SI (R/DN/s)	SV (R/DN/s)
September 2006	10.8	8.1
January 2007	10.4	7.9

The next figure shows the SV calibration data fitted by a quadratic equation:

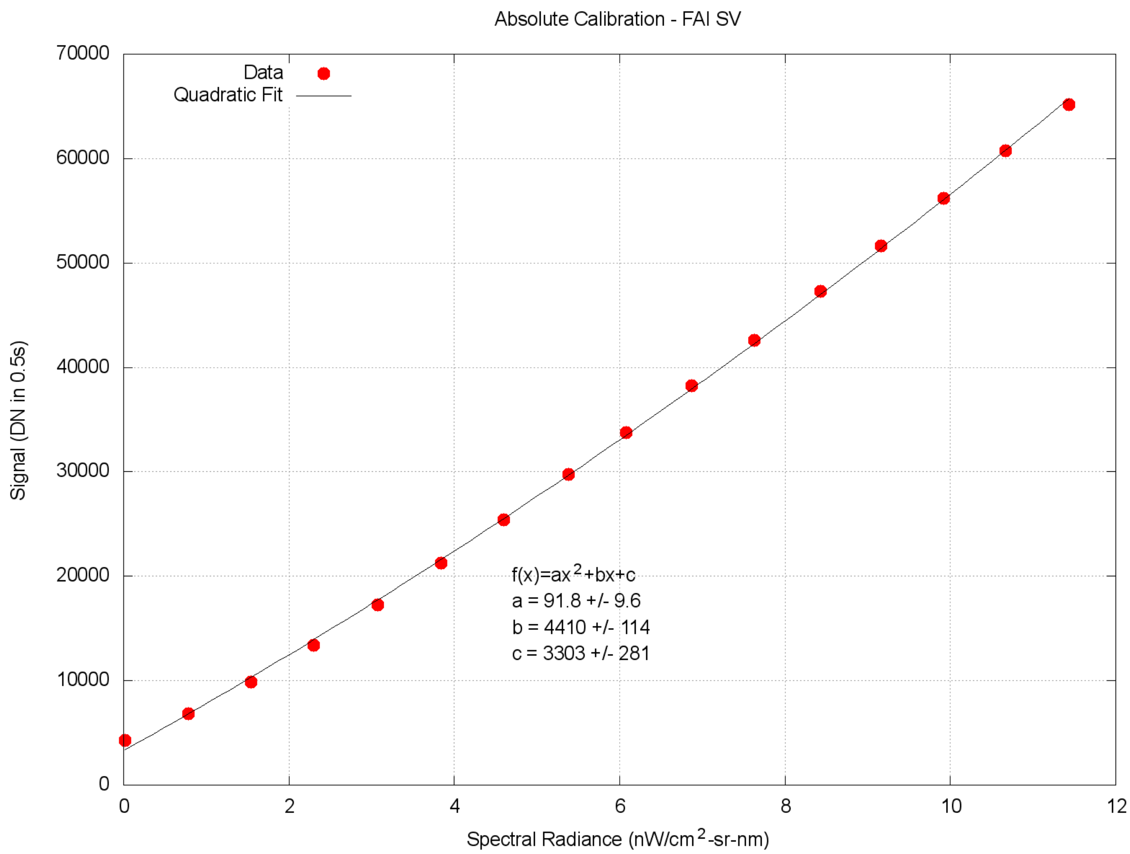

If the curve is correct, the responsivity increases with the spectral radiance in a linear fashion: i.e. the first derivative of the curve is a linear function. This implies that there is a signal-level dependent calibration factor that should be used rather than that derived from the linear fit to the data. The cause of the non-linearity has been discussed with technical personnel, and nobody has been able to provide an explanation. If the curvature were downward rather than upward, causes such as saturation effects could be invoked. The other possibility that is being pursued is that there is a non-linearity in the measurements of the lamp radiance within the integrating sphere instrument.

It is convenient to change the above plot to more useful units. The figure below shows the source brightness in kilorayleighs (kR) plotted against the net signal in DN/s. The quadratic function that fits the curve is $\mathbf{y=-10^{-8}x^2 + 0.0093x + 20.4}$.

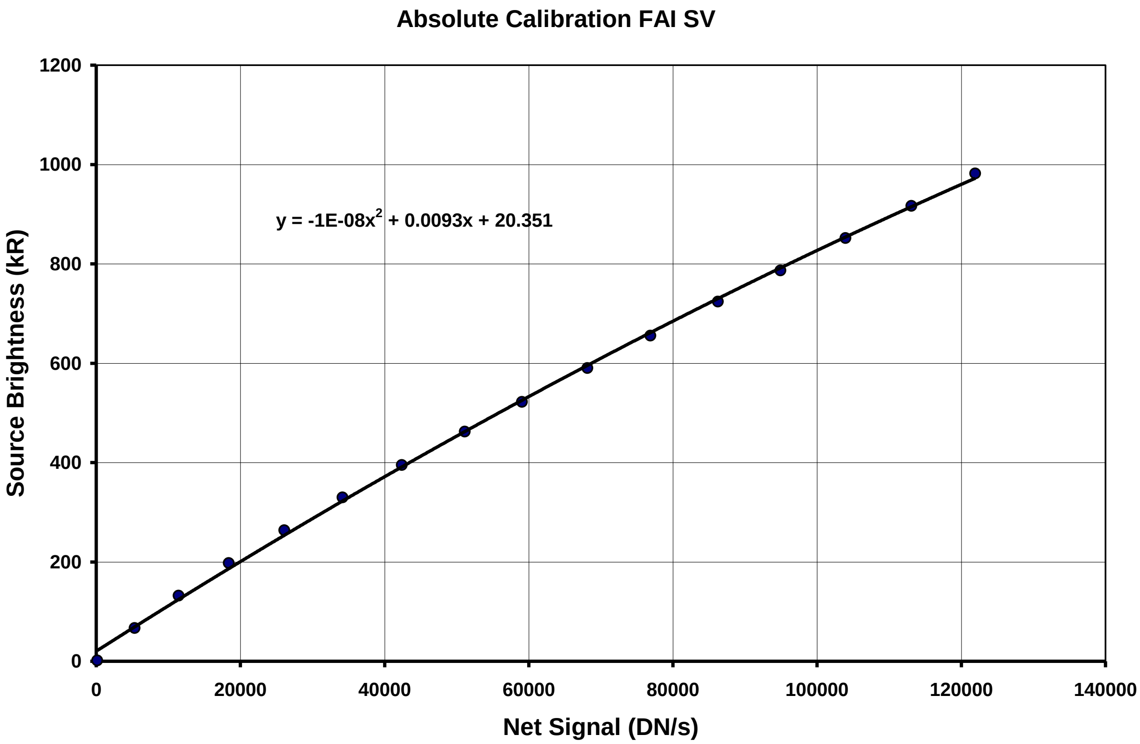

The first derivative gives the calibration factor in kR/DN/s as a function of the net signal in DN/s: Calibration factor = -2E-08x + 0.0093. If the brightness is given in rayleighs, then the calibration factor is -2E-05x + 9.3. The plot below shows the variation of calibration factor with the net signal. For airglow and typical aurora, it is expected that the brightness will be less than about 40 kR which means that the expected range in the calibration factor will be between about 8.5 and 9.3. For this range, the uncertainty should be under 5%. For weak aurora and airglow the value 9.3 is a good approximation.

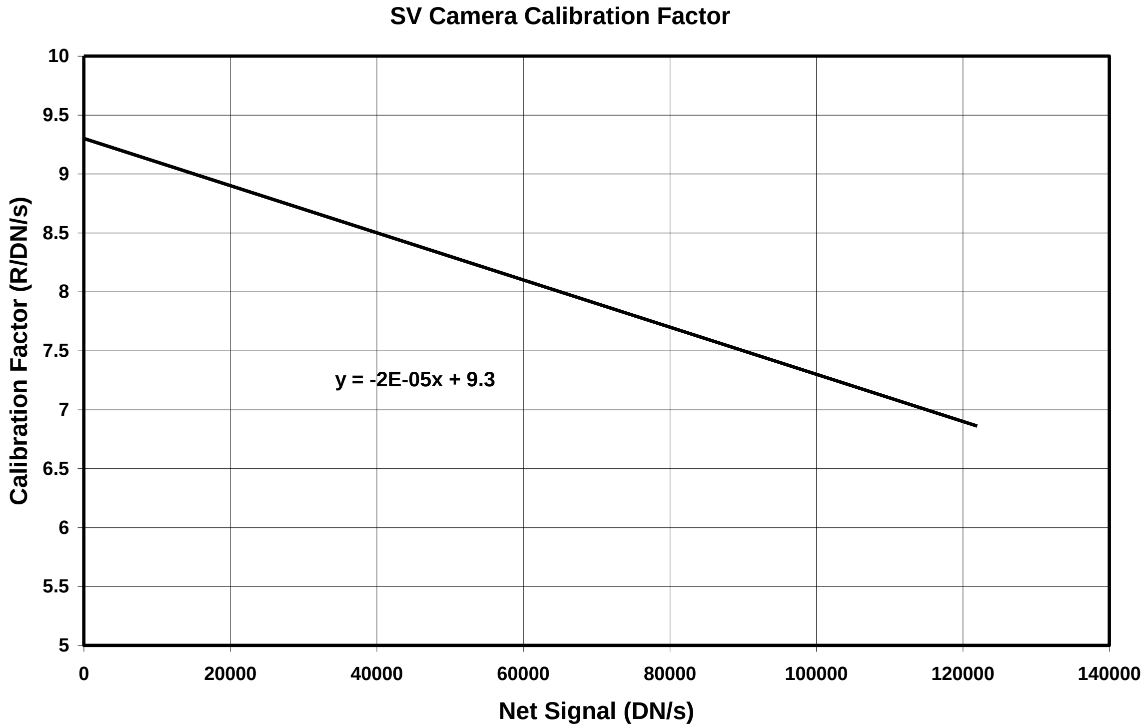

c. Estimated calibration uncertainty

The sources of calibration uncertainty are the measured fit to the graphs shown above, the optical passbands, and the output of the integrating sphere.

The estimation process is relatively straightforward for the SV camera. The optical passband is obtained from the measured interference filter curve that was provided by the manufacturer, Barr Associates. Their curve for a light cone of 7 degrees half angle (f/4 to match the camera optical module) is shown below along with a rectangle having the same area as the actual curve. It is the width of the rectangle that is used to provide the bandwidth in the calibration calculation.

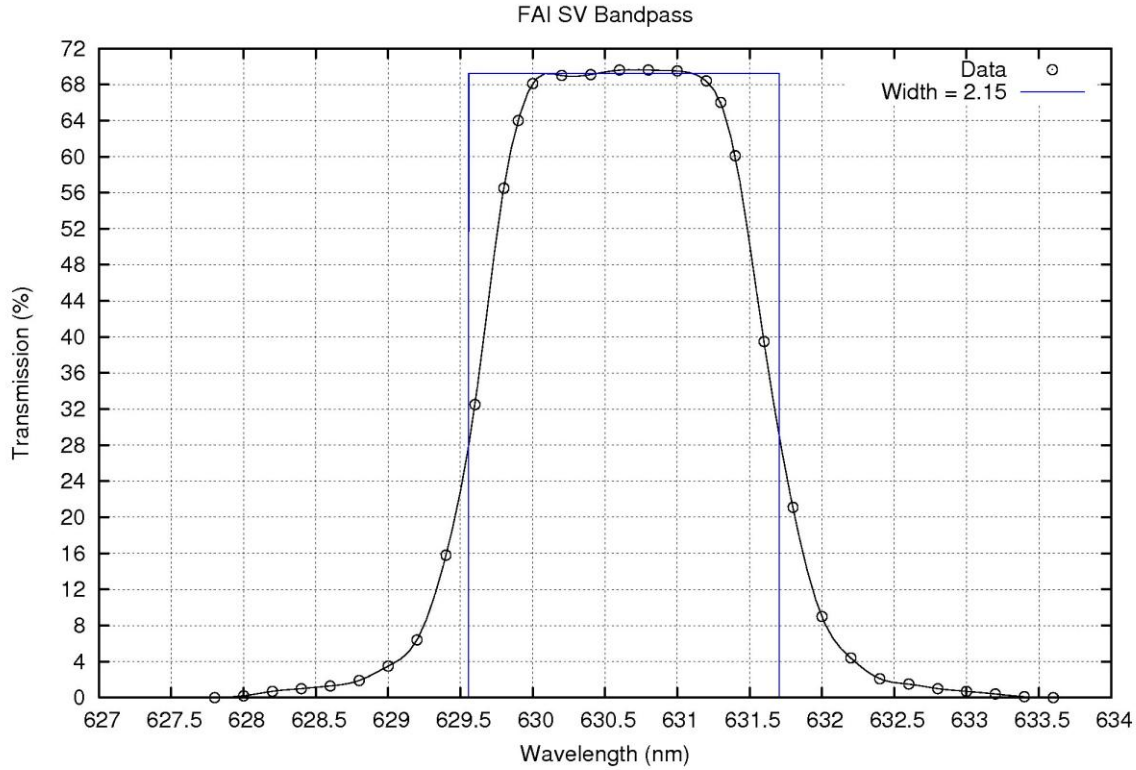

Without additional high-resolution measurements of the filter passband when it is in the instrument, a reasonable estimate for the bandwidth is 2.15 +/-0.1 nm. The estimated overall uncertainty is given in the table below.

Calibration factor	Source	Bandwidth	Total (RMS)
5%	4%	5%	8%

For the SI camera there is another factor that needs to be addressed: the spectral distribution of light from aurora and the integrating sphere are different, so a correction may be necessary. Progress has been made based on auroral band intensities given in the literature, but better data are desirable. For a description of the analysis done so far, see Appendix 1: Predicted SI Response to Airglow and Aurora. It is important to be aware that the calibration factor depends to some degree on the atmospheric composition and the energy distribution of the precipitating electrons. This is because the emission bands from different molecules are differently distributed across the SI passband. The approach used in Appendix 1 is to relate the total number of rayleighs from the SI passband to the equivalent intensity of the OI 557 nm emission. For the auroral tables used, the factor is about 23: i.e. the equivalent OI 557 nm emission rate equals the emission rate measured within the SI passband divided by 23.

3. Correction for non-uniform response

Optical systems normally have their highest responsivity near the optical axis with a fall-off towards the edges of the field of view. This variation can be corrected by measuring the response to a uniform light source that fills the field of view. For FAI, this correction takes the form of an array of normalization factors that is multiplied by the image. A normalization array was obtained for each camera in September 2006. It was subsequently determined that the active area of the CCD was misaligned with the optical field of view for the operational camera modes, and it was therefore necessary to repeat the non-uniformity response test in January 2007 using the correct area of the CCD. The analysis was carried out using the same integrating sphere images that provided the absolute calibration data presented above. The signal level was much higher than the magnitude of the drops in DN value that were still present at that time. The report on the non-uniformity analysis follows.

a. January 10 Integrating Sphere Measurements – FAI SI

A total of 45 images of a variable intensity integrating sphere were taken at UNH on January 10, 2007 using the SI camera. The uniformity array was found by removing the offset and dark current, then linearly fitting β values for a given location on the CCD (e.g. pixel location [23,138]) with DN over all the images, where β for any given pixel in an image is

$$\beta = \text{avg(center 36 pixels)/(pixel DN value)}.$$

The reason for the linear fit of β to all the 45 values for a single pixel is that there is a small linear variation of β with signal level. The uniformity correction is applied to each pixel of an image array by first removing the electronic offset and the dark current contributions and then multiplying the net signal by the normalization factor, β, for that pixel.

The non-uniformity is obvious in the raw image shown below. The negative DN values result from subtracting the offset and dark current, which is done by removing an average of three 0.1s images.

FAI SI Image (FAI_070110_121200.SDF)

Date (yyyymmdd) = 20070110
CCD Temperature = 4.672 C
Set CCD Temperature = 4.672 C
Exposure = 0.100 s

Time (UT) = 12:12:00.000
NCOLS = 280
NROWS = 256
Mode = 4

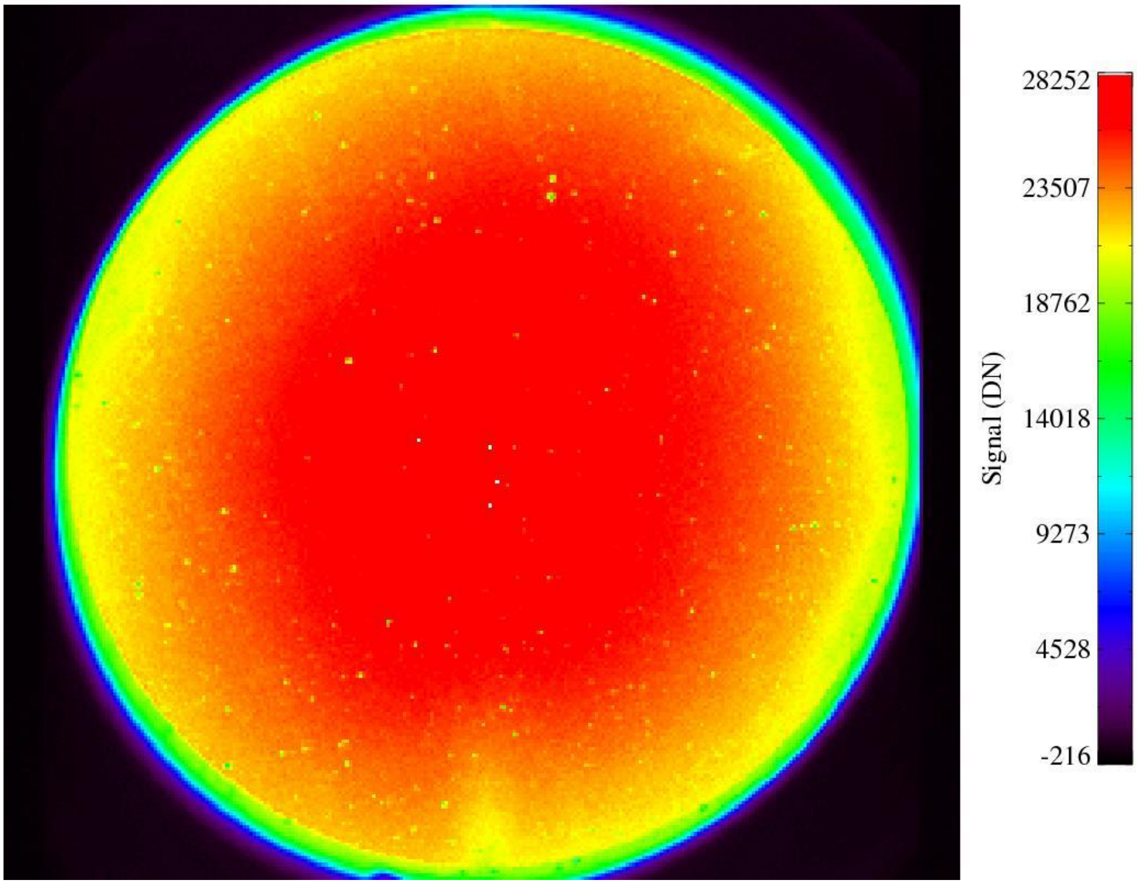

The non-uniformity effect is demonstrated more clearly in the following figure that shows the data plotted for 3 selected rows of the same image.

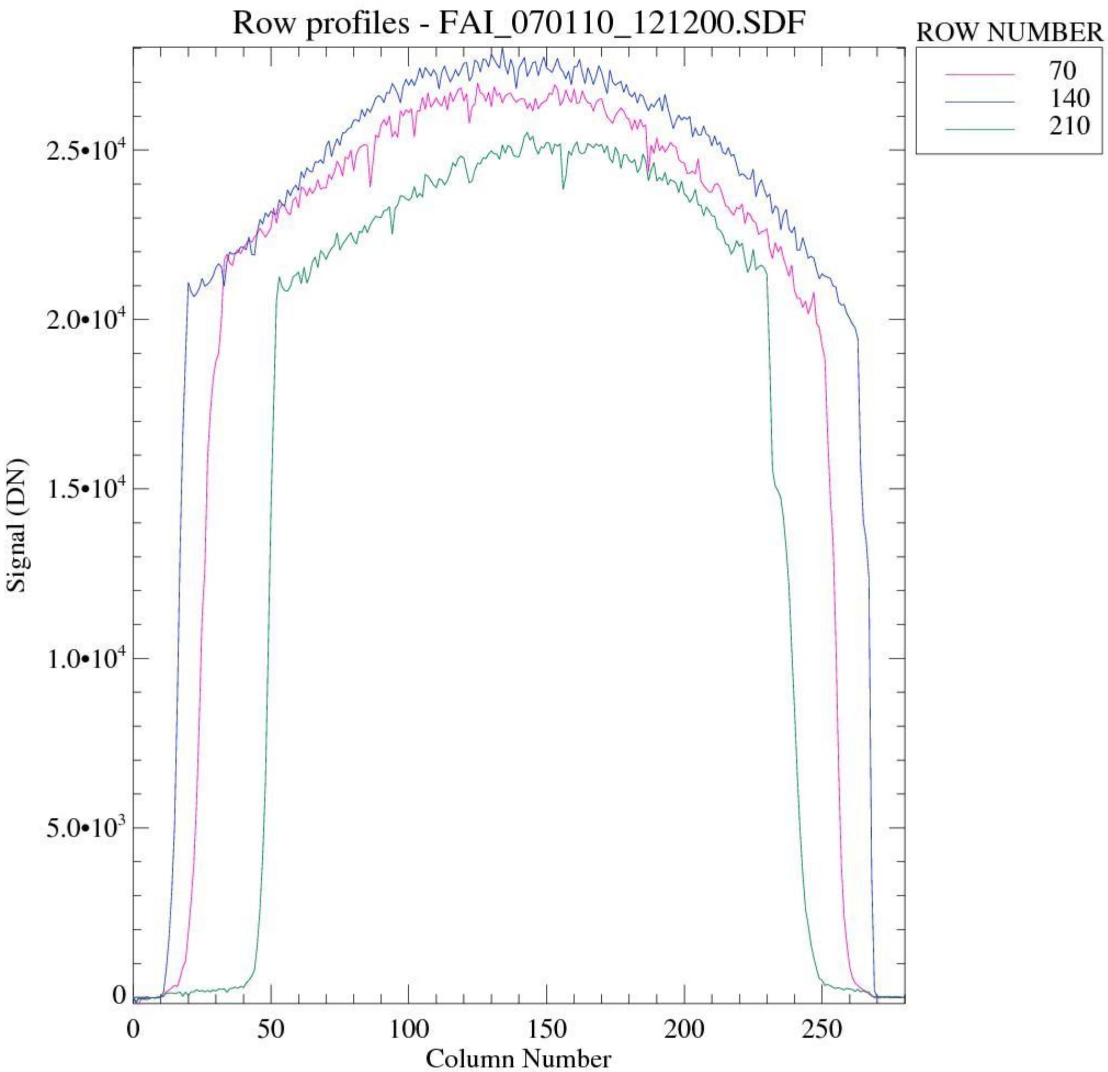
Row profiles - FAI_070110_121200.SDF
ROW NUMBER
70
140
210
Signal (DN)
2.5•10^4
2.0•10^4
1.5•10^4
1.0•10^4
5.0•10^3
0
0
50
100
150
200
250
Column Number

The corrected image and the resulting row profiles are shown below. It is clear that the non-uniformity of the camera response can be accounted for in the routine data analysis.

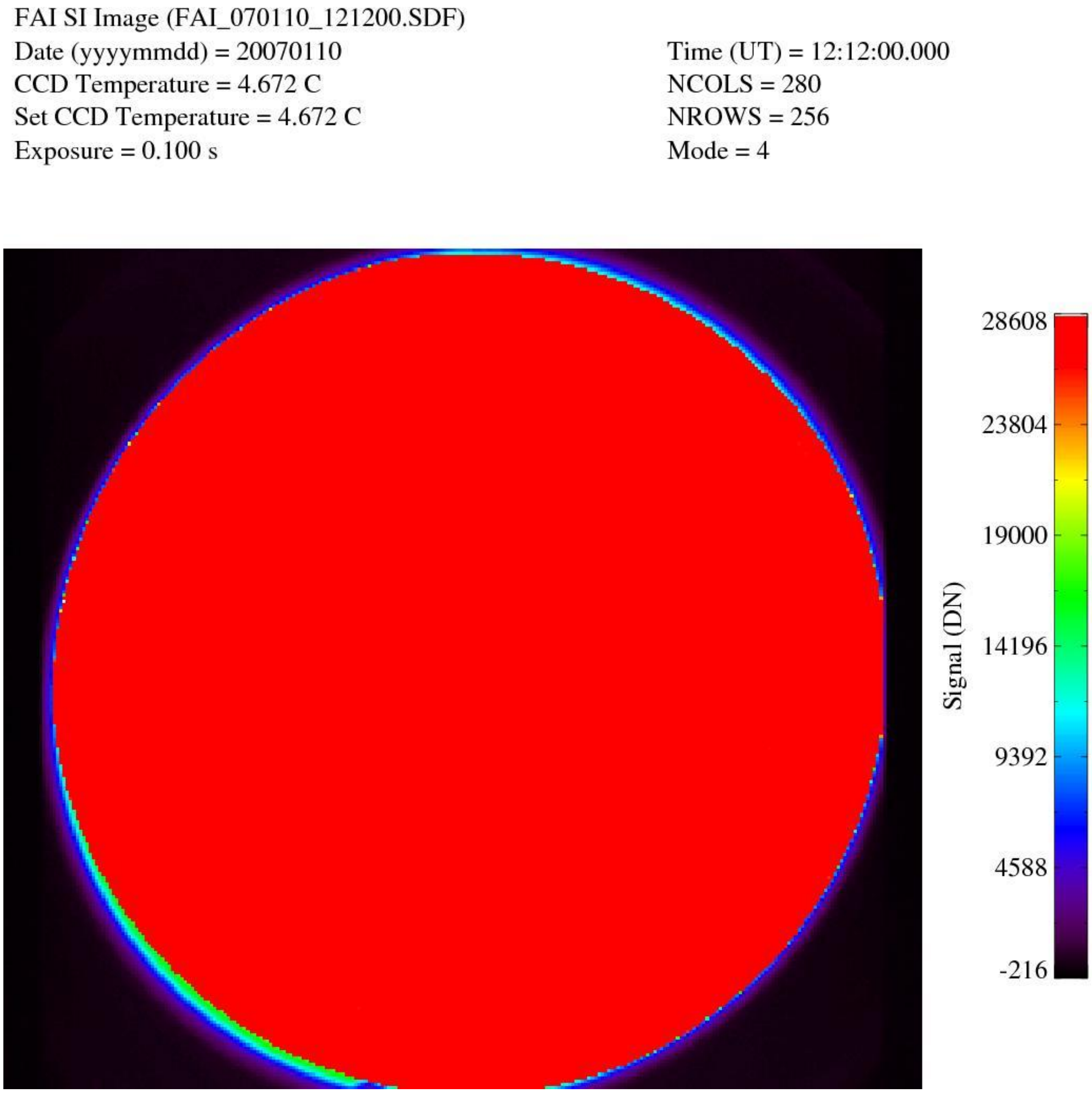

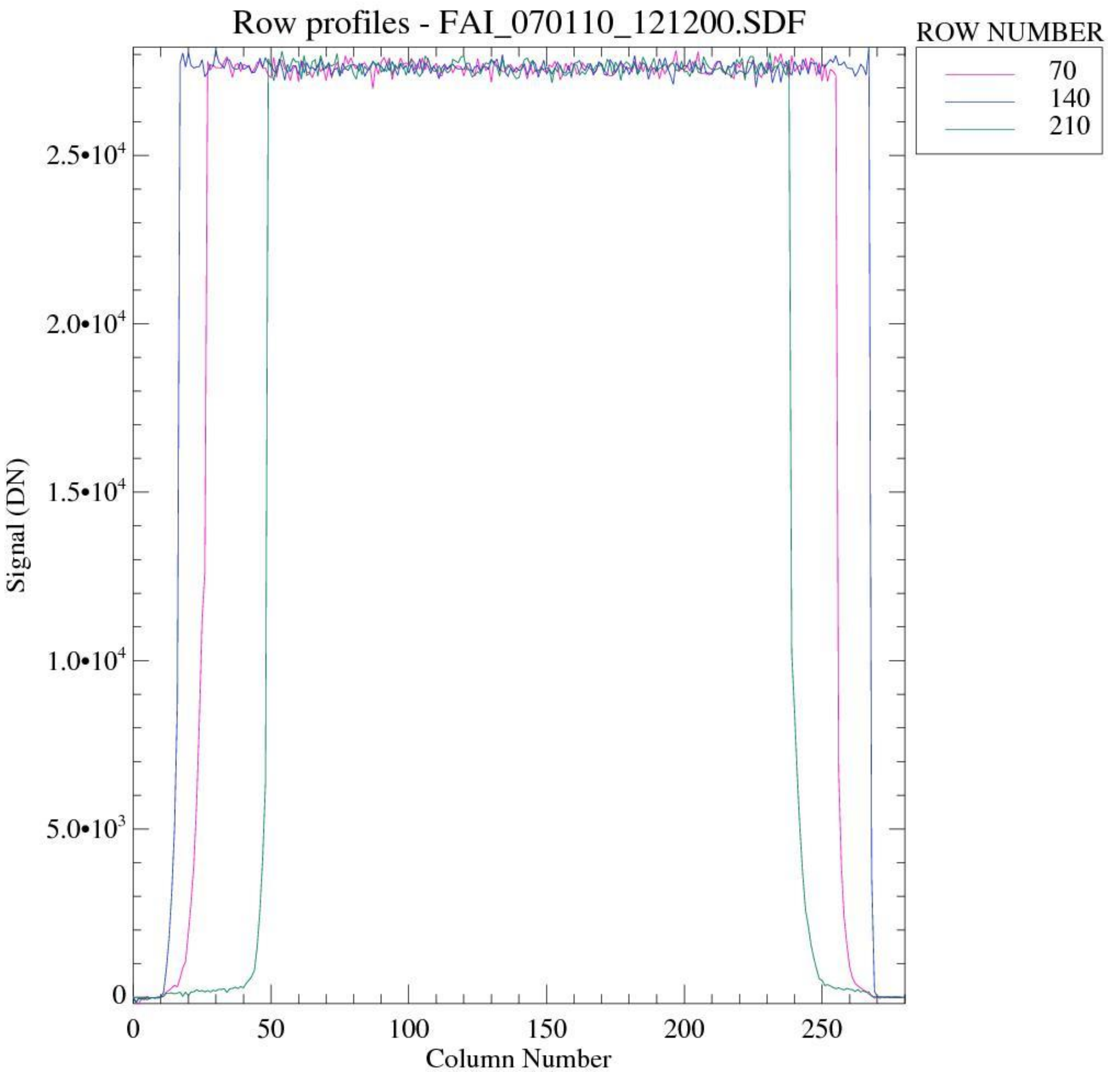
Row profiles - FAI_070110_121200.SDF
ROW NUMBER
70
140
210
2.5•10^4
2.0•10^4
1.5•10^4
1.0•10^4
5.0•10^3
0
Signal (DN)
0
50
100
150
200
250
Column Number

b. January 12 Integrating Sphere Measurements – FAI SV

A total of 42 images of a variable intensity integrating sphere were taken at UNH on January 12, 2007 using the SV camera. The procedure to find the array of normalization factors was identical to that for the SI camera.

The non-uniformity is obvious in the raw image shown below. The negative DN values result from subtracting the offset and dark current, which is done by removing an average of three 0.1s images.

FAI SV Image (FAI_070112_124637.SDF)
Date (yyyymmdd) = 20070112
CCD Temperature = 4.672C
Set CCD Temperature = 4.672C
Exposure = 0.500 s

Time (UT) = 12:46:37.000
NCOLS = 280
NROWS = 256
Mode = 4

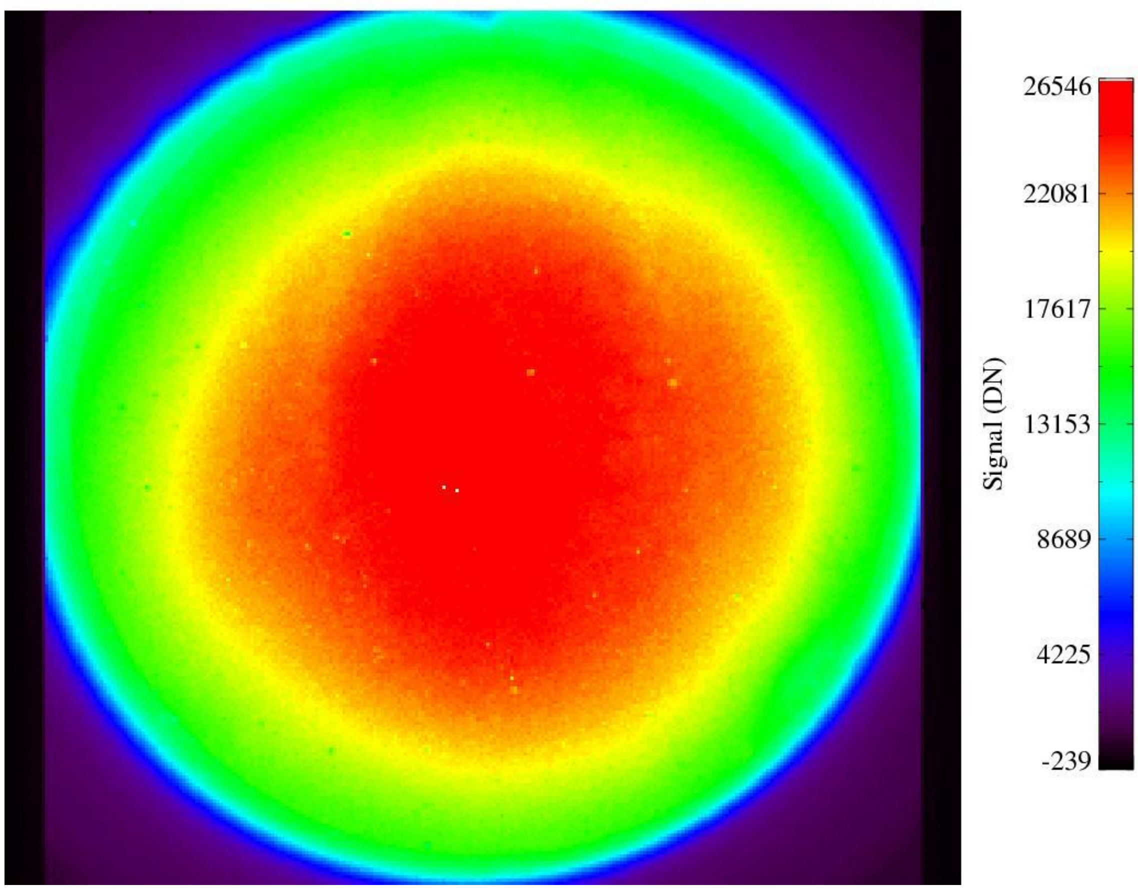

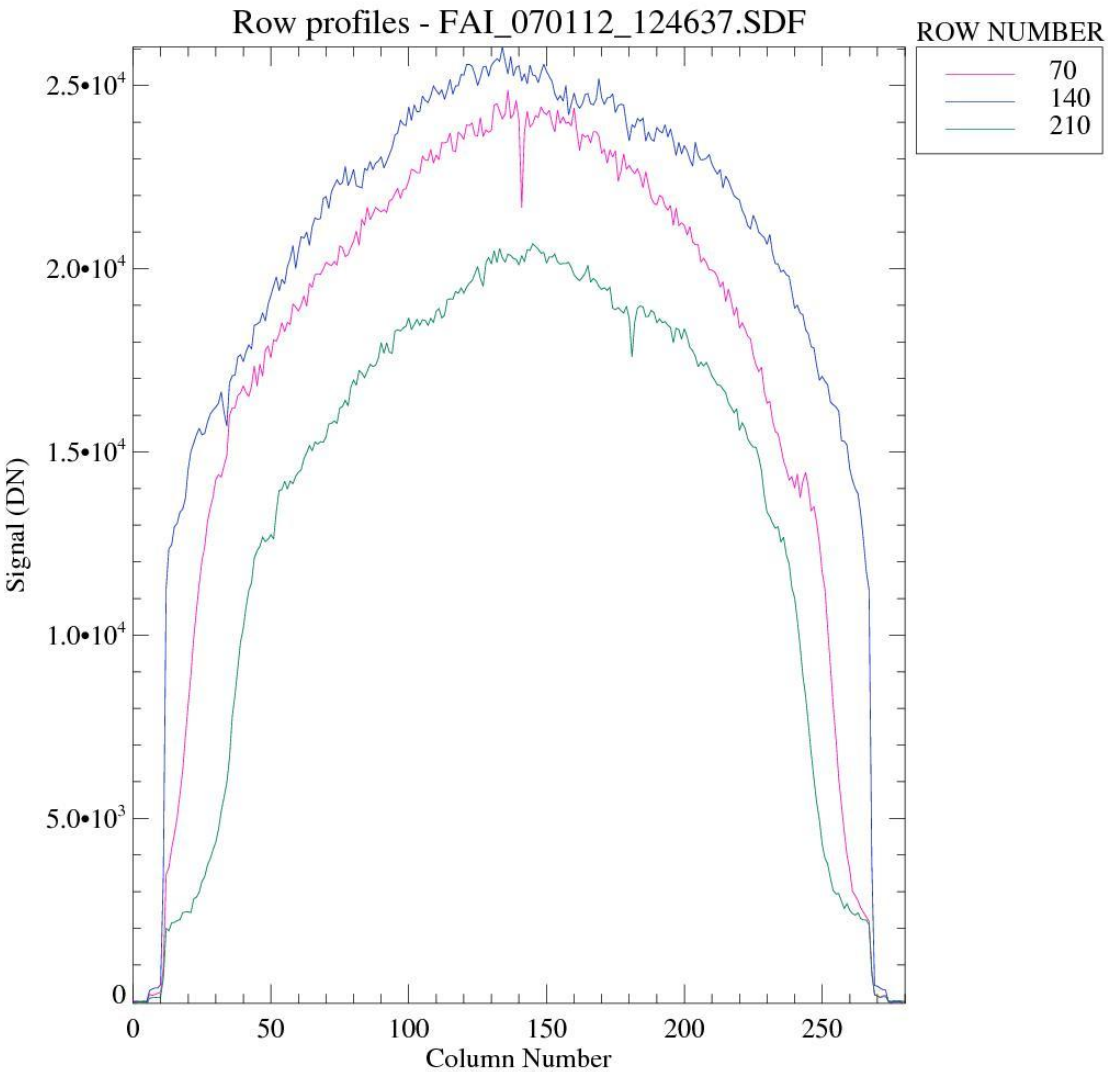
Row profiles - FAI_070112_124637.SDF
ROW NUMBER
70
140
210
Signal (DN)
Column Number
2.5•10⁴
2.0•10⁴
1.5•10⁴
1.0•10⁴
5.0•10³
0
0
50
100
150
200
250

The corrected image and the resulting row profiles are shown below. It is clear that the non-uniformity of the SV camera response can be accounted for in the routine data analysis.

FAI SV Image (FAI_070112_124637.SDF)
Date (yyyymmdd) = 20070112 Time (UT) = 12:46:37.000
CCD Temperature = 4.672C NCOLS = 280
Set CCD Temperature = 4.672C NROWS = 256
Exposure = 0.500 s Mode = 4

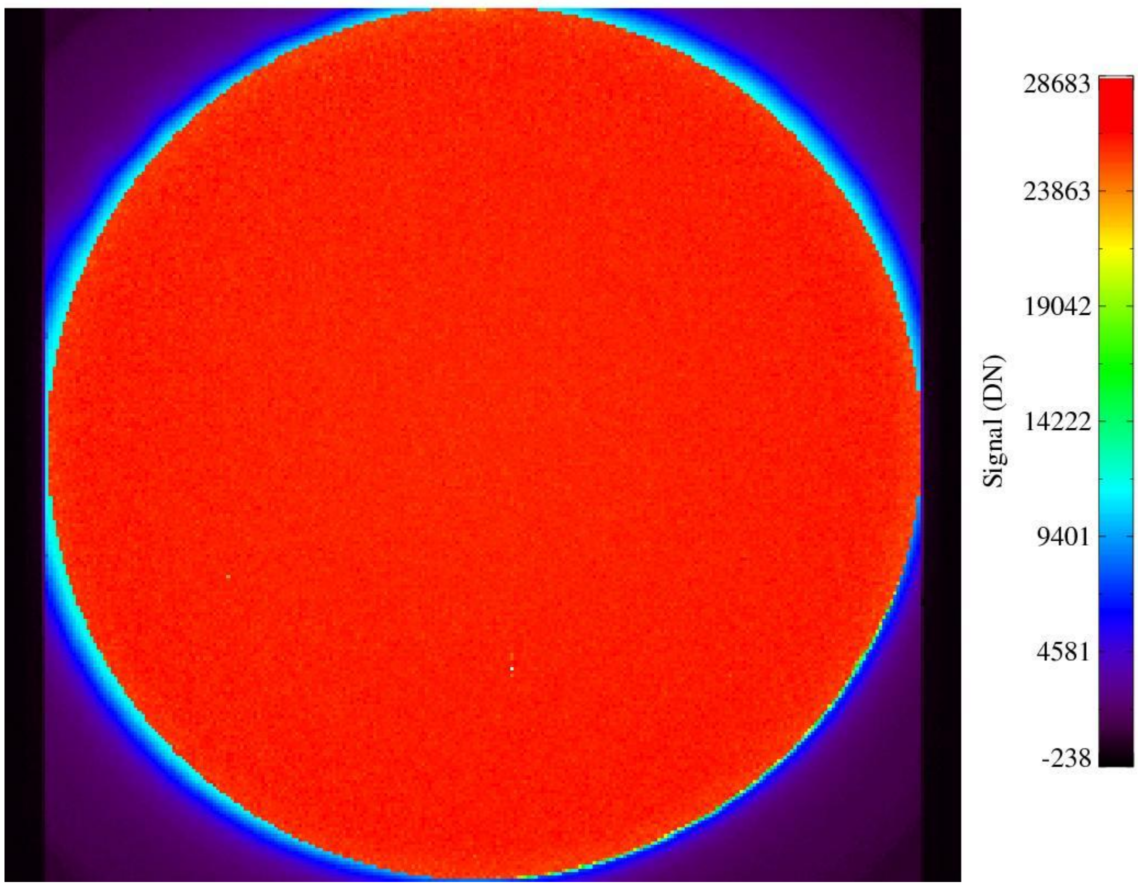

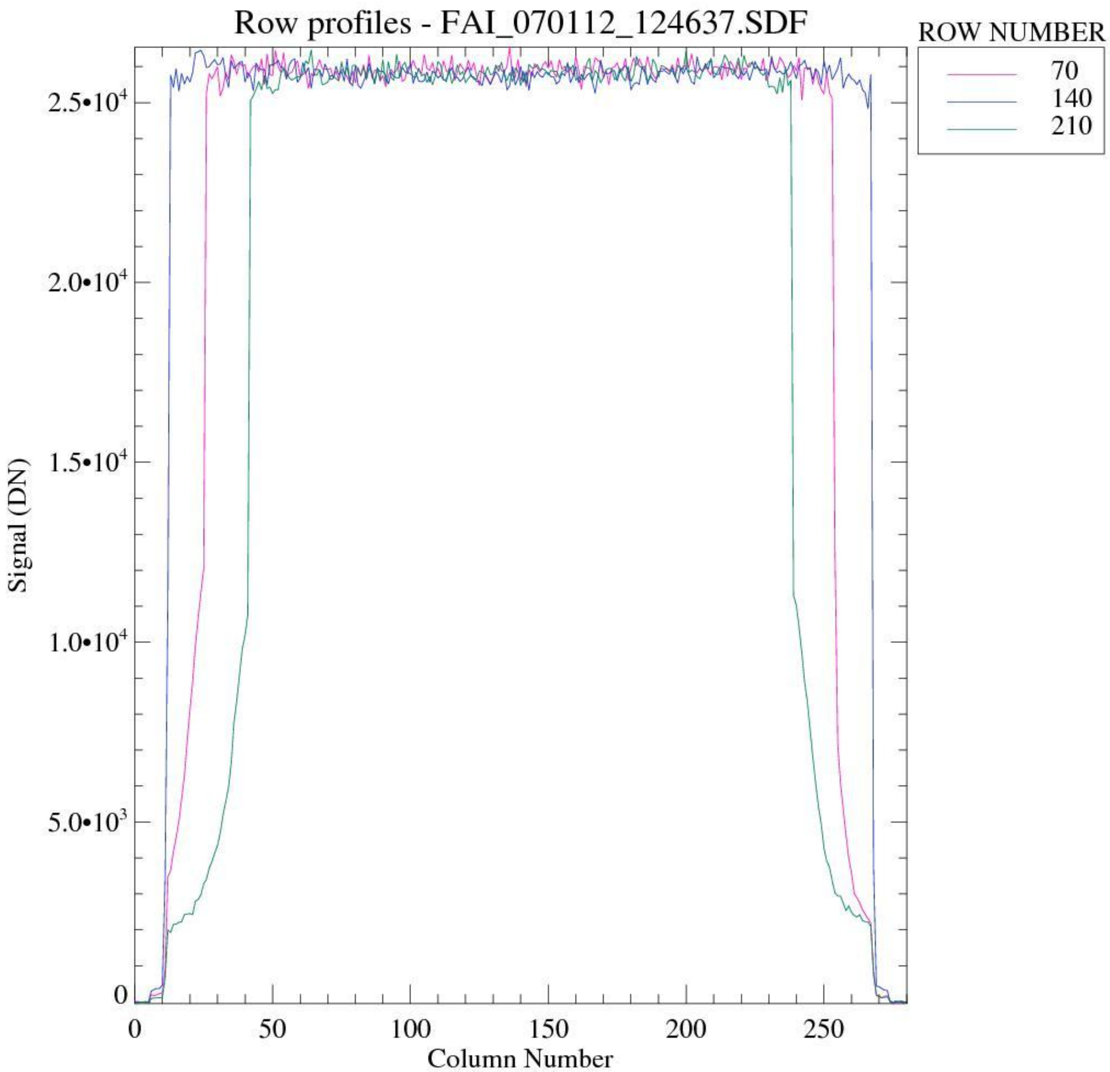

One table of normalization factors was constructed for each camera. These will be applied during routine processing of the mission data. For Mode 4 the table will be used as is, but for Modes 2 and 3 the normalization factors will be averaged over the number of pixels that are binned in each mode.

4. Response linearity with exposure time and pixel binning

The linearity of the response of the cameras with exposure time was checked using the early data (June 2006) from Routes. This was done by measuring the dark current over a range of exposure times at a fixed CCD temperature. There were three independent measurements made at each exposure time for each camera. The linearity of the response with exposure time is confirmed for each camera by the graphs below.

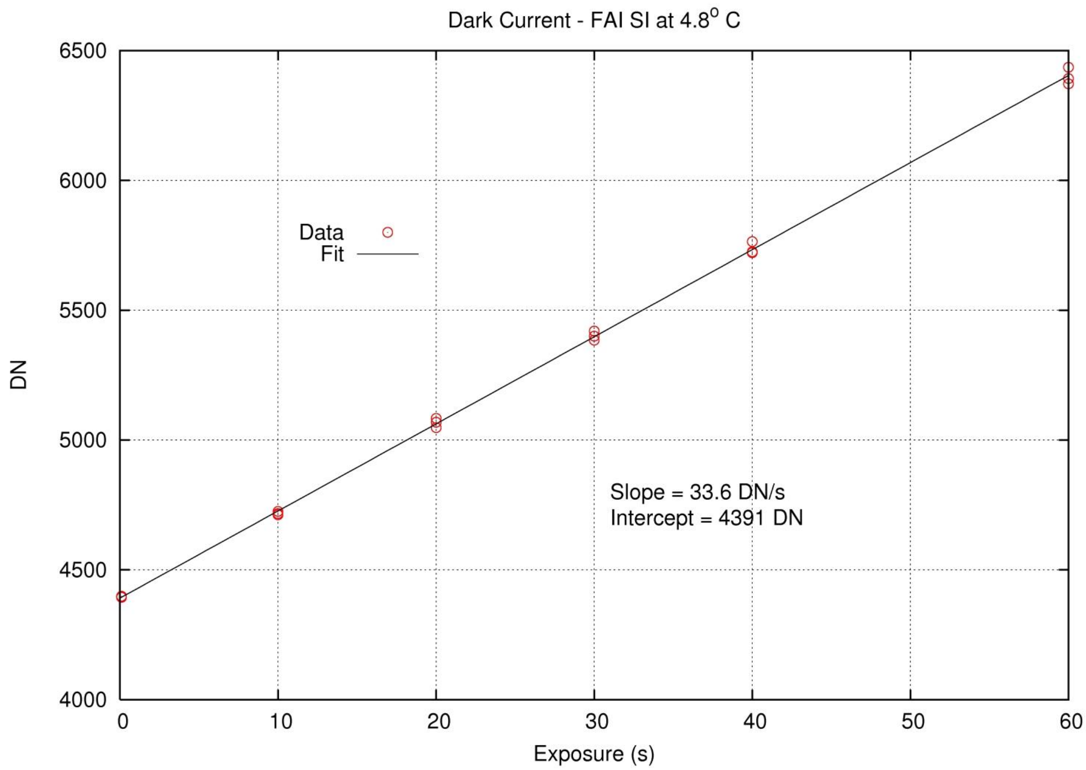

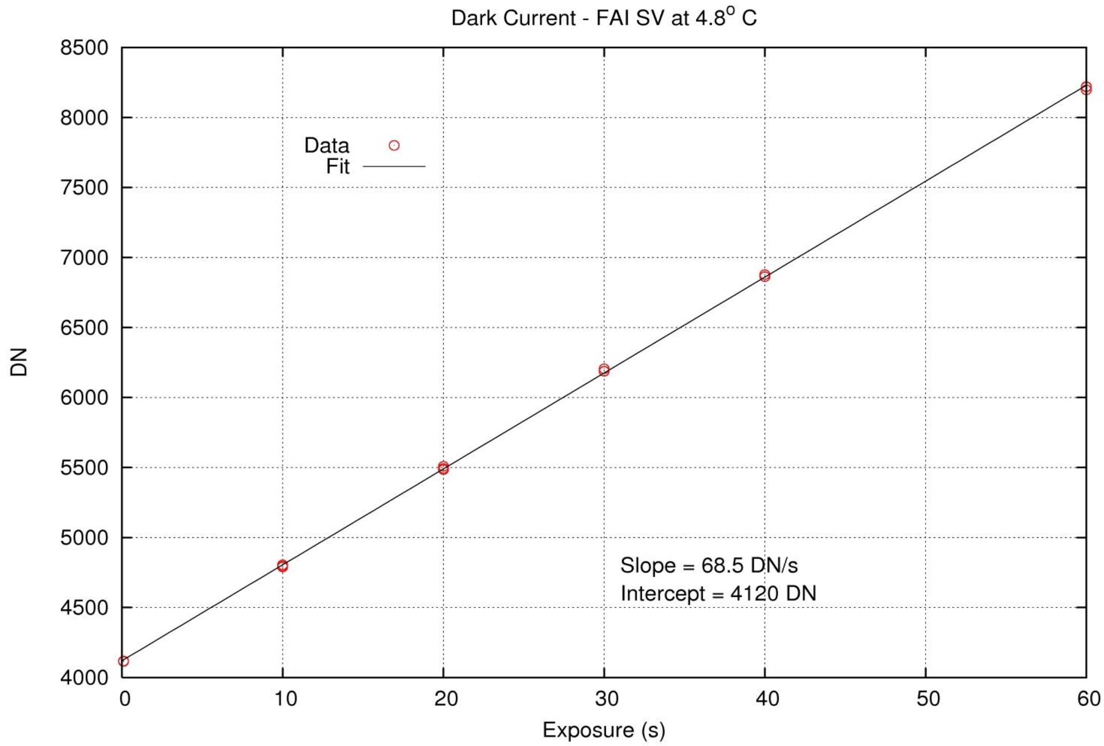

Confirmation of the linearity of response with binning was more elusive. The analysis of the early test data was based on the assumption that the data offset was a single constant number determined only by the electronic setting at the preamplifier, whereas the measurement of the offset was later found to vary. This variation required a different measurement procedure to independently determine the offset. The procedure involved taking a very short dark exposure (1 ms) that ensured that the output was dominated by the offset rather than the dark current. Once the 'offset' image was subtracted, the dark current signal varied with the Mode as expected, i.e., as the number of binned pixels in each Mode.

5. Mean dark current as a function of CCD temperature

For this analysis, the mean dark current has been taken to be the mean of the dark current in the centre 20 by 20 (or 21 by 21) pixel block of pixels. It is of course also essential to know how the dark current in each pixel varies with CCD temperature. The dark current cannot be measured reliably in space with the required accuracy because the cameras do not have shutters. Therefore, laboratory measurements must be used to characterize the dark current.

Four sets of data are available: one set from the David Florida Laboratory taken by Routes on July 7, 2006, two sets from the optical calibration laboratory at the University of New Hampshire taken on September 15, 2006 and December 28, 2006/January 1, 2007, and one set from the University of Calgary taken on July 24, 2007. The results from these measurements are summarized in this section.

a. Measurements at Routes AstroEngineering

In the first data set, obtained by Routes AstroEngineering on July 7, 2006 using a thermal chamber at the David Florida Laboratory, the amount of useful data was limited because a software problem rendered many of the measurements unreliable due to faulty values of CCD temperature in the image headers. For the data that appeared to be consistent, the offset that was subtracted from the raw data was determined from the intercept of the plot of dark current versus exposure time. The slope of the same graph gives the mean dark current at the fixed CCD temperature (see previous graph for 4.8ºC). The measured dark current at 4.8º C from the Routes data was 33 DN/s for SI and 68 DN/s for SV.

b. Measurements at the University of New Hampshire

The first measurements at UNH were made on September 15, 2006 at 5 degree C intervals between 0ºC and 20ºC. Three dark images at an exposure of 20 s were made at each temperature for each camera. The offset was removed by subtracting the mean DN level of 6 offset columns (CCD columns 275 to 280). The net dark current data and the fitted curve to the data are shown in the next two figures.

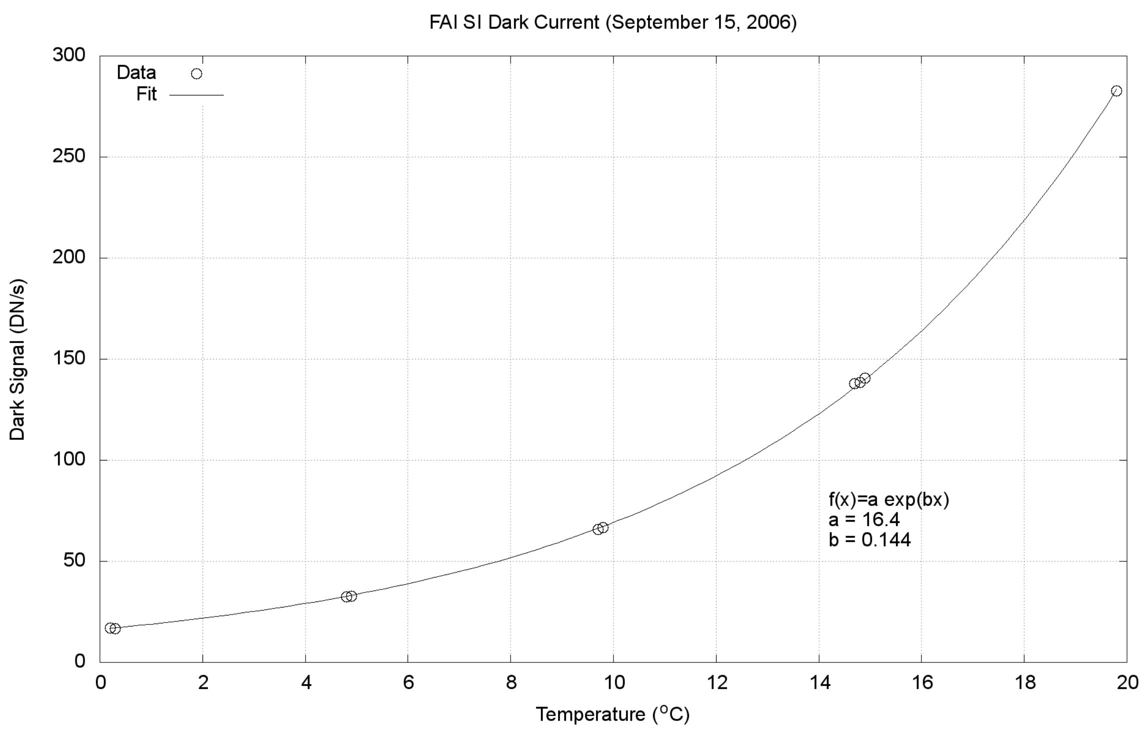

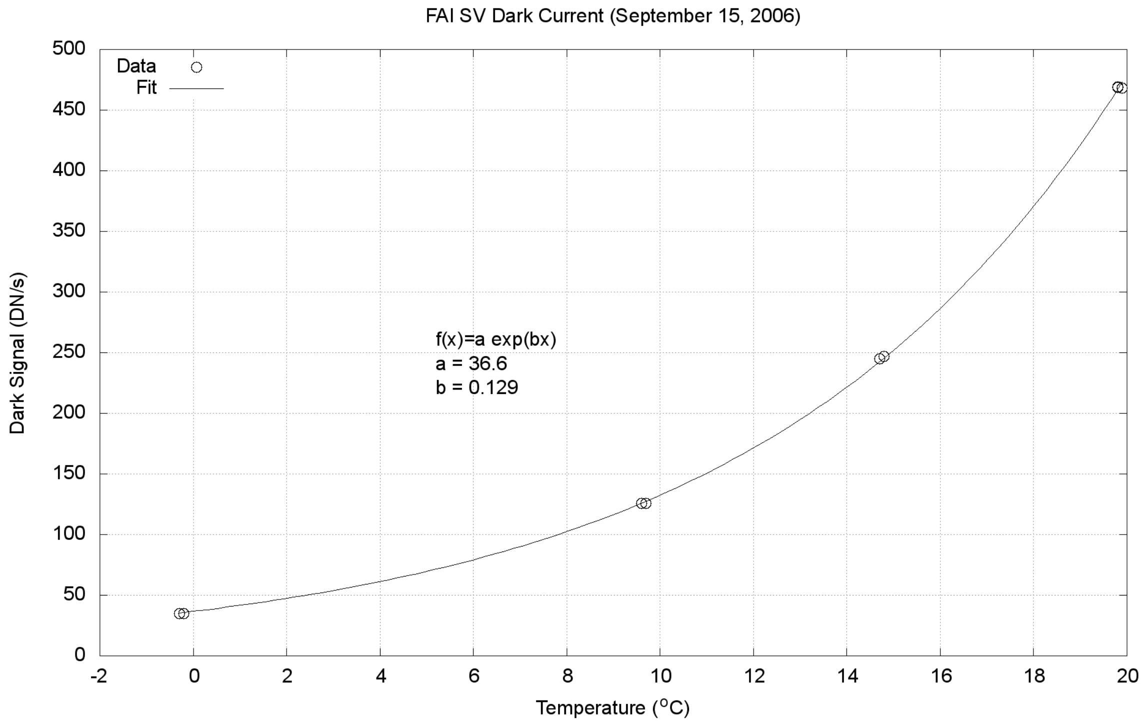

The UNH measurements on December 28, 2006 and January 1, 2007 were made at temperature increments of about 2 degrees in order to improve the resolution. The range covered was 0ºC to 20ºC. The instrument was purged with dry nitrogen during the measurements to prevent condensation. The net dark current was obtained by subtracting the mean of three 1ms-exposure images from the mean of three 10s-exposure images taken at the same temperature. This single step removed the offset, the dark current that accumulated during the image transfer to the storage region of the CCD, and the dark current that accumulated during the readout from the storage region. The results shown in the graphs below are very similar to those in the September 2006 set. The fitted curve can be used to calculate the mean dark current at temperatures between 5 and 20 degrees C. The results here are for the central 21 by 21 pixel portion. A more thorough analysis is required to characterize the dark current over the entire CCD on a pixel-by-pixel basis.

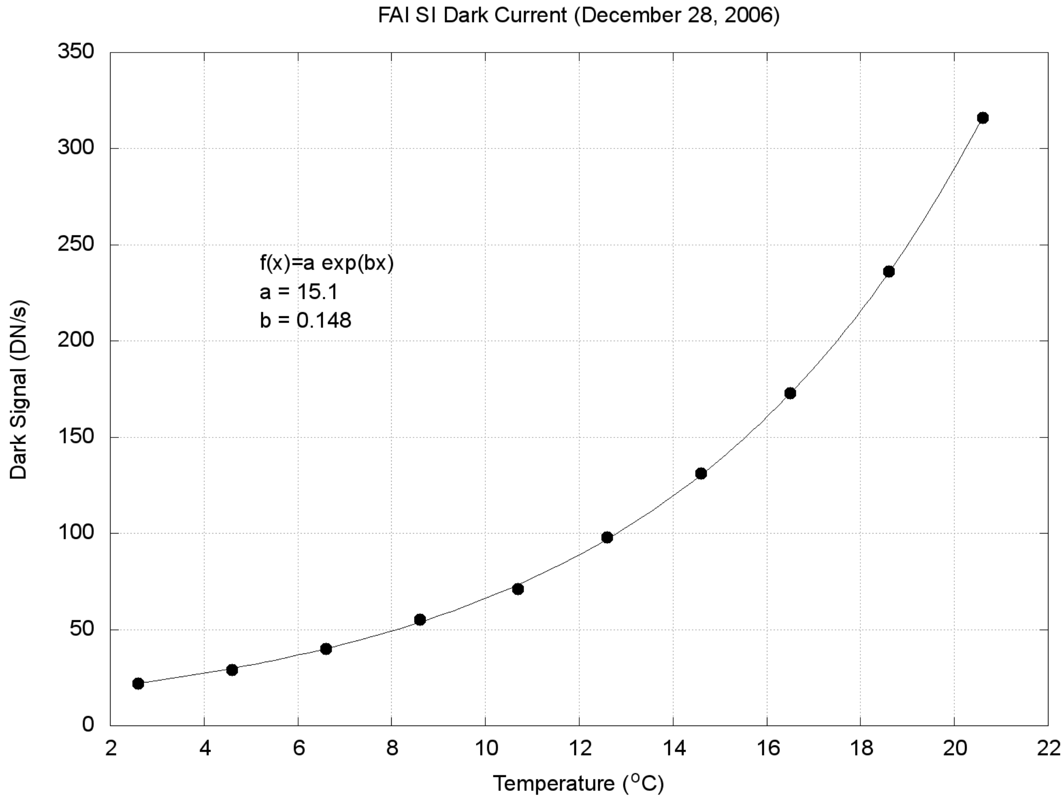
FAI SI Dark Current (December 28, 2006)
f(x)=a exp(bx)
a = 15.1
b = 0.148
Dark Signal (DN/s)
Temperature (°C)
0
50
100
150
200
250
300
350
2
4
6
8
10
12
14
16
18
20
22

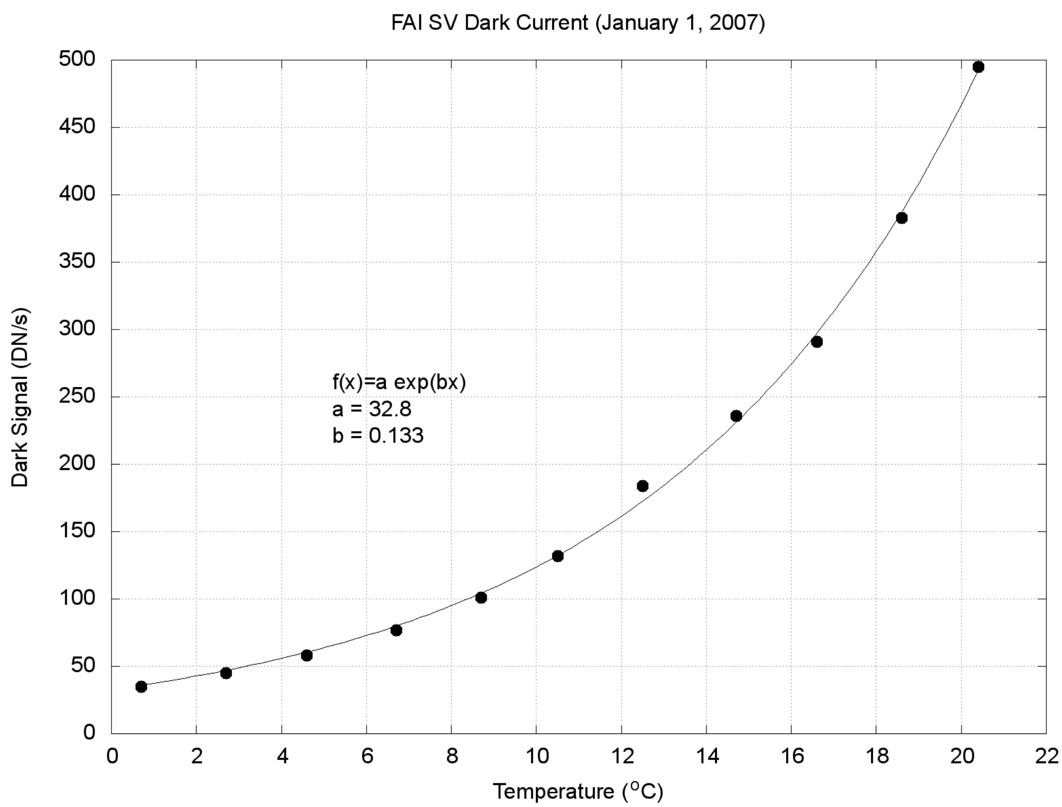
FAI SV Dark Current (January 1, 2007)
f(x)=a exp(bx)
a = 32.8
b = 0.133
Dark Signal (DN/s)
Temperature (°C)
0
50
100
150
200
250
300
350
400
450
500
0
2
4
6
8
10
12
14
16
18
20
22

c. Measurements at the University of Calgary

Measurements of dark current carried out at Routes and UNH had two obvious deficiencies: the measurements did not extend to low enough CCD temperature; and all early data suffered from ubiquitous spurious drops in DN values which increased the noise in the data. The DN drop-out problem was corrected in late 2006, and then in July 2007 a new set of dark current measurements was made at the University of Calgary covering the CCD temperature range of -16ºC to +20ºC in steps of 2ºC.

i. Dark Current Characterization

A library of dark images was taken at the U of C consisting of five 1ms images, five 0.5s images, and five 10s images from each camera, at temperatures ranging from -16 ^{o}C to +20 ^{o}C in two degree increments. The 10-second exposures were used to create a pixel-by-pixel fit to enable the removal of the dark current from all FAI images, given the correct CCD temperature. The fit was found as follows.

The net dark current for each pixel in the 256x256 imaging area was obtained by subtracting the mean of the 1ms signal for the same pixel at the same temperature. The net dark current for each pixel was plotted against temperature, and a curve was fitted to that plot in the form,

$$DC = A[0] \cdot \exp(A[1] \cdot T) + A[2]$$

Here DC is the dark current in DN/s, T is the CCD temperature in degrees C, and the A values are constant fitting parameters. Generally, the fitted curve for a single pixel looked like the following:

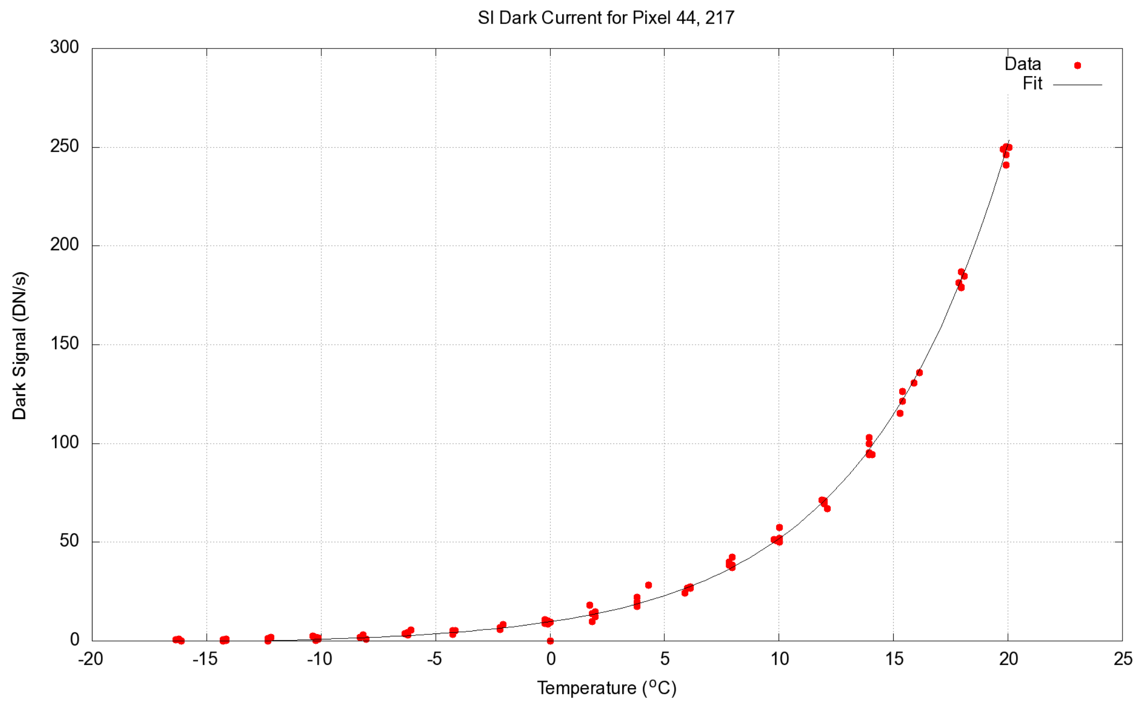

For the SI CCD, the average fit to all the pixels is

$$DC = 16.9 \cdot \exp(0.140 \cdot T) - 0.99,$$

and for the SV CCD the fit is,

$$DC = 37.3 \cdot \exp(0.127 \cdot T) + 1.46$$

Results for the central 20x20 area of each CCD are shown in the following two graphs. The fitting parameters are in close agreement with those found for the entire array. The fitting procedure was carried out for each pixel and the fitting parameters for each pixel were saved for mission data processing. For each image that is received from orbit, the CCD temperature information for that image will be used with the fitted dark current parameters to calculate and subtract the dark current for each pixel.

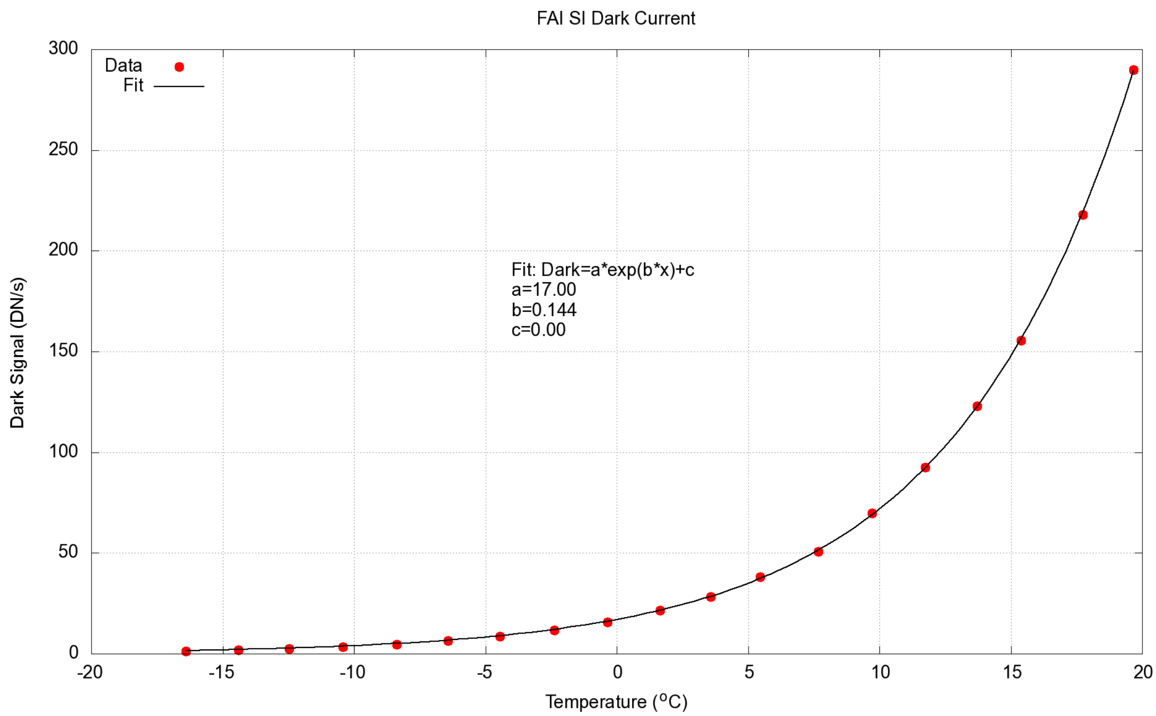
FAI SI Dark Current
Data
Fit
Fit: Dark=a*exp(b*x)+c
a=17.00
b=0.144
c=0.00
Dark Signal (DN/s)
Temperature (°C)
300
250
200
150
100
50
0
-20
-15
-10
-5
0
5
10
15
20

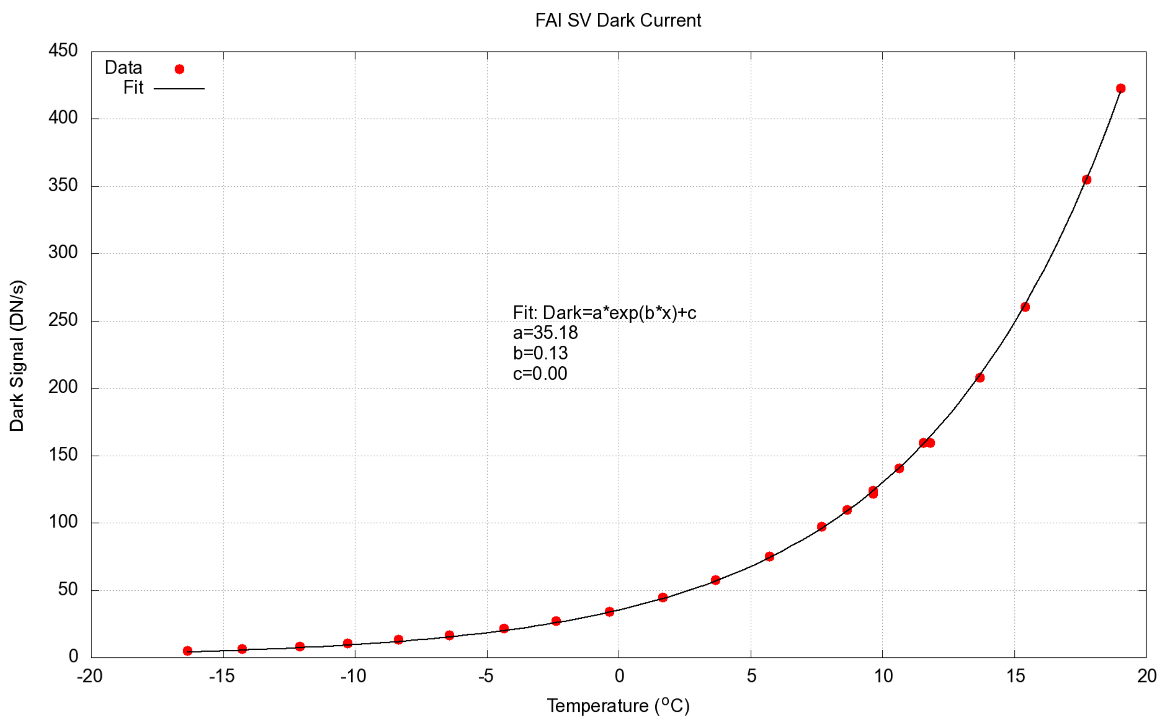
FAI SV Dark Current
Data
Fit
Fit: Dark=a*exp(b*x)+c
a=35.18
b=0.13
c=0.00
Dark Signal (DN/s)
Temperature (°C)
450
400
350
300
250
200
150
100
50
0
-20
-15
-10
-5
0
5
10
15
20

The agreement between measurements of dark current made at UNH and U of C over a range of temperatures is very close as can be seen from the fitting parameters given in the following table for three dates: September 15, 2006 by Routes, December 28, 2006 at the University of New Hampshire and July 24, 2007 at the University of Calgary. The fitted dark current variation with temperature has the form $DC = ae^{bT}$ where T is in degrees C and a and b are the fitted constant parameters. The calculated dark current values (DN/s) at 20ºC also agree well.

Dark Current versus Temperature

Date	a(SI)	b(SI)	DC(20ºC)	a(SV)	b(SV)	DC(20ºC)
Sept. 15, 2006	16.4	0.144	292	36.6	0.129	483
Dec. 28, 2006	15.1	0.148	291	32.8	0.133	469
July 24, 2007	17.0	0.144	303	35.2	0.130	474

The measured dark current vs. temperature for each CCD is shown in the next two figures along with the curves given by the CCD manufacturer. The manufacturer's curve has been shifted vertically by the amount necessary to make the 20ºC values of dark current approximately the same as the measured dark current in units of DN/s. The shapes of the curves are similar but not identical, demonstrating the importance of making laboratory measurements of the dark current.

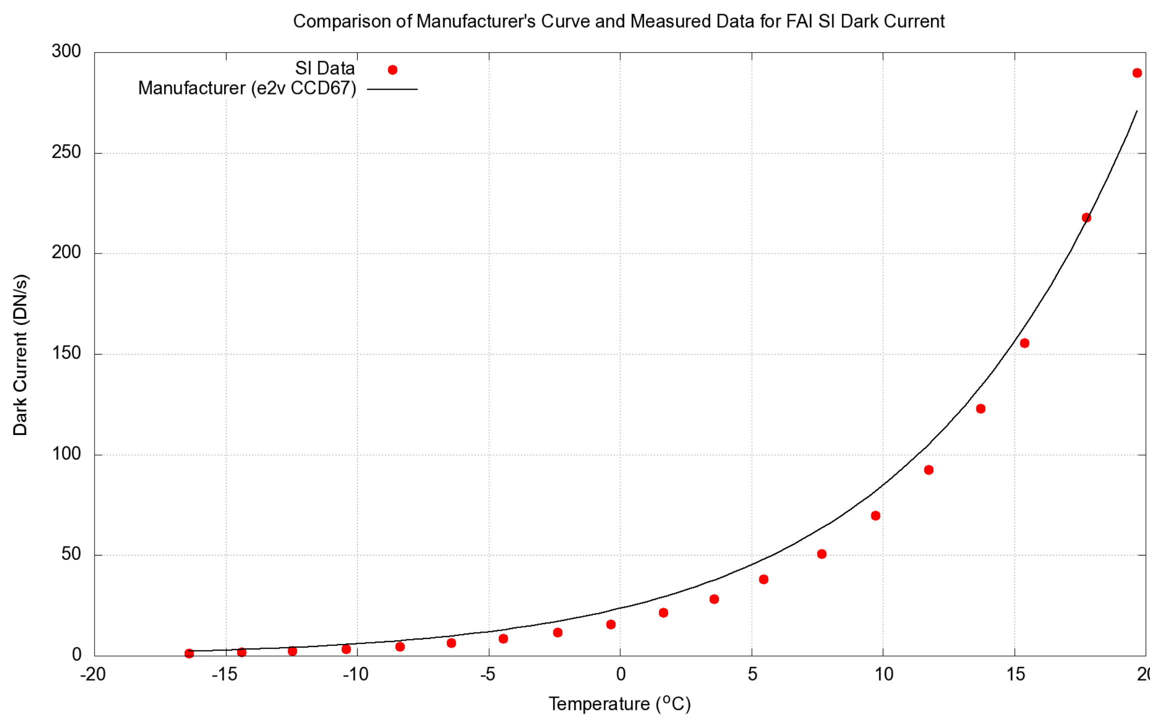

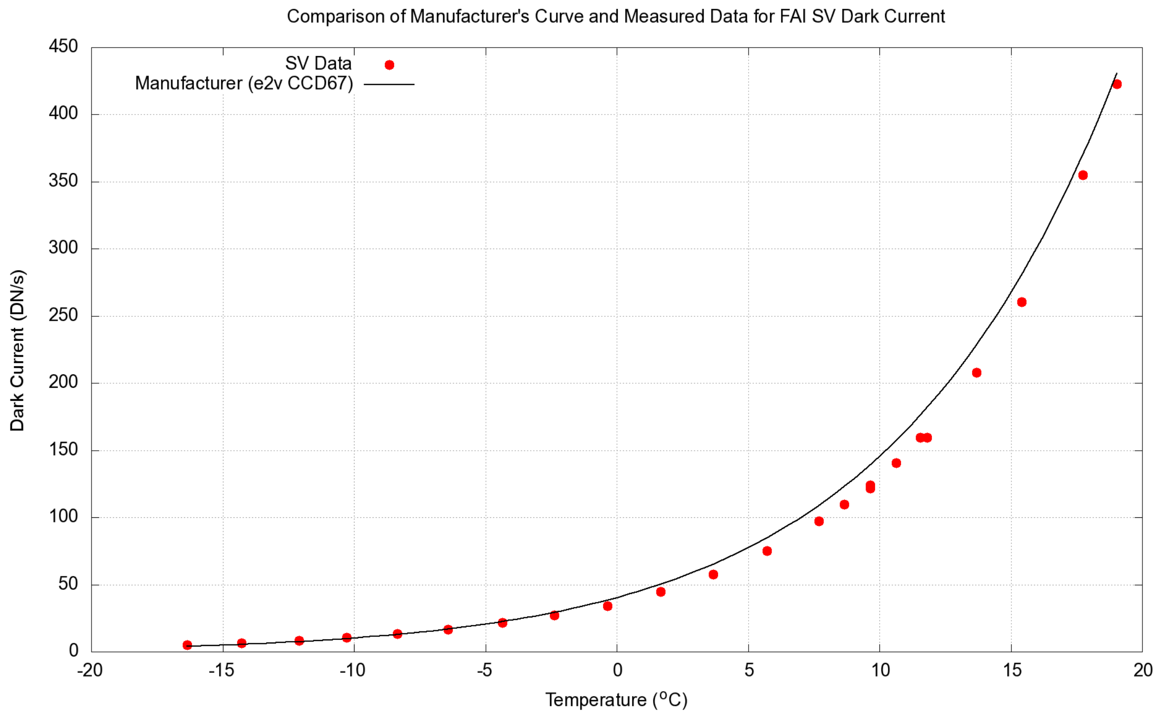

ii. Hot Column Removal

A second, very similar fit was done to remove hot columns in the FAI data that appear when the temperature is above about -5 °C. The fit for this purpose was found using the 1ms exposures from the dark current library. The hot columns are produced at readout and do not contribute to the dark current, and thus have a different temperature-dependent signal than does the true dark current. As with the dark current, an exponential fit was performed for each pixel across the range of temperatures in the library after the dark current and electronic-induced offset was removed. If the remaining signal was above 40 DN at 25°C (theoretically it should be zero), the curve was accepted. If the curve did not reach the threshold, no correction was performed. This acts to select the hot columns and leave the other pixels untouched. The fits were saved and used along with the CCD temperature information from the image to remove the hot columns when an image is displayed.

The following images show the effect of the dark current and hot pixel removal on a 0.5 second exposure for the SI and SV cameras, at a temperature of 5.8 °C.

SI camera

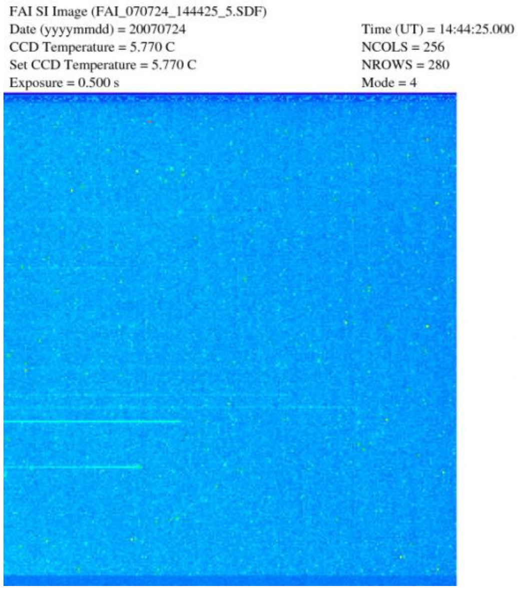

Before Removal

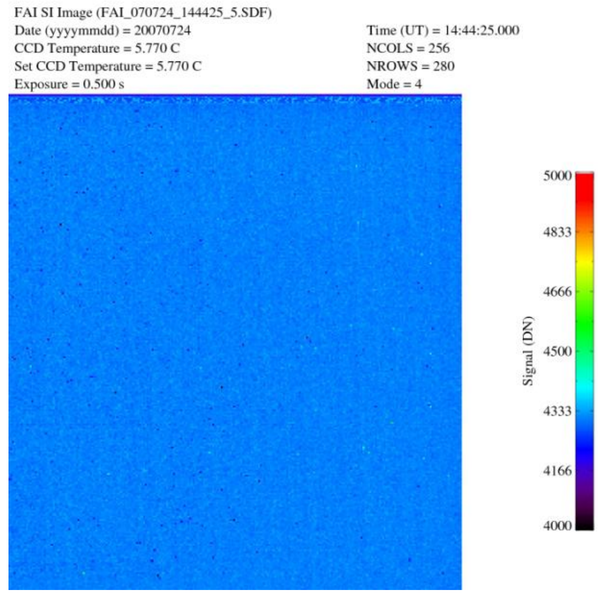

After Removal

SV camera

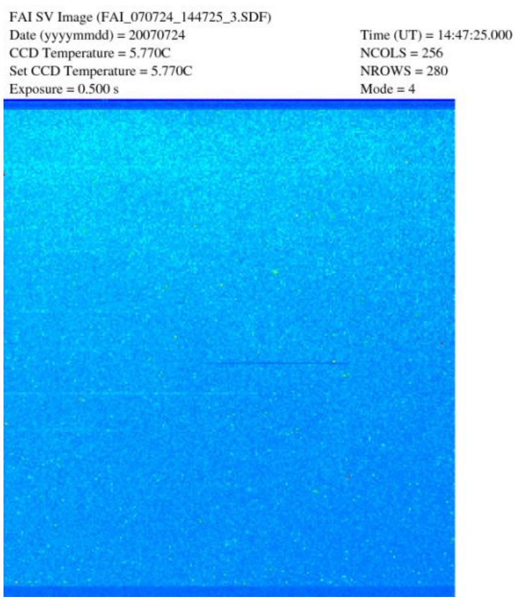

Before Removal

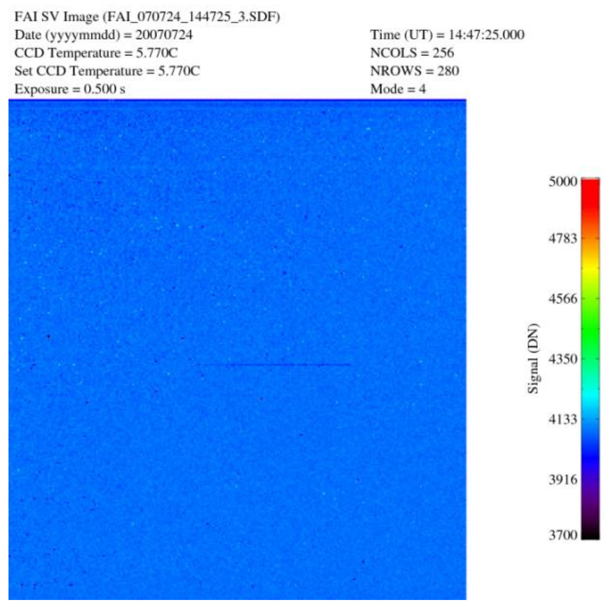

After Removal

d. Correction for dark current gradients

The dark current in each pixel accumulates during the finite time required for the data to be transferred from the image area to the storage area and for the storage area to be read out. This results in signal gradients along both the columns and rows that can be observed in the dark current images. Fortunately, these gradients can be removed from the data using information about the transfer times involved, the dark current rate at the temperature of the CCD, and the operation mode (2, 3, 4). With the addition of the exposure time, a corrected dark current image can be constructed for any CCD temperature and exposure time.

The table below gives the total readout time per image along with the components that make up the total. The readout time remains constant for each Mode.

	Mode 4	Mode 3	Mode 2
Transfer to storage	5µs • 256 rows	5µs • 256 rows	5µs • 256 rows
Rows to output register	25µs •256 rows	25µs •256 rows	25µs • 256 rows
Output shifts	4.5µs •280 cols •256 rows	5.0µs • 140 cols •128 rows	5.5µs •70 cols •64 rows
Total readout time	330ms	96ms	31ms

The figure below shows the measured and calculated average gradient along the columns. The agreement verifies the expected cause of the gradient. The accumulated dark current is largest for row 256 and least for row 1.

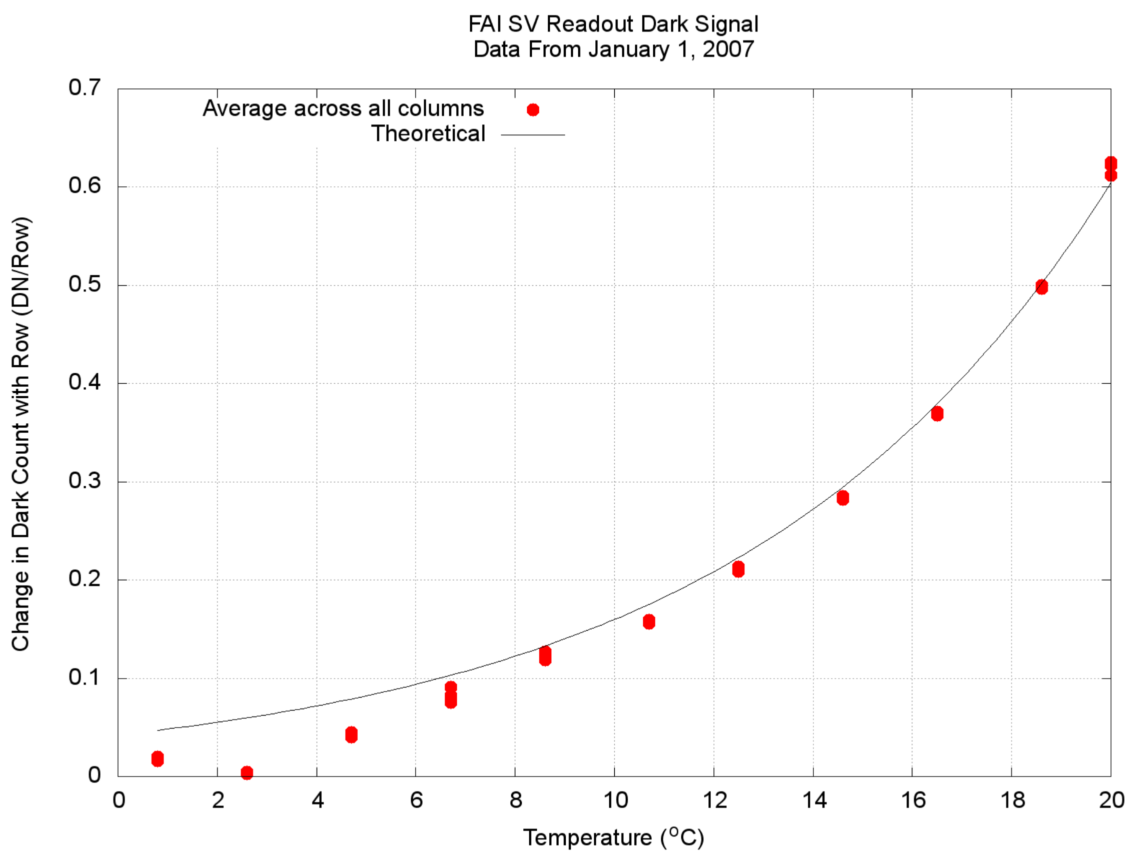

What follows is a brief description of the procedure to synthesize the recorded dark current for each pixel of an image.

Let the CCD column number = x
Let the CCD row number = y
Let the dark current rate = R (DN/s) (data numbers per second)
DC(x,y) is the dark current in DN for pixel (x,y)
DC(X,Y) is the dark current in DN for superpixel (X,Y). Superpixels are used in Mode 2 (default is 4 x 4 pixels) and Mode 3 (default is 2 x 2 pixels).
The transfer times were provided by Burley Scientific.

Mode 4

There are 5 components to the dark current:

1. Frame transfer before exposure
   DC(x,y) = R*4.5µs*(256-y)

2. Exposure period
   DC(x,y)=R*Exposure time

3. Frame transfer of image to storage
   DC(x,y)=R*4.5µs*256

4. Parallel shifts from storage to horizontal transport register
   DC(x,y)=R*25µs*y

5. Readout for Mode 4
   DC(x,y)=R*4.5µs*(x+(y-1)*280)

The total dark current for Mode 4 is the sum of the above components. It is assumed for simplicity that R is the same for all pixels. In practice R = R(x,y).

Mode 3

a. For Mode 3, change step 5 above to

DC(X,Y)=R*5.0µs*(X+(Y-1)*140)*4 for X =1 to 140 and Y = 1 to 128

b. Then sum components 1 to 4 for each pixel

c. Bin into superpixels (2 by 2) for X = 1 to 140 and Y = 1 to 128

$$DC(X,Y)=\sum_{n=0}^{1}\sum_{m=0}^{1} DC(2X-n,2Y-m) \text{ for } X=1 \text{ to } 140 \text{ and } Y=1 \text{ to } 128$$

d. Finally, sum this with the Mode 3 version of step 5 to obtain the dark current in superpixel X,Y.

Mode 2

a. For Mode 2, change step 5 above to

$$DC(X,Y)=R*5.5\mu s*(X+(Y-1)*70)*16 \text{ for } X = 1 \text{ to } 70 \text{ and } Y = 1 \text{ to } 64$$

b. Then sum components 1 to 4 for each pixel

c. Bin into superpixels (4 by 4) for X = 1 to 70 and Y = 1 to 64

$$DC(X,Y)=\sum_{n=0}^{3}\sum_{m=0}^{3} DC(4X-n,4Y-m) \text{ for } X=1 \text{ to } 70 \text{ and } Y=1 \text{ to } 64$$

d. Finally, sum this with the Mode 2 version of step 5 to obtain the dark current in superpixel X,Y.

The readout times for each Mode are shown in the table below. These impose a limit to the rate at which images can be transferred to telemetry.

The relative contribution of the ‘readout’ portion of the dark current diminishes with exposure time as illustrated in the figure below.

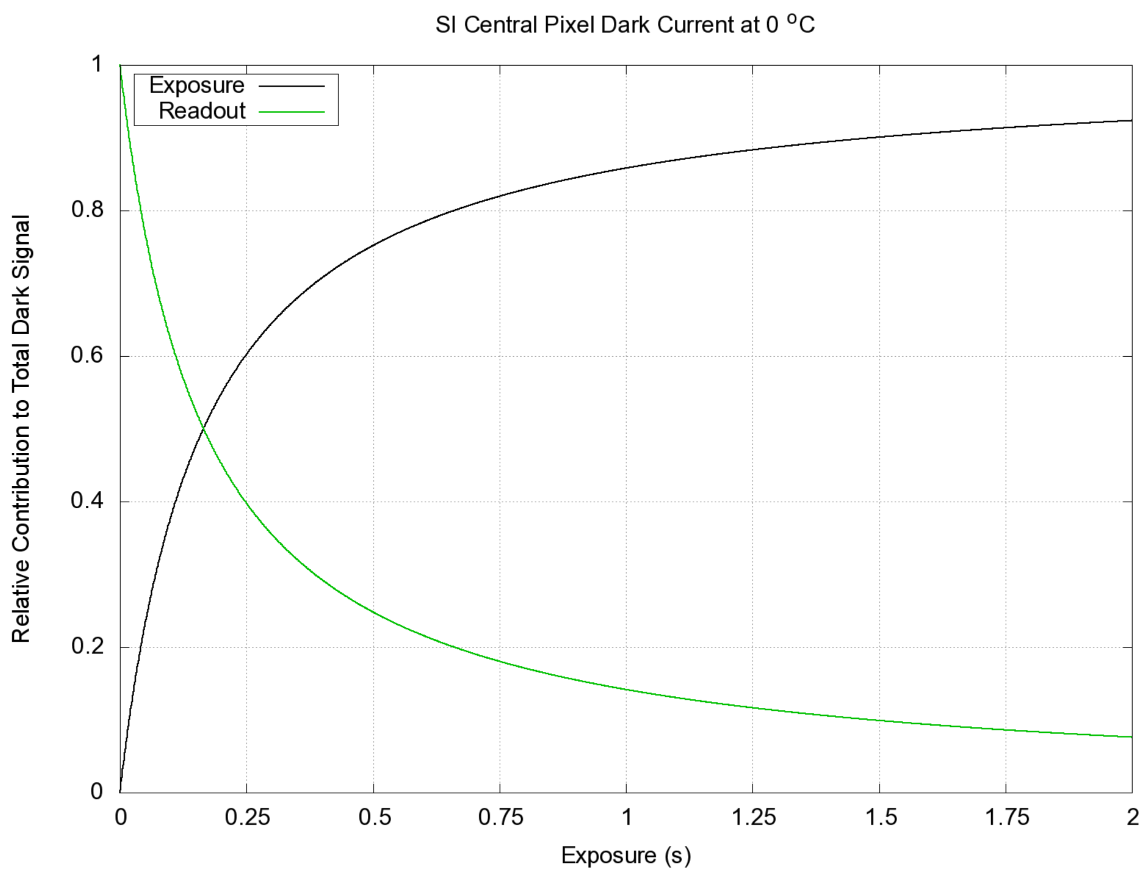

6. Measured field of view and baffle performance

For this test FAI was positioned on a rotation table in the dark room at UNH and a small light source was located on the wall. Images of the light source were taken over a range of rotation angles of the camera. The exposure time was increased outside the field of view (FOV) to provide a larger dynamic range. The two figures below show the results. The location of the sharp drop in signal marks the edge of the FOV. These plots show that for SI the FOV is 26 degrees with an uncertainty of about 1 degree. For SV the FOV is 25 degrees with an uncertainty of about 1 degree. Within the measurement error, it can be concluded that the FOVs are the same for the two cameras, as expected.

Beyond the FOV, the signal drops to about 1% within 1 degree, and appears to drop to about .001 % within about 2 degrees. The asymmetry from one side to the other looks strange, as does the knee in the SI plot. It was planned to make the measurements for two orthogonal directions, but time did not permit. Until star fields are available it is necessary to assume that the baffle performance is rotationally symmetric.

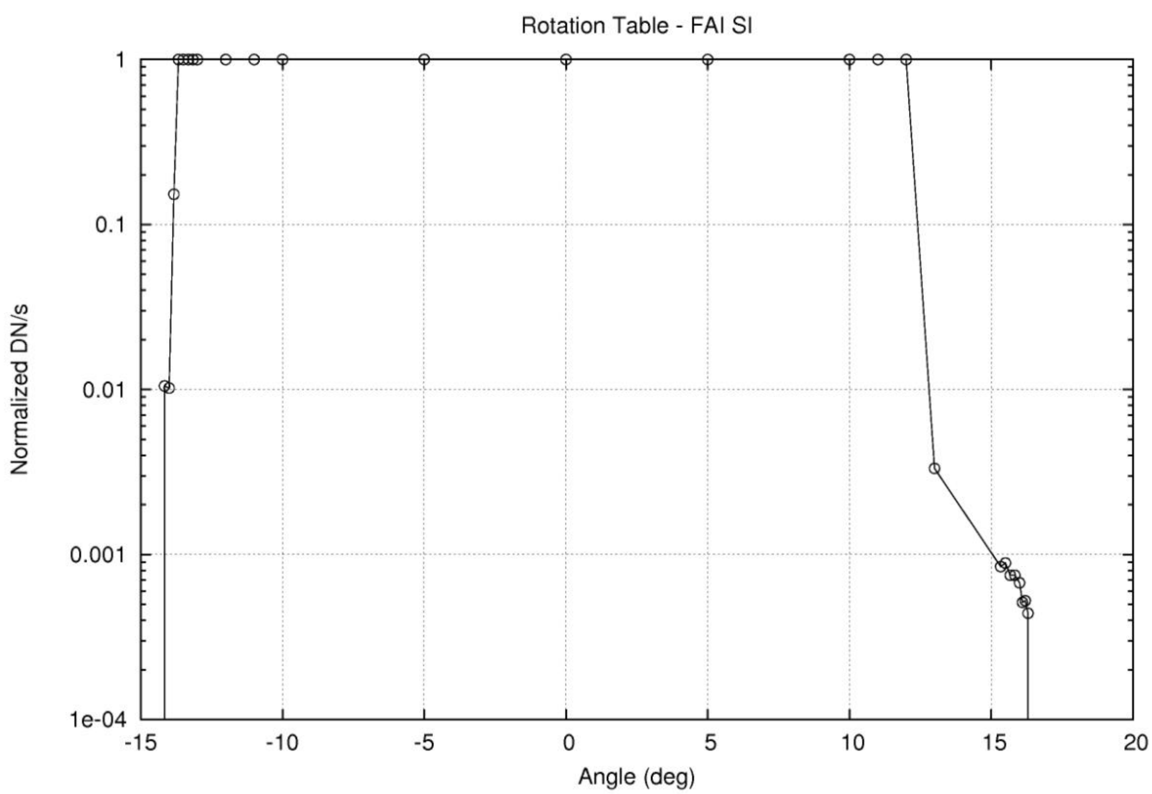

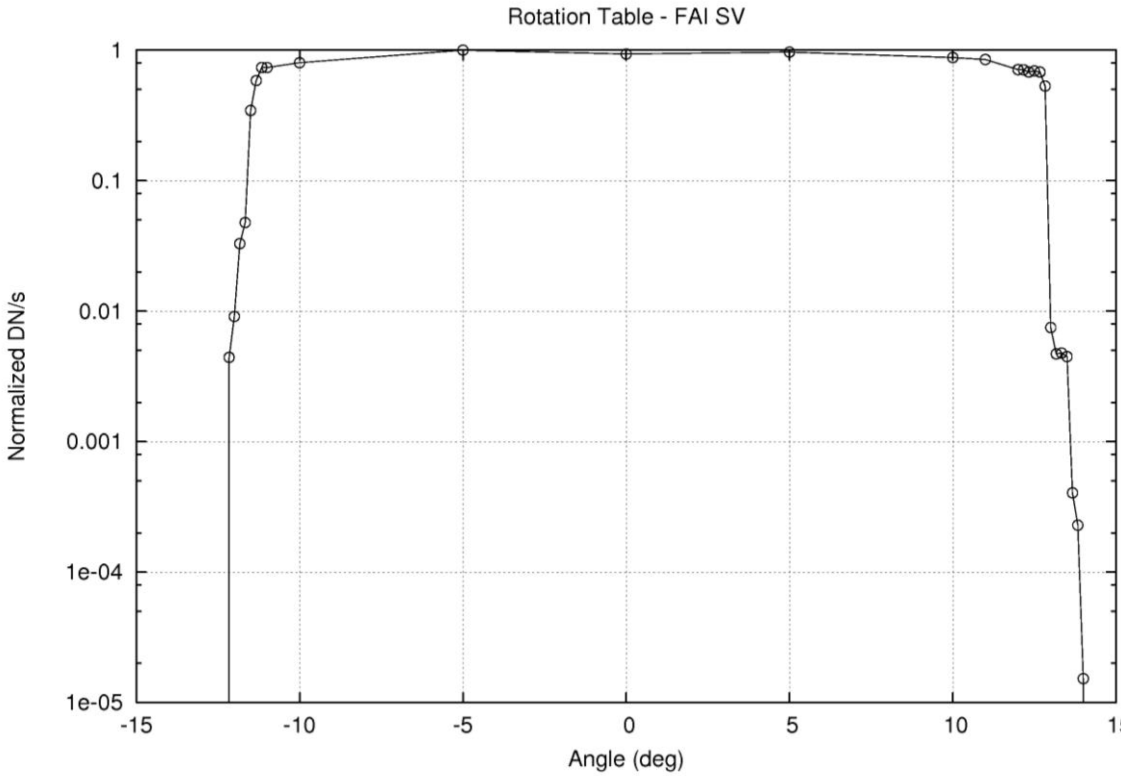

Combining measurements of the angular FOV with the image of the FOV on the CCD it is possible to determine the angle per pixel which is a fundamental parameter for data analysis. Using 26 degrees as the FOV and 246 as the diameter of the FOV on the CCD, the angular resolution is 26/246 = 0.106 deg/pixel.

FAI Camera Angular Resolution = 0.106 deg/pixel

7. Focus and resolution tests

a. Tests at Routes using strips

A very simple resolution test was carried out at Routes in June 2006. Black and white parallel strips of width 1.4 cm were attached to a flat board and located at a distance of 7.8 m so that the 0.2 degree angular separation of one spatial period subtended by the camera corresponded to two pixels at the CCD. The images are reproduced below and indicate that the resolution is set by the pixel size because the strips are clearly visible.

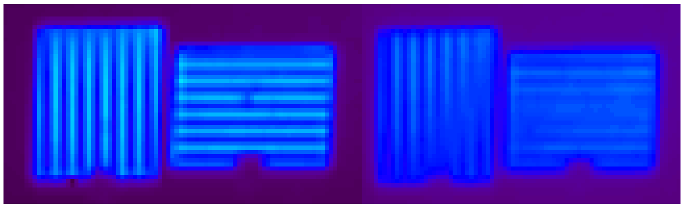

SI SV

It is evident that the resolution of the SI camera is superior to that of the SV camera. An estimate of the contrast for SI (max-min/max+min) is 0.35.

b. Point spread function

Point sources (small light bulbs) were imaged at both Routes (June 9, 2006) and UNH (October 11-13, 2006). The source at Routes had an angular extent of less than one pixel, whereas the source at UNH had an angular extent of about 2 pixels due to the smaller room size. Inspection of the images of the point sources indicated that the cameras are in good focus. The first figure below is a plot of the UNH source showing both the data and a Gaussian fit. The full-width-half-max (FWHM) of the fit is 2.5 pixels.

The UNH light source was imaged at several different angles with respect to the optical axis during the FOV test. The fit to these is shown below for the SV camera. The SI measurements could not be used because the analog-to-digital converter (ADC) was saturated at 65536 (16 bits) by the light level. The results for the SV camera show that the broadening of the point image away from the centre of the field is relatively small, and the same can safely be expected for the SI camera.

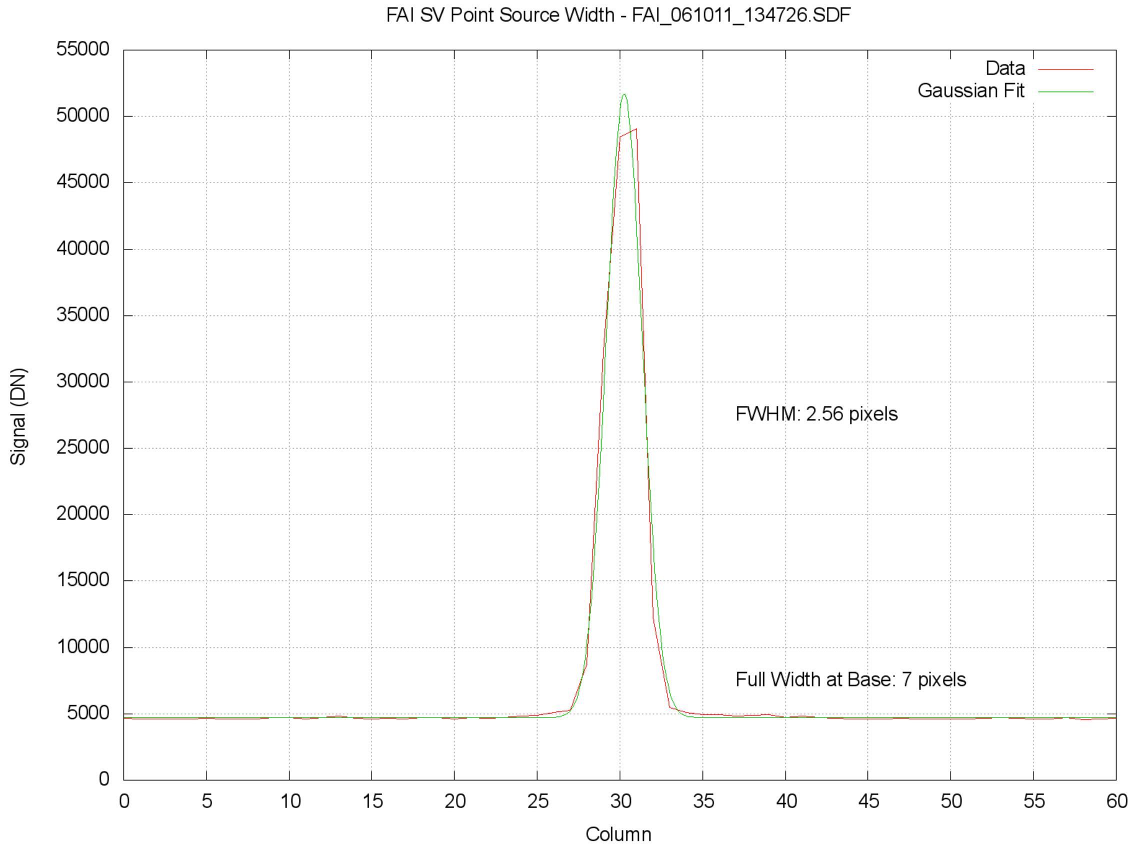
FAI SV Point Source Width - FAI_061011_134726.SDF
Data
Gaussian Fit
FWHM: 2.56 pixels
Full Width at Base: 7 pixels
Signal (DN)
Column
0
5000
10000
15000
20000
25000
30000
35000
40000
45000
50000
55000
0
5
10
15
20
25
30
35
40
45
50
55
60

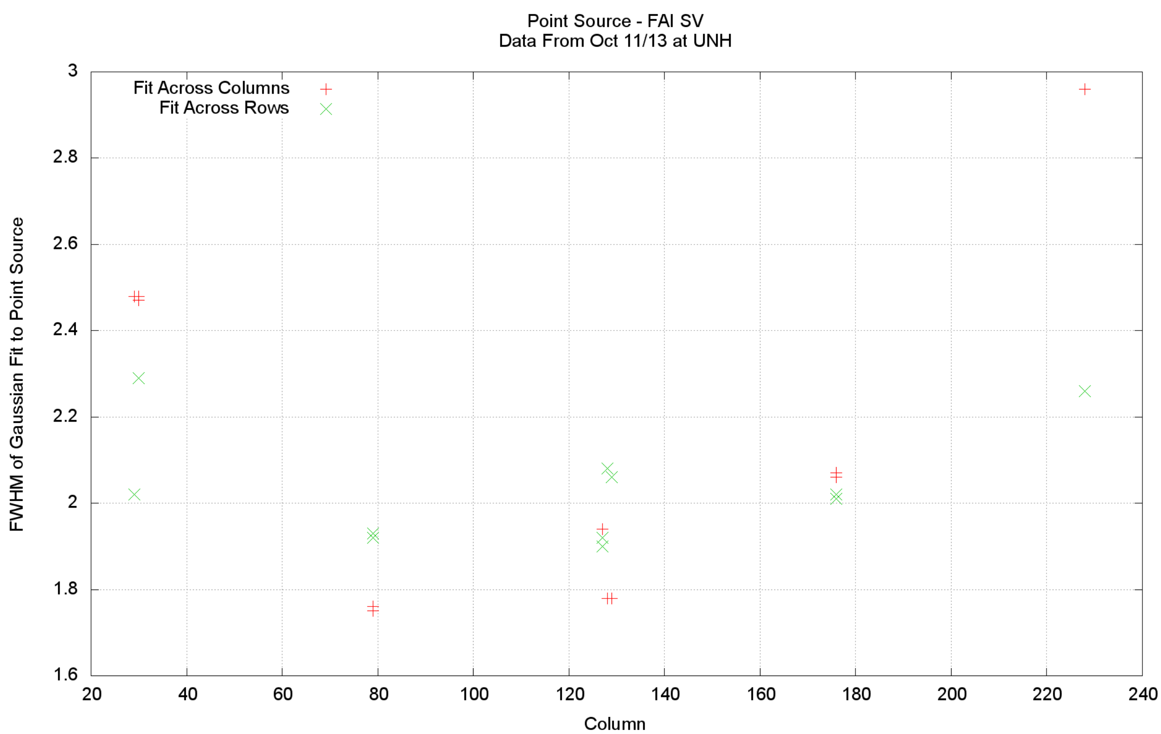
Point Source - FAI SV
Data From Oct 11/13 at UNH
Fit Across Columns
Fit Across Rows
FWHM of Gaussian Fit to Point Source
Column
1.6
1.8
2
2.2
2.4
2.6
2.8
3
20
40
60
80
100
120
140
160
180
200
220
240

From the Routes data of June 9, 2006, the point spread function for both cameras could be obtained. The next two figures show the FWHM for a few available angles. The profiles are narrower than for the Routes data as expected due to the smaller angular size of the source. The resolution at the CCD is very near the Nyquist limit of 2 pixels, i.e. two features must be separated by 1 pixel to resolve them.

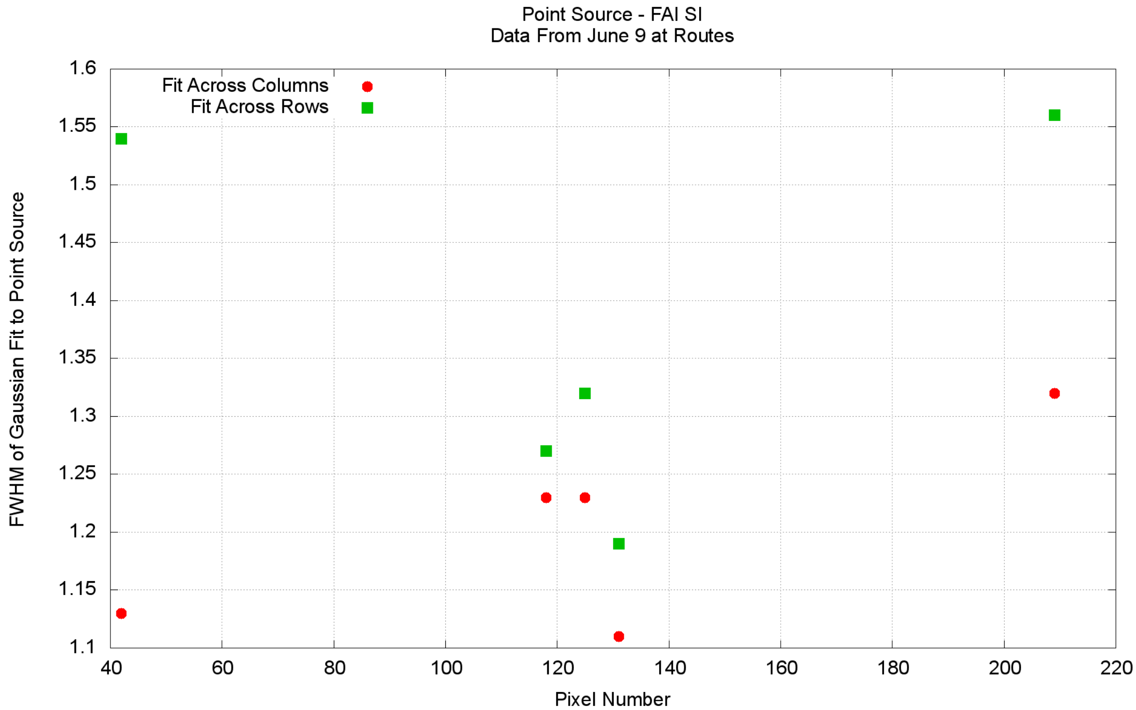

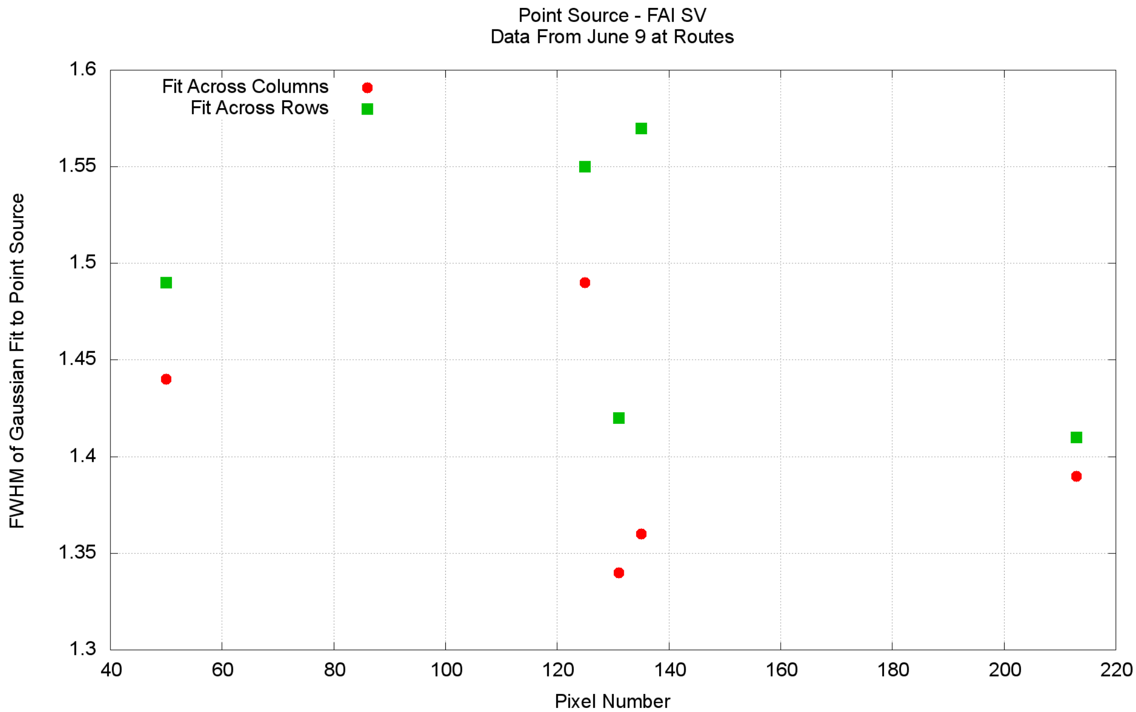

c. USAF resolution chart

Two collimators were provided by UNH for the purpose of assisting with the testing and characterization of the cameras. A set of 35 mm test slides came with each collimator. One version of the 1951 USAF resolution test pattern was imaged by each camera, and qualitative inspection of the test pattern showed that the resolution of the SI camera is near the 2 pixel limit and the resolution of the SV camera appears to be between 2 and 3 pixels. The images below were taken at Routes on June 13, 2006.

SI

SV

8. Image distortion

The first figure below is an image of a rectilinear checkerboard pattern obtained at UNH in October 2006. The pincushion distortion in the image is obvious. The obstruction at the bottom is not part of the checkerboard. The correction for the distortion would move the image pixels to a rectilinear grid.

Because the distortion is regular, i.e. pincushion, and therefore radially symmetrical, it can be corrected by the application of a third-order polynomial that relates the measured pixel radii (R_{meas}) to the corresponding radii (R_{cor}) in a perfect image:

$$R_{cor} = (a*R_{meas}^3+b*R_{meas}^2+c*R_{meas}+d)*R_{meas}$$

Here, the radius is normalized, i.e. R=1 at the edge of the image. The parameter d ensures that the corrected image is the same size as the measured image. For a perfect lens, a, b, and c are 0.0 and d = 1. Once these parameters have been determined, all images can be routinely corrected for distortion.

A preliminary approach to finding the parameters has been essentially through a process of iteration and inspection, i.e. empirical. The second image below shows the same checkerboard image as the first image, but after correction for distortion. Although there is an obvious improvement, at a future time the coefficients will be determined in a completely objective manner by solving for the coefficient values for both cameras.

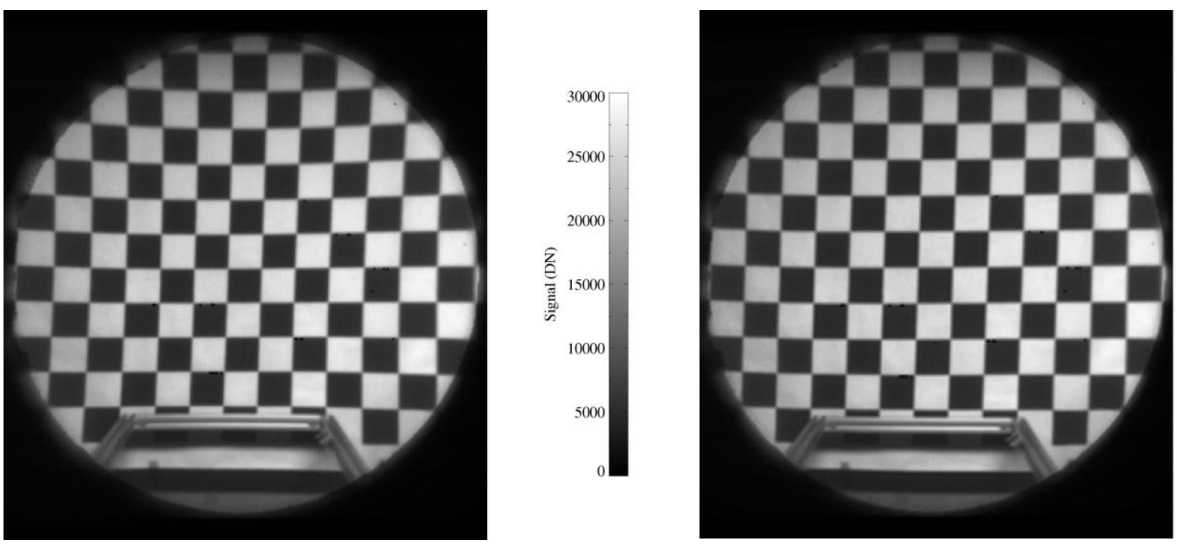

9. Noise characteristics

a. Read noise

The two following figures show the measurements of the read noise. The data were obtained from the offset columns on January 23, 2007. The standard deviation of about 7.5 DN agrees well with the expected read noise.

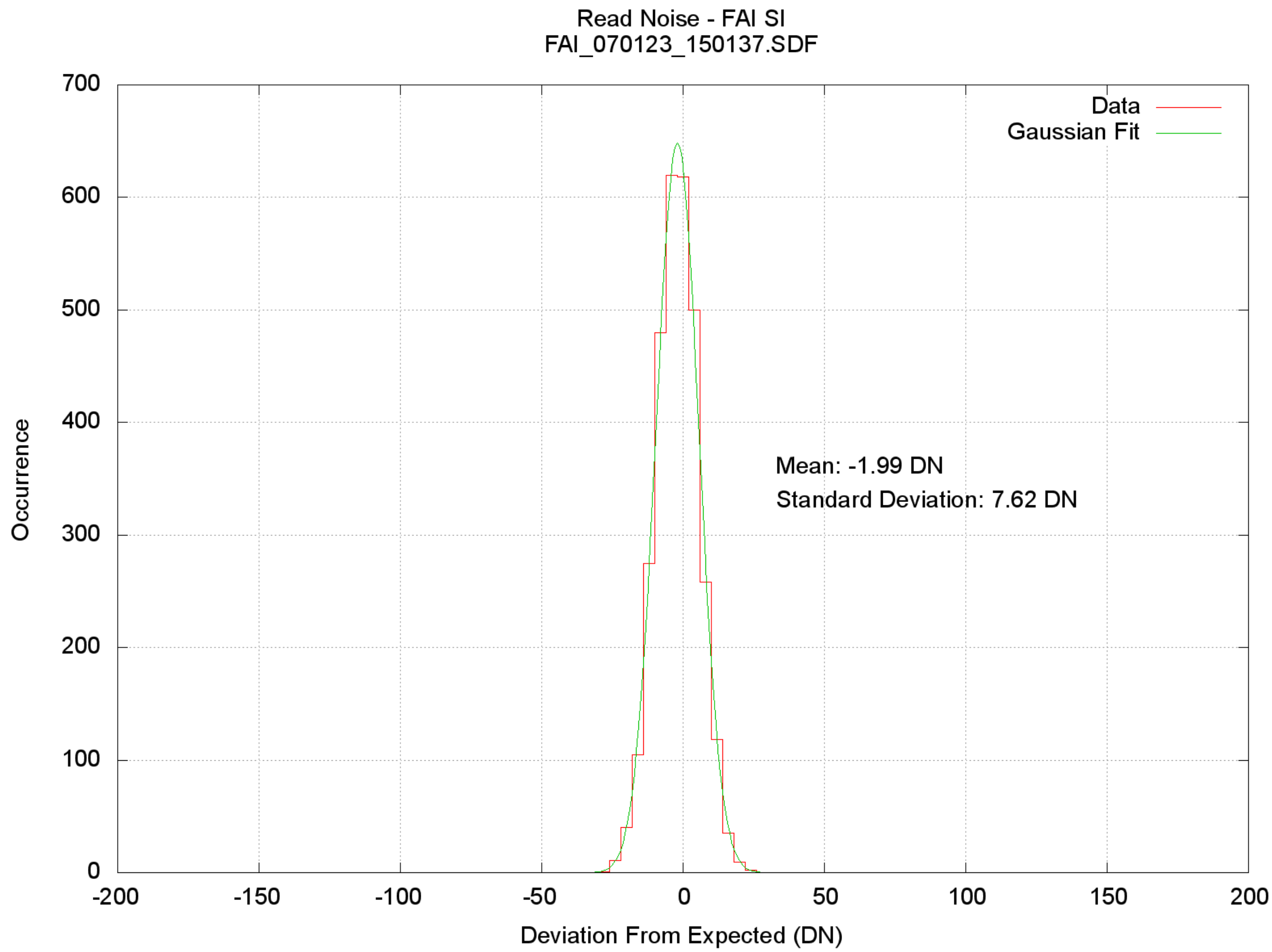
Read Noise - FAI SI
FAI_070123_150137.SDF
Data
Gaussian Fit
Mean: -1.99 DN
Standard Deviation: 7.62 DN
Occurrence
Deviation From Expected (DN)
0
100
200
300
400
500
600
700
-200
-150
-100
-50
0
50
100
150
200

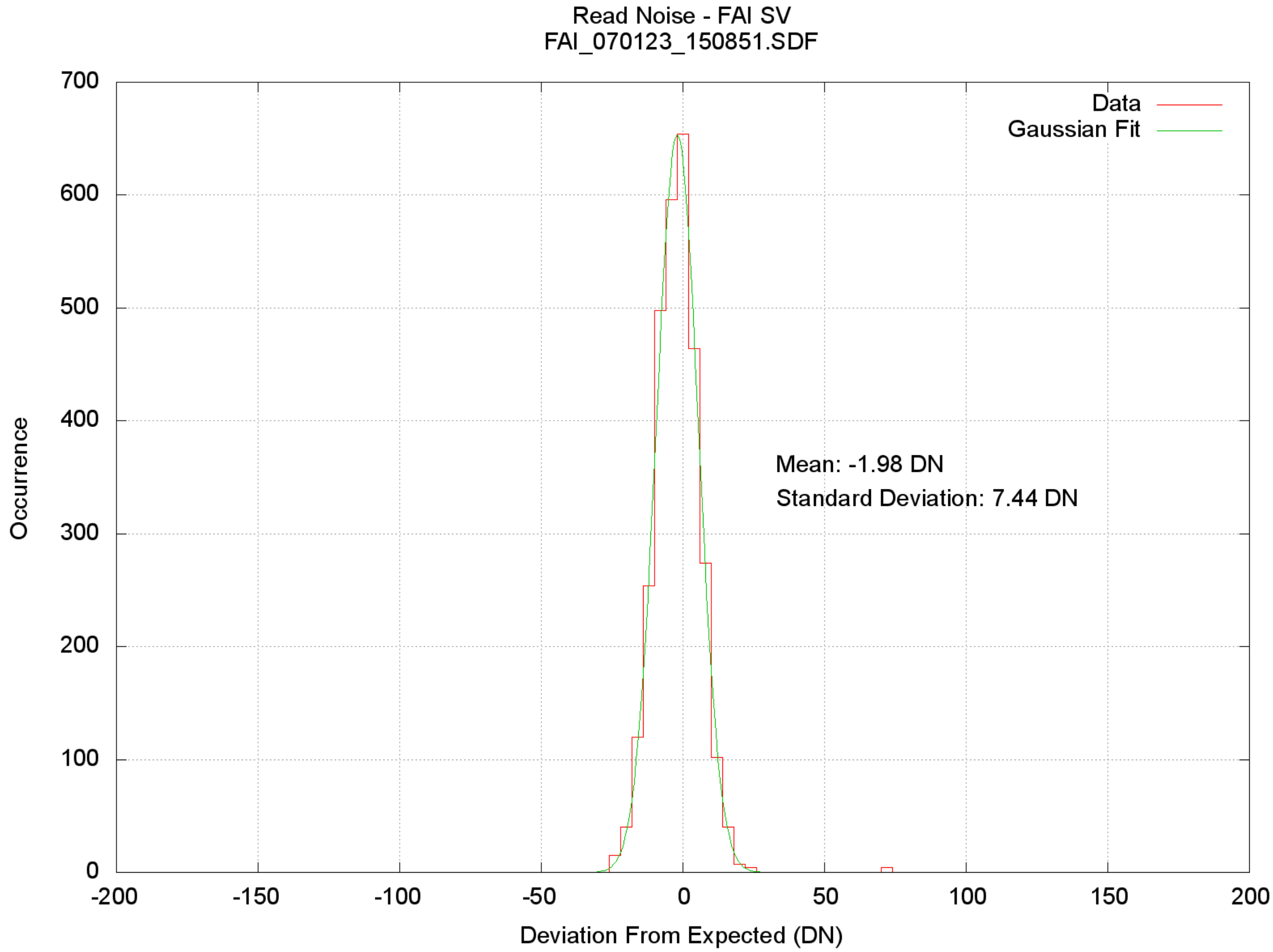

b. Offset tests

It was discovered during the course of the analysis that the measured electronic offset was not constant but varied with the signal level. Modifications to the instrument hardware and software greatly reduced the effect. Nevertheless, it is important to record the presence of a condition that causes a depression of the measured offset that increases with increasing signal. Fortunately, the effect is negligible for signal levels below about 20,000 DN as the figure below shows.

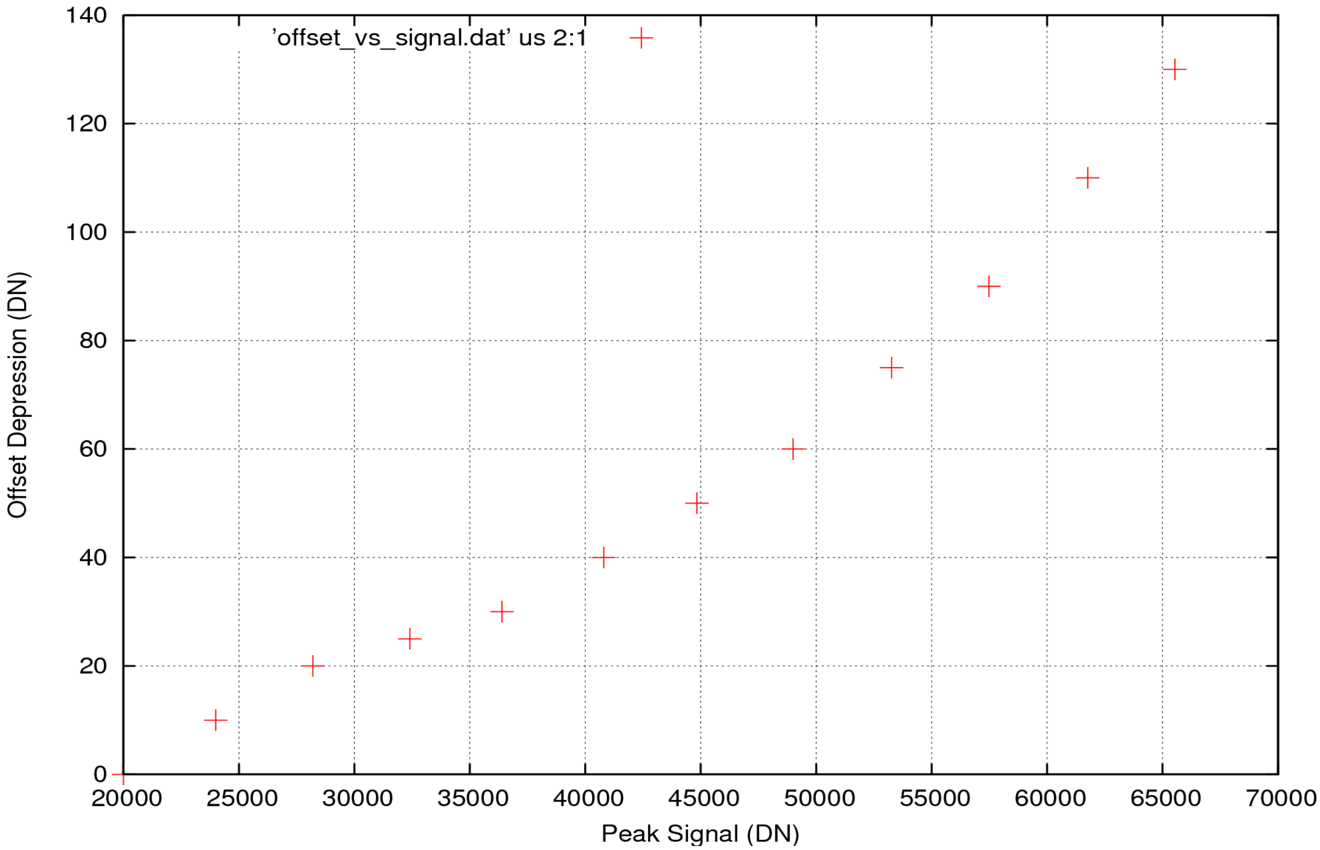

c. S/N calculations

The calculation of expected S/N can be estimated from either the responsivity based upon the parameters of the cameras, or the responsivity determined from the measurements of the calibrated integrating sphere intensities. Both methods must be considered approximate. The table below shows both the calculated and measured responsivity. The agreement is very good considering the uncertainties in some parameters such as the transmission of the optical systems. The calculated responsivity is used here.

Camera	Calculated Responsivity	Measured Responsivity
SI	.105 DN/R·s	0.0965 DN/R·s
SV	.097 DN/R·s	0.107 DN/R·s

The background for the calculated responsivity is set out in a document entitled "Background Material for ePOP-FAI Operations Planning", written in 2004 and revised in April 2005. It is included in this report as Appendix 2. The calculated S/N is based on the instrument parameters for the default operating modes, the measured dark current, and the estimated contribution from airglow (see Appendix 4 for the procedure used to estimate the NIR airglow contribution). The table below gives a summary of the input data.

Item	SI	SV
Read noise	7 DN/s	7 DN/s
Binning	1 x 1	2 x 2
Exposure	0.1s	0.5s
Airglow	18000 R	100 R
Dark Current at 5 º C	33 DN/s	68 DN/s
Dark Current at 15 º C	147 DN/s	247 DN/s
Responsivity (DN/s/pixel)	.0965	.107

The plots below show the calculated S/N for a range of emission intensities. For the SV camera, plots are shown for two CCD temperatures because the dark current noise is the primary limitation to the S/N. From the figure it can be seen that for a CCD temperature of 5 ºC a S/N of 3 is attainable for an OI 630 nm emission rate of about 225 R. The performance of the SV camera is strongly dependent on the CCD temperature.

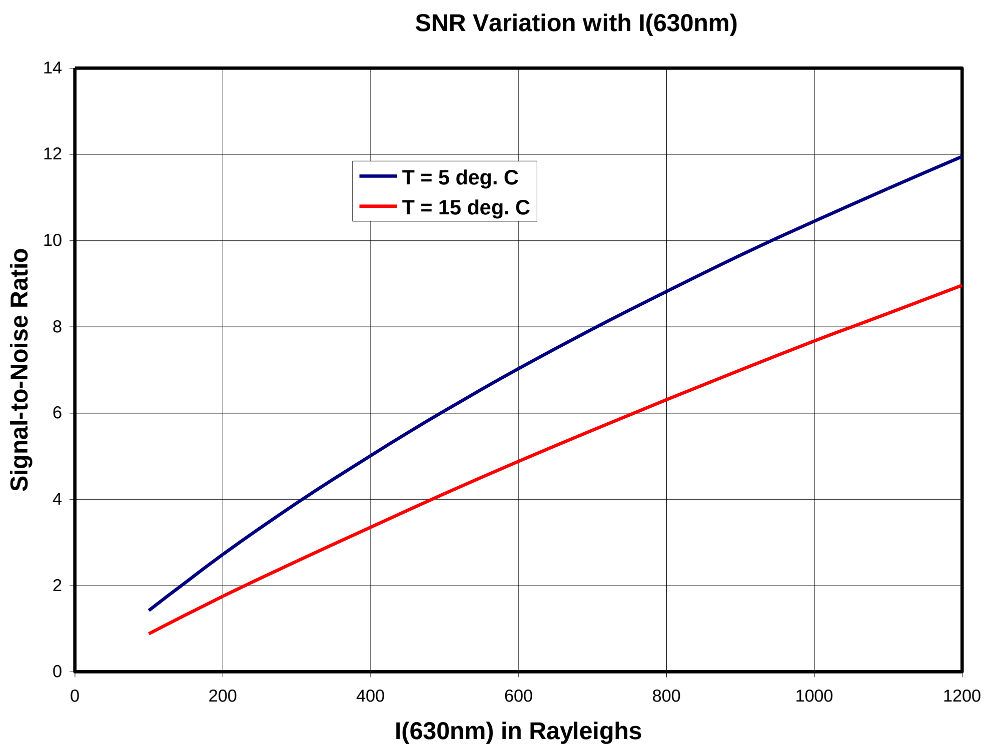

There are other ways to demonstrate the dependence of the S/N on the CCD temperature. The next figure shows the S/N at 2 intensities (150 R and 300 R) over a range of temperature. The measured dark current has been used for the calculations.
It is clear that the CCD temperature must be kept low for airglow observations.

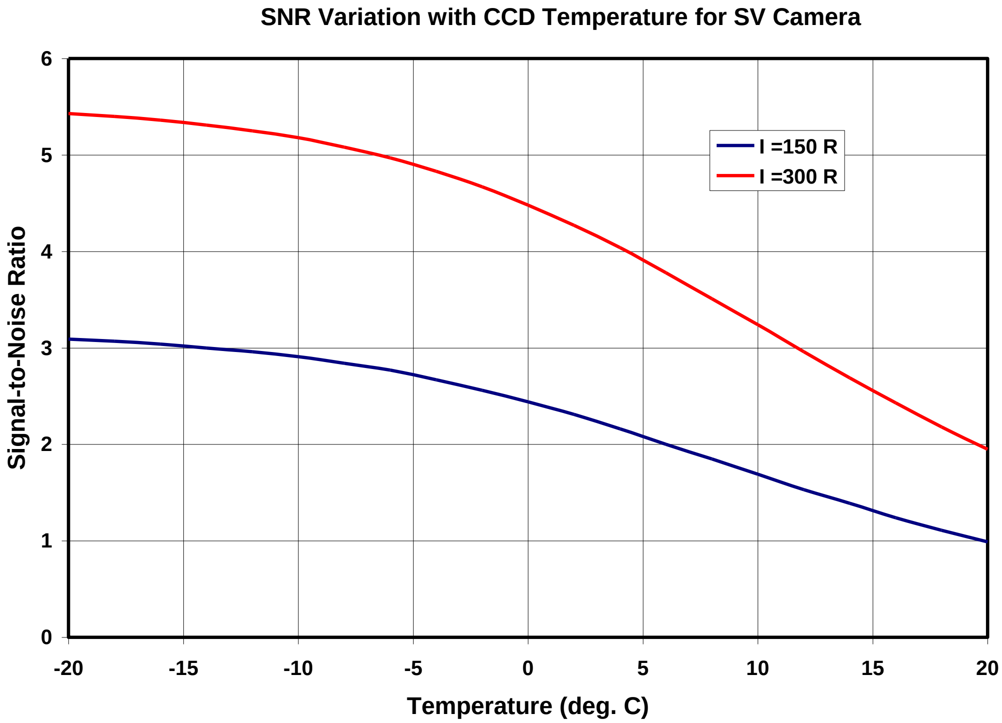

The next figure shows the required intensity level for S/N =3 as a function of the SV CCD temperature. For the SV camera, the read noise dominates at CCD temperatures below about 0 º C, and the dark current noise dominates for higher temperatures.

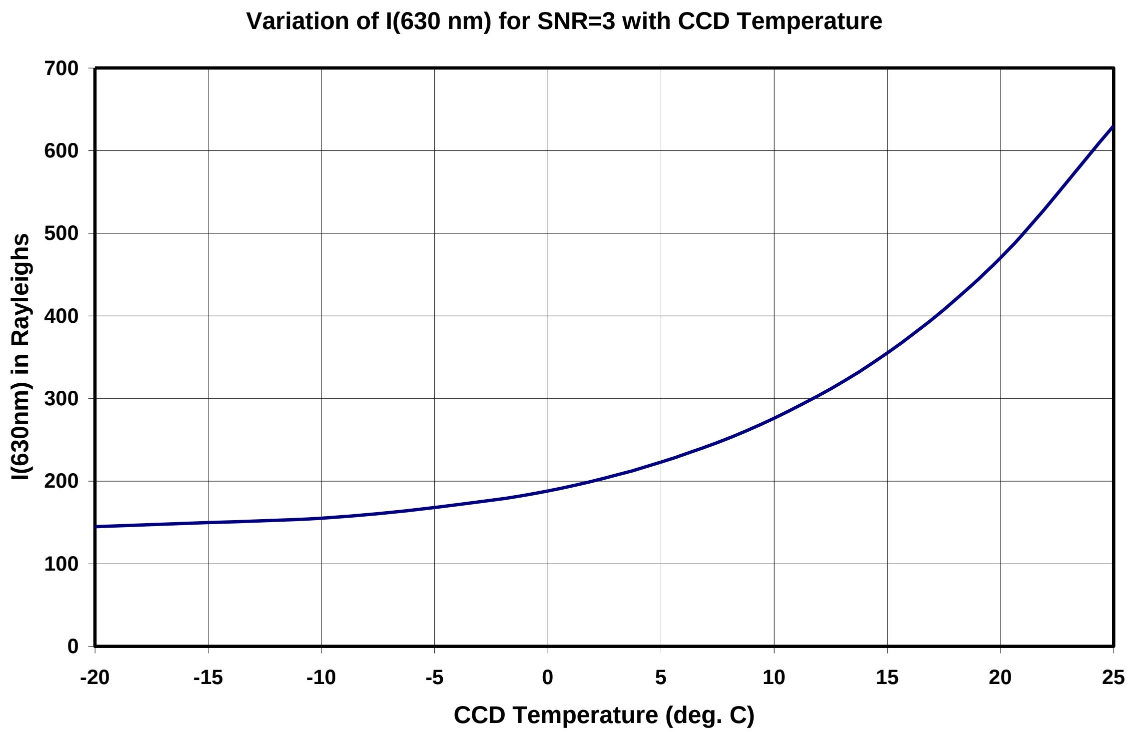

For the SI camera, the S/N is affected more by the NIR airglow than by the CCD temperature at all temperatures, so only one plot is shown below for the SI camera. The intensity scale refers to the equivalent auroral intensity of the OI 557 nm emission; the actual NIR intensity is about 23 times larger. The derivation of this factor for the SI camera is described in Appendix C. From the plot, using the default operating parameters, a S/N of 3 is achievable for an equivalent 557 nm intensity of about 250R.

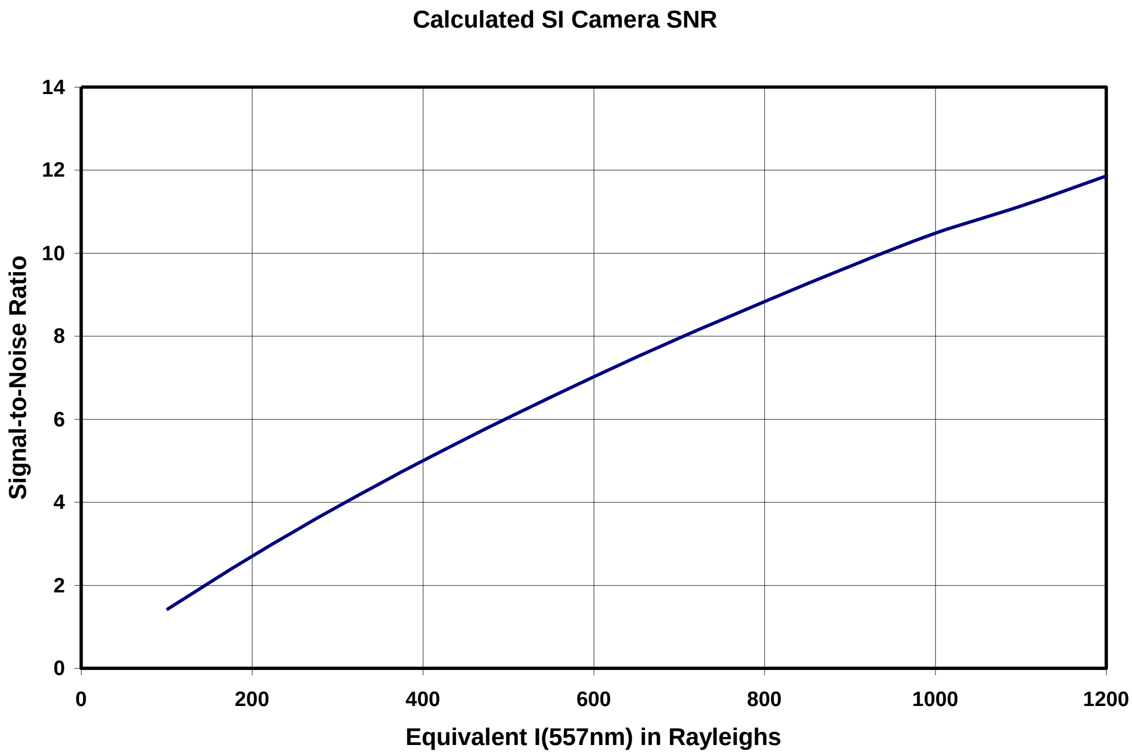

d. Photon transfer curves

Three images of a uniform light source were taken at various intensities (including dark current) for both cameras on January 10th and 12th at UNH. Two of three images at each intensity were used to generate a photon transfer curve using the method outlined in Chris Cully's University of Calgary Phys 603 report (see also Janesick, JR, et al., Charge-coupled device charge-collection efficiency and the photon transfer technique. Optical Engineering, 26 (10) pp. 972-980, October 1987). The 20x20 central area was extracted from each image and we plot signal vs. noise, where

$$Signal = \overline{X1_i} - \overline{D}$$

$$Noise = \sqrt{\frac{\sum [(X1_i - \overline{X1_i}) - (X2_i - \overline{X2_i})]^2}{2N_p}}$$

$X1_i$ is a pixel from the first image, $X2_i$ is a pixel from the second image, $\overline{D}$ is the average dark current from the 20x20 area, and N_p is the number of points (=400).

The results are as follows:

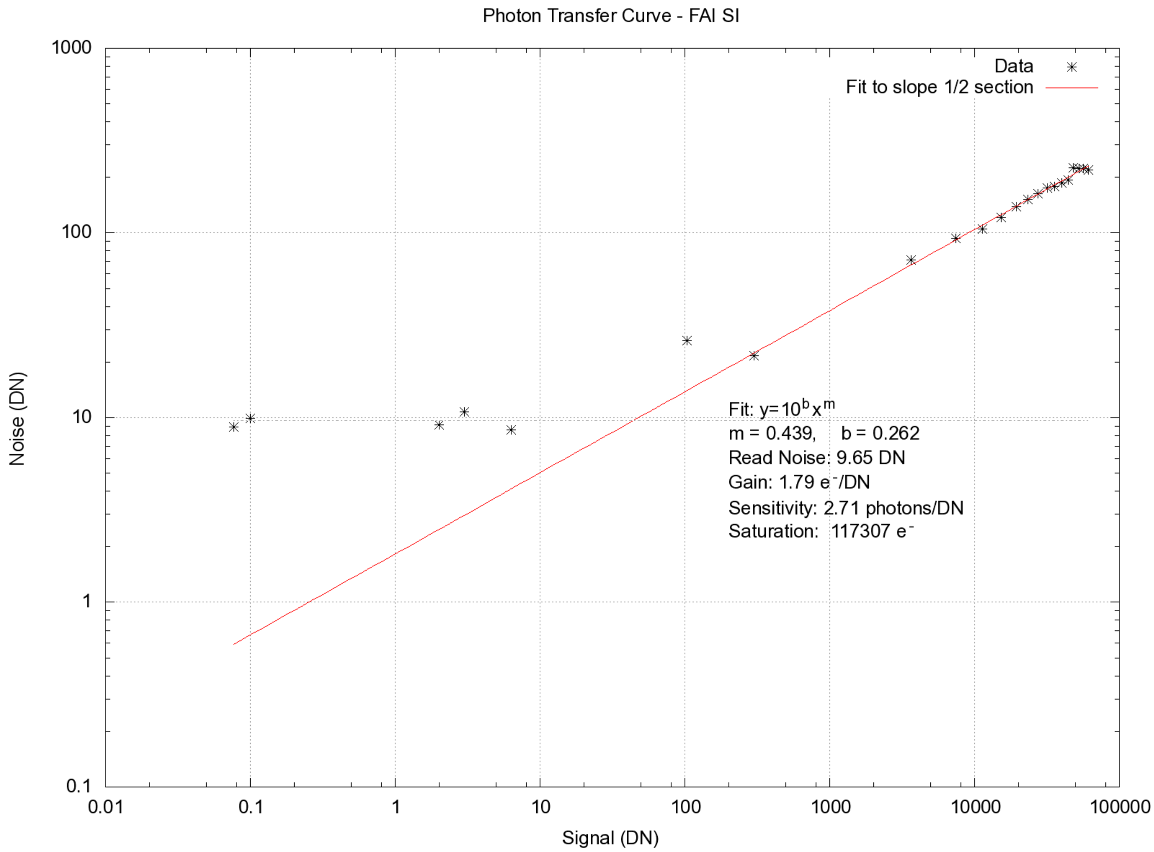
Photon Transfer Curve - FAI SI
Data
Fit to slope 1/2 section
Fit: y=10^b x^m
m = 0.439, b = 0.262
Read Noise: 9.65 DN
Gain: 1.79 e-/DN
Sensitivity: 2.71 photons/DN
Saturation: 117307 e-
Noise (DN)
Signal (DN)
1000
100
10
1
0.1
0.01
0.1
1
10
100
1000
10000
100000

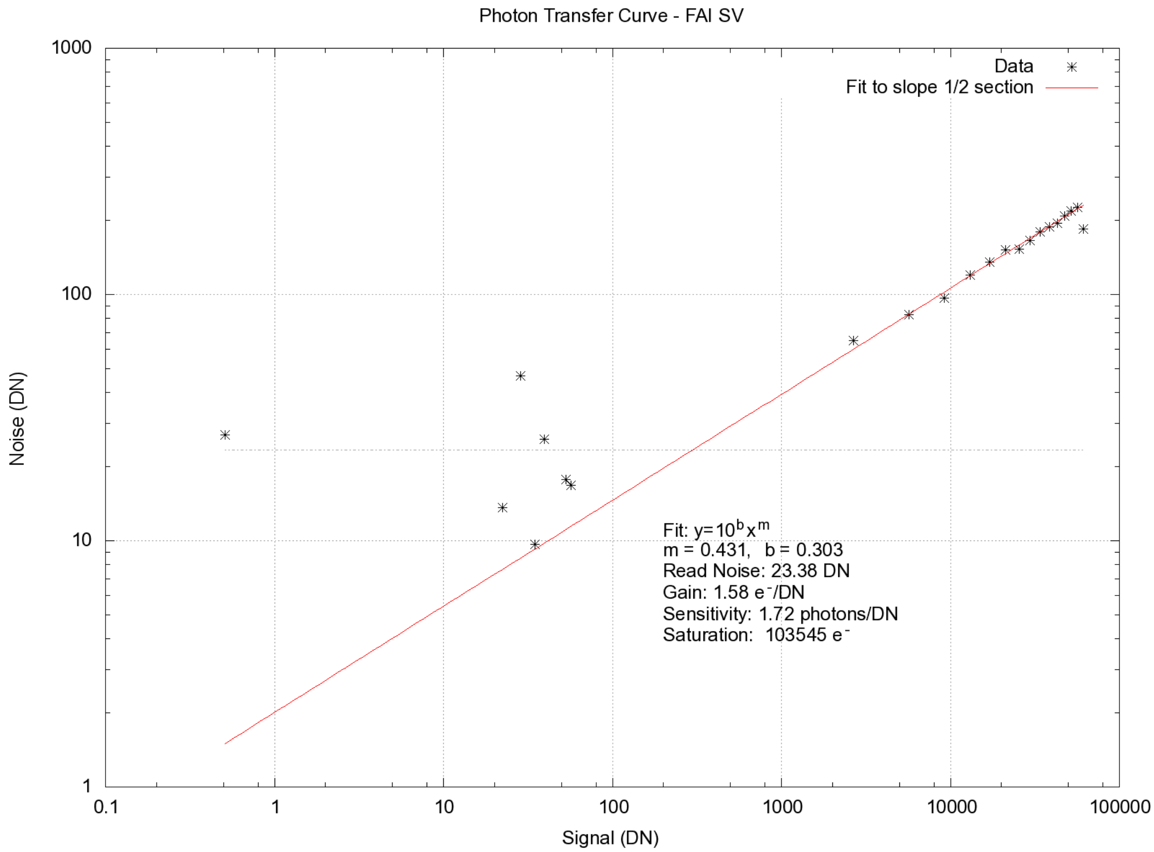

The fixed pattern noise was eliminated by subtracting the two frames, leaving only shot noise. Full saturation was not obtained for either camera, so the top portion of the curves is somewhat cutoff. A fit to the data (excluding the dark current points) showed a slope of 0.439 for SI and 0.431 for SV. The theoretical slope is 0.5. The gain is the signal value at the intersection of the best fit line with unity noise, and was found to be 1.79 e^-/DN for SI and 1.58 e^-/DN for SV. The read noise is the noise value found for the dark current images, and averages to 9.65 DN for SI and 23.4 DN for SV. The high value for the SV camera can be attributed to bit flips that occurred in the data due to a memory problem in FAI at the time of testing. The sensitivity is given by the gain divided by the quantum efficiency, and turns out to be 2.71 photons/DN for SI and 1.72 photons/DN for SV, assuming quantum efficiencies of 0.66 and 0.92 for SI and SV, respectively. The full well depth is the gain multiplied by 65535, corresponding to 117307 e^- for SI and 103545 e^- for SV.

10. Conversion from electrons to data numbers (DN)

The conversion from electrons to DN was set electronically by Burley Scientific to be between 1 and 2 electrons/DN. An accurate knowledge of this number is not of great importance when the absolute calibration is based on laboratory measurements of a light source in which case only the input photon flux and the output signal are necessary. However, it is of interest to be able to determine as many parameters as possible.

There are two ways to check the electron/DN conversion rate. The first method uses the photon transfer curve obtained from experimental data and the second method involves the comparison of dark current measurements with those provided by the CCD manufacturer. The photon transfer method (see the previous section) yields 1.79 electrons/DN for the SI camera and 1.58 electrons/DN for the SV camera. The table below shows the results of comparing the manufacturer's data sheet with the measured dark current at UNH and U of C. The dark current measurements are shown as an average per pixel over the CCD as well as an average per pixel for an area that is 20 by 20 pixels. The ratio of the manufacturer's measurements (in electrons/s/pixel) to the measurements at UNH and U of C (in units of DN/s/pixel) yields the number of electrons per DN for the camera. Although the average is about 1.7 electrons/DN, the large variation indicates that this is not a very reliable method.

CCD Dark Current at 20 degrees C

	Camera	Data Sheet (el/s)	UNH (DN/s)	U of C (DN/s)	el/DN UNH	el/DN U of C
CCD Average	SI	529	292	278	1.8	1.9
20 by 20 Average	SI	747	292	303	2.6	2.5
CCD Average	SV	498	496	473	1.0	1.1
20 by 20 Average	SV	780	483	474	1.6	1.6

Some improvement in accuracy is expected by comparing the entire curve of measured dark current vs. CCD temperature with the calculated variation given by the manufacturer in the form of an equation. The expression for the dark current variation with temperature is provided by e2v for the CCD67 AIMO device as

$$\mathbf{DC(T) = DC(293K) \bullet 1.14x10^{6} \bullet T^{3} \bullet e^{-9080/T}}$$

The following figure shows this curve for the SI camera along with the fit to the measured dark current. The calculations have been multiplied by 0.5 to obtain reasonable agreement. The reciprocal of this multiplier, i.e. 2.0 is the number of electrons per DN (i.e. the step size of the ADC in electrons). It is obvious from the figure that the shape of the manufacturer's curve is different from the measured variation for some reason, and this imposes considerable uncertainty in the electrons/DN obtained from overlaying the curves.

Of the two methods, the photon transfer function technique is likely the more reliable because it depends only on measured data. Fortunately, the number of electrons per DN is not needed in the data analysis.

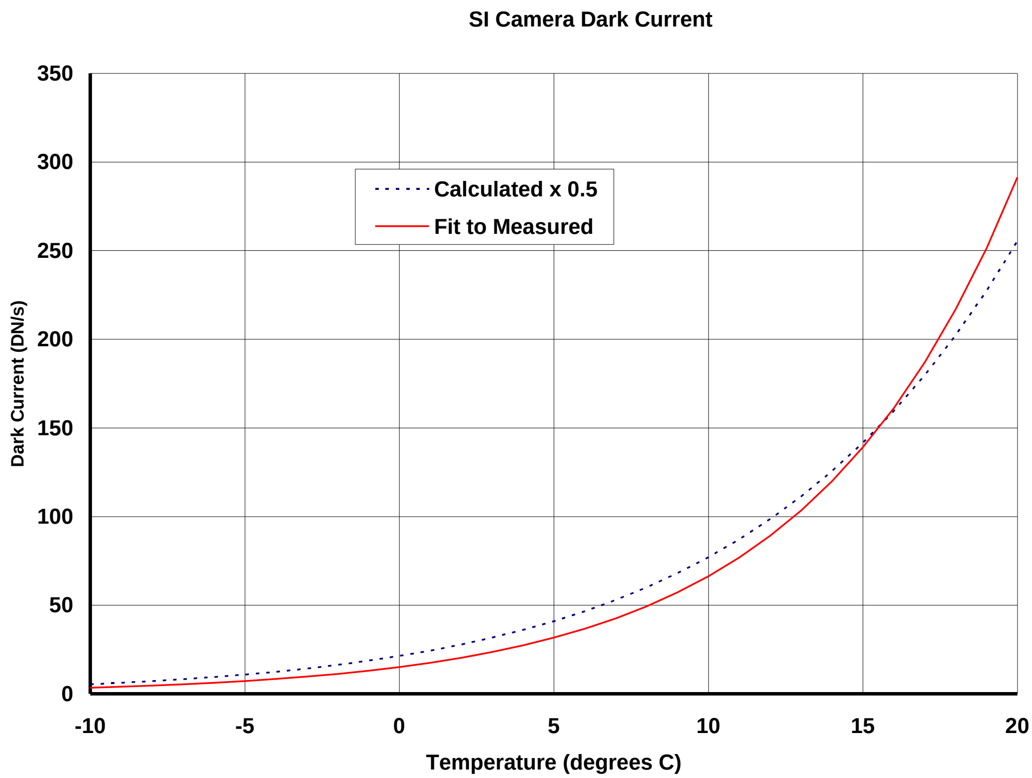

11. FAI Optical Filter Characteristics

a. SI Camera

The SI camera filter transmission versus wavelength is shown in the figure below. Between 630 and 680 nm the transmission increases rapidly from 0 to 90% and remains at 90% for longer wavelengths. The filter is a Schott glass filter, RG645 that is inherently very stable and reliable. The transmission characteristics were not checked independently: the curve shown below was provided by the manufacturer.

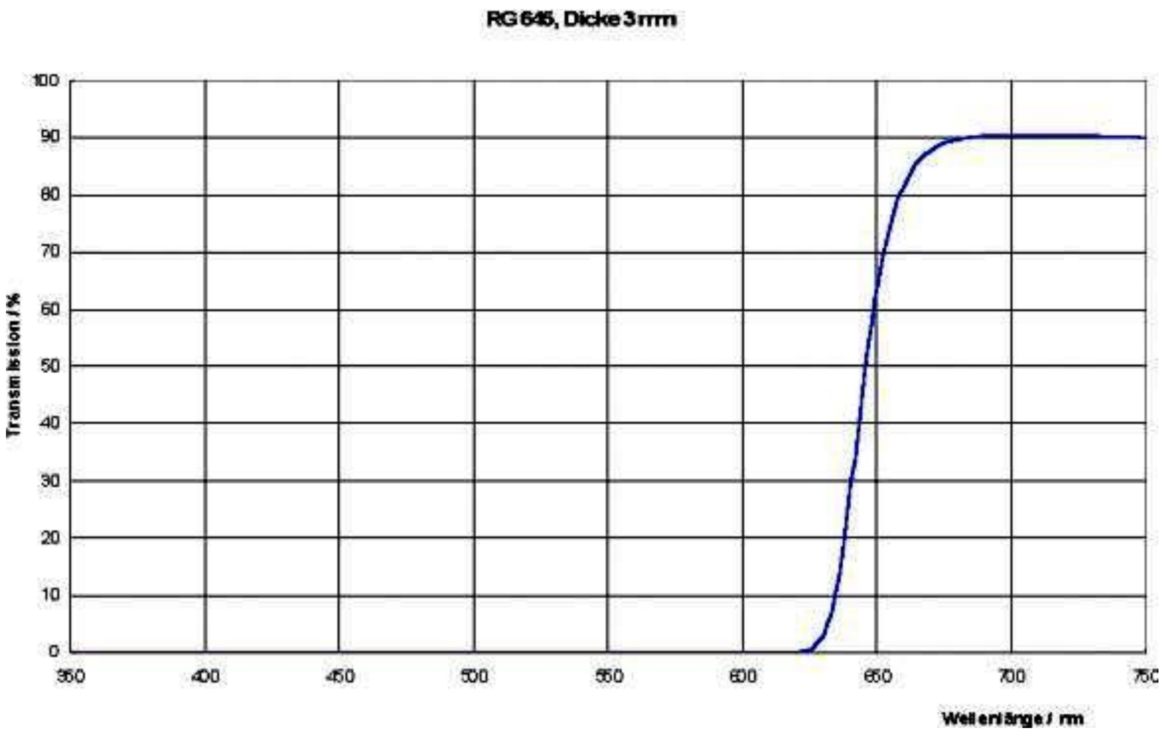

b. SV Camera

The SV bandpass filter was produced by Barr Associates. It is a special metal oxide filter with a 2.0 nm passband whose spectral position is relatively insensitive to variations in temperature. The manufacturer's measurement of the passband is shown below for a cone of incident light with a half-cone angle of 7 degrees corresponding to the f/4 speed of the optical system. The centre wavelength of the filter is at 630.7 nm. The OI 630 nm emission will be at the short-wavelength edge of the flat transmission peak.

In Section B.2.a it is shown that for calibration purposes the area under the transmission curve is the same as that of a rectangular filter of width 2.15 nm.

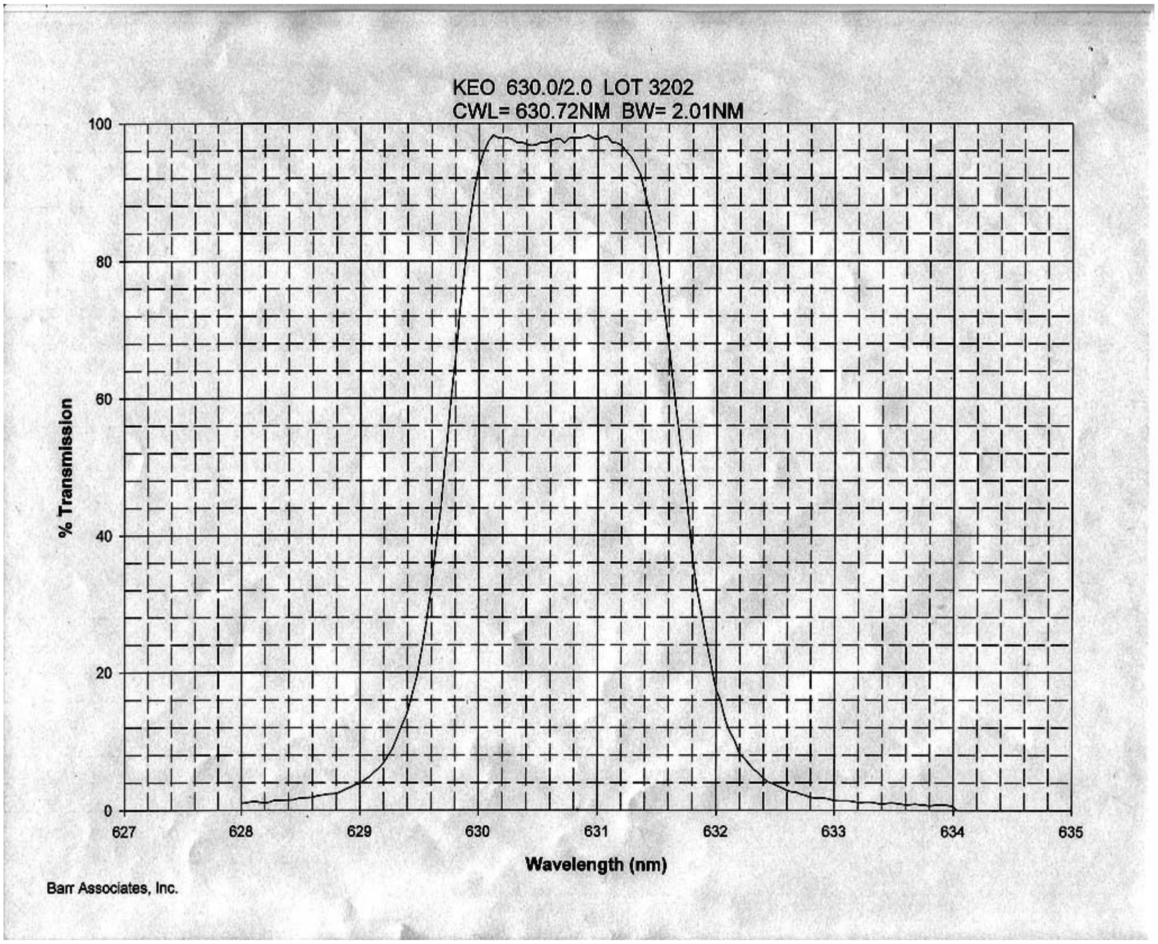

On December 17, 2007 the SV filter passband was checked at the University of Calgary at room temperature using a white light source and an Acton Research Corporation Spectra Pro 500 monochromator. The measurements were made with the SV camera using appropriate exposure times. Images were taken at 0.1 nm steps from 628 to 632 nm and at 0.2 nm steps across the wings of the filter passband. Some results are shown in the figure below. The slit width was too wide to provide the resolution necessary to measure the detailed shape, but the general characteristic of the filter was confirmed. In particular, it was verified from the long wavelength portion of the curves that the passband does not shift with location on the CCD.

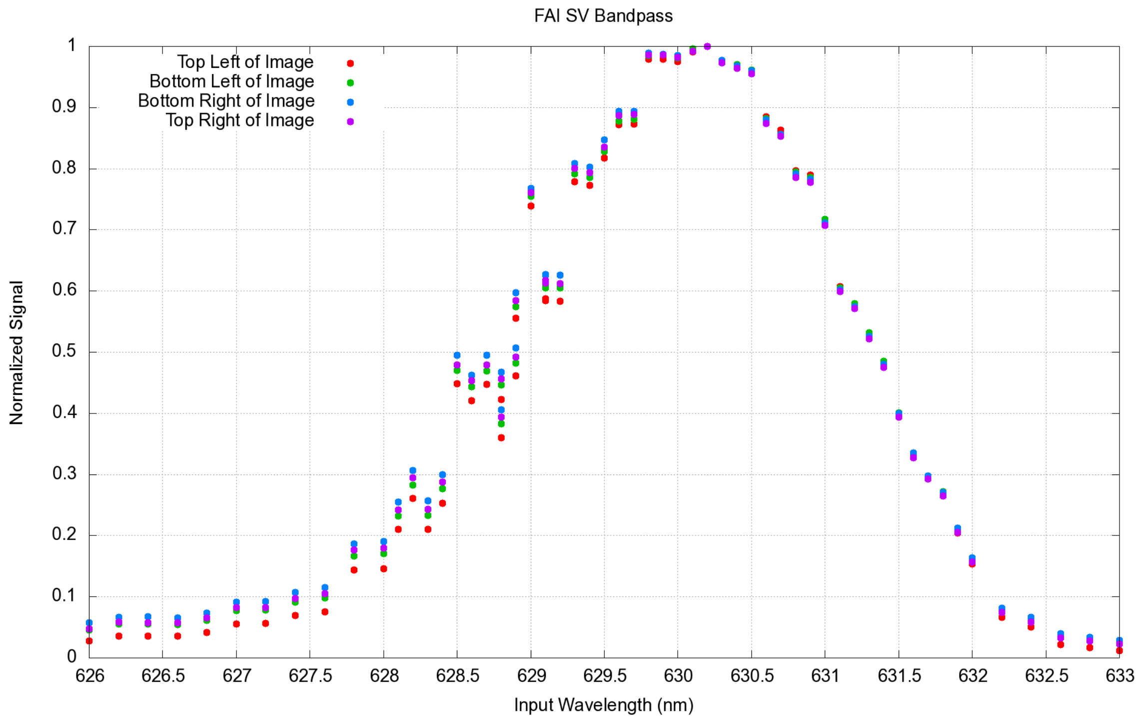

12. Parameter table

During the course of the FAI development there has been an effort to try to keep abreast of the basic instrument parameters. Numerous revisions have been made. Included here is the latest revision. It is unlikely that there will be further changes of a significant nature.

a. Instrument components

This table provides in one place a list of some of the important instrument parameters. Most of the information was provided by manufacturers and contractors but some is based on the characterization measurements. None of this information is expected to change now that the flight instrument fabrication and testing have been completed.

FAI Instrument Component Data Table

Category	Item	Parameter	Value	Source
Optics	Baffle	FOV	27.5 ^{o}	Routes
Optics	Baffle	Vanes	4	Routes
Optics	Lenses	Elements	7	Coastal Optical Design
Optics	Lenses	Focal Length	68.9 mm	Coastal Optical Design
Optics	Lenses	f-number	4.0	Coastal Optical Design
Optics	Lenses	Field of view	27 degrees (full)	Coastal Optical Design
Optics	Lenses	Image Size	33 mm diam.	Coastal Optical Design
Optics	Lenses	Transmission	0.8	Estimate (18 surfaces)
Optics	SI filter	Transmission	0.9 (λ>650 nm)	Schott RG645 3 mm
Optics	SV filter	Transmission	0.68 (λ=630.3 nm)	Barr (14^o cone)
Optics	SV filter	Half-width	2.0 nm	Barr (14^o cone)
Optics	Taper	Reduction	5:1	Schott Fiber Optics
Optics	Taper	Image circle	6.6 mm diam.	Coastal
Optics	Taper	Transmission	0.5	Estimated
CCD		Pixel size	26μm x 26μm	e2v CCD67
CCD	QE	SV band	0.92	e2v CCD67
CCD	QE	SI band	0.66 effective	Calculated (LLC)
CCD SI		Dark current	529e^-/s @ 293K	e2v spec sheet
CCD SV		Dark current	498e^-/s @ 293K	e2v spec sheet
CCD		Full well	600K electrons	e2v spec sheet
CCD		Readout	0.33 seconds	150 kHz (Burley)
CCD		Read noise	~10 electrons rms	Measured (Jan. 07)
CCD		Output	1.5μV/e^-	E2v CCD67
Electronics	ADC	Input	0 to 5.0 V	Burley Scientific
Electronics	ADC	Output	16 bits	Burley Scientific
Electronics	ADC	Conv. Time	1.2μs/pixel	Burley Scientific
Electronics	Conversion	SV	1.58 e^-/DN	Measured (Jan. 07)
Electronics	Conversion	SI	1.79 e^-/DN	Measured (Jan. 07)
General		Power	19W – 28W	FAI ICD
General		Mass	7.7 kg	Maximum from ICD
General		Telemetry	1.5 Mbits/s	FAI ICD

b. Requested Satellite Orbital Parameters

This table lists the expected orbital configuration. These numbers have been used to calculate some of the expected camera properties.

Basic Orbital Parameters

Period	103 min	Requested
Apogee	1500±50 km	Requested
Perigee	325±25 km	Requested
Inclination	80±10 degrees	Requested

c. Camera operations

The following table provides the selected default operational parameters. The calculated spatial characteristics listed are based on these parameters.

Preliminary Default Operational Parameters and Characteristics

Item	Camera	Value	Comment
Pixel binning	SV	2 by 2	Preliminary
Pixel binning	SI	1 by 1	Preliminary
Exposure time	SV	0.5s	Preliminary
Exposure time	SI	0.1s	Preliminary
Cycle time	SV	30 s	Preliminary
Cycle time	SI	1.0 s	Preliminary
Responsivity	SV	0.107 DN/R·s	Measured (Jan.07)
Responsivity	SI	0.0965 DN/R·s	Measured (Jan.07)
Camera FOV (angular)	Both	26 degrees	Measured (Jan. 07)
One Pixel FOV (angular)	Both	0.106 degrees	For 246 pixel image diam.
Pixel size from perigee	SV	0.4 km	For aurora at 220 km
Pixel size from perigee	SI	0.4 km	For aurora at 110 km
Pixel size from apogee	SV	4.7 km	For aurora at 220 km
Pixel size from apogee	SI	2.6 km	For aurora at 110 km
Image diam from perigee	SV	48 km	For aurora at 220 km
Image diam from perigee	SI	98 km	For aurora at 110 km
Image diam from apogee	SV	580 km	For aurora at 220 km
Image diam from apogee	SI	630 km	For aurora at 110 km
Intensity for S/N =3	SV	225R	For default parameters
Intensity for S/N = 3	SI	250R	Equiv. 557 nm value

13. Dynamic range

The dynamic range of the FAI cameras can be calculated from the measured or calculated responsivity and the 16-bit range of the A/D converter. The saturation level is then 65536 DN minus the sum of the electronic offset, dark current and airglow contributions. For the minimum useful signal it is a common practice to choose the signal (in DN/s) that corresponds to a S/N of 3. The dynamic range is then found by dividing the saturation level by this minimum useful signal. The following table shows the dynamic range and saturation level (in rayleighs) for the three operational modes. The calculations used the default exposure times of 0.1 and 0.5 s for SI and SV respectively. The numbers in brackets are the equivalent OI 557 nm auroral intensities.

Camera	Mode	I for SNR=3.	Saturation (R)	Dynamic Range
SV	1	750	1.14E+06	5095
SV	2	225	2.87E+05	1278
SV	3	100	7.16E+04	318
SI	1	5200 (226)	6.36E+06	1222
SI	2	2300 (100)	1.59E+06	306
SI	3	1070 (46)	3.97E+05	76

14. Unexplained Camera Behaviour

During the testing, characterization and calibration of FAI, we encountered some behaviour that we could not explain nor remove by changes to the hardware or software. These items are listed below along with the steps that were taken (if any) to compensate.

a. Non-linear calibration

The graphs of light intensity versus camera response are not linear as expected, but have a slight downward curvature. The calibration factor (R/DN/s) for each camera is not constant but varies with the slope of the calibration curve. Assuming a straight line rather than the curved line introduces a small error in the absolute calibration of the cameras. It is planned to use the varying calibration factor in the routine analysis of SV data.

b. Signal-dependent variation in angular response

The UNH calibrated integrating sphere was used to obtain the correction for the non-uniformity of response of the cameras across the CCDs. As described above, this was done for every pixel, expressed in relation to the value of 1.00 for the central area of the CCD. Although the resulting array of correction factors should be independent of the signal strength, upon closer inspection it was found that the correction factor increases with the signal level above about 20,000 DN. In practice, such large signals are not expected to be realized very often, but it was nevertheless decided to include the small adjustment for signal level in the routine data processing.

c. Unexpected variation in electronic offset measurement

It was earlier assumed that the electronic offset in the signal chain is a constant and therefore does not have to be monitored closely. However, it was found during the analysis of characterization data that the measured offset does indeed vary a small but significant amount relative to the readout noise. It is not independent of the binning mode, nor is it independent of the incoming light level. The offset variation was reduced but not eliminated by means of hardware changes.

It was decided that the prudent approach is to measure the offset for each image. This was achieved by enlarging the number of CCD columns being read out to include the 6 offset columns on each side of the image area. The technique that produced the best results was to find the average DN level of the last six offset columns that are read out. This technique was shown to be very reliable in practice and will be incorporated in the routine data processing.

d. Ramp-up of recorded signal in first few rows of CCD

There is a small ramp-up effect of a few DN for the first CCD rows that are being read out for each image. This occurs only for the SI camera, and after some investigation it became clear that the effect was linked to the flight cable between the camera and the Electronics Unit. Changes to the cable at Routes did not cure the problem, but it was decided not to have a new cable manufactured unless the ramp-up effect becomes serious.

e. Comparison of CCDs

There are surprising differences in the performance of the two CCDs. The SV CCD was selected for that camera because it was reported by the manufacturer to have lower dark current than the other two, but measurements have shown that the SV CCD has about 1.6 times more dark current than the SI CCD. The SV camera has also consistently not performed as well as the SI camera during tests of readout noise, optical resolution, etc. Why the SV CCD and indeed the SV camera appear to have inferior performance characteristics is not understood.

f. Halo effect

There is a slight mismatch between the physical size of the optical taper and the size of the circle of light on the optical taper due to the field of view of the camera. This can be seen as a weak circle of light in the CCD images likely due to a small amount of light that is scattered in the fibres. This small halo effect is not expected to adversely affect the performance of the cameras.

Acknowledgement

The characterization of the Fast Auroral Imager was possible only because many individuals provided the necessary assistance in a timely and professional manner. The instrument was not developed in the conventional way in which a prime contractor assumes all the responsibility for all phases of the development and testing. In our case, which involved a number of organizations, a high degree of cooperation and good will was required (and received) in addition to technical excellence. The principal organizations involved were Routes AstroEngineering, Burley Scientific, the University of New Hampshire, and the University of Calgary. A partial list of individuals who made a significant contribution to the testing phase includes the following:

Burley Scientific: Greg Burley
Routes AstroEngineering: Blair Gordon, Don Asquin, Paul Marchand, Danny Ng
UNH: Marc Lessard, Brent Sadler, Phillip Fernandez, Sarah Jones
UofC: Greg Enno, Bob Hum, Peter King

C. Appendices

1. Predicted FAI-SI Response to Aurora

A. Introduction

Until now a comprehensive investigation of the expected response of the FAI-SI camera has not been undertaken. There are two parts to this investigation. The first task is the calculation of the number of CCD electrons that are produced per second as a consequence of the distribution of auroral emissions in the spectral region 650 nm to 1100 nm. This requires knowledge of the optical system, the filter transmission, the quantum efficiency of the CCD as a function of wavelength and other characteristics of the selected CCD. The second part involves the assessment of the contribution to the CCD signal from the airglow background emissions that are also distributed throughout the SI passband. The results from this study provide necessary information about the expected signal-to-noise ratio, dynamic range and saturation levels. I have used a convenient auroral reference for this assessment: 1 kR of OI 557.7 nm that is known as IBCI aurora. It should be pointed out that there will be iterations to these calculations whenever updated information is available such as instrument parameters and emission intensities. For that reason I have used linked Excel Worksheets for the calculations.

B. The instrument

Here is the input information that has been used in the calculations:

Camera f-number: 0.8
Transmission of the lens system: 0.8
Transmission of the fibre optic taper: 0.5
Pixel size: 26 µm x 26 µm
Read noise: 10 electrons rms
Single pixel mode
Exposure: 1.0 second
Filter: Schott Glass RG645, 3 mm thick, with transmission 0.9 (650-1100 nm)
Quantum efficiency of CCD: e2v CCD67 AIMO BI for Basic Midband Coated CCD
Dark signal: 164 electrons/pixel/second at $0^{o}C$

C. The aurora

My prime source was the book Aurora by Alister Vallance Jones. He tabulated emission rates for the primary auroral bands in the 650-1100 nm spectral region: N_2 First Positive, O_2 Atmospheric, O_2^+ First Negative and the Meinel N_2^+. As given, they are calculated for an IBCIII aurora. For calculation efficiency I binned the auroral intensities into 50 nm bins from 650 nm to 1100 nm (9 bins) and selected the appropriate quantum efficiency at the estimated ‘centre of mass’ of the emissions in the bin for each band.

D. The airglow

The literature provides a range of emission rates for the OH Meinel and O_2 Atmospheric bands in the nightglow. The O_2 Atmospheric Band is not observed from the ground due to self-absorption; however it is bright when viewed from above the atmosphere. It varies a great deal with location, time and dynamic influences such as tides and gravity waves. From the HRDI experiment on the UARS satellite the zenith brightness was found to vary from 2 kR to 12 kR with a mean value of about 6 kR (Yee et al. JGR Vol. 102, pp.19,949-19,968, 1997). This is also the value obtained by Wallace and Hunten (JGR, Vol. 73, p. 4813, 1968) deduced from observations of the O_2 (0,1) band.

The OH bands have been measured by many people and show a large variation. For the first estimation I have used a recent set of observations made in Russia by Bakanas (Physics of Auroral Phenomena, Proc. XXV Annual Seminar, Polar Geophysical Institute, Apatity, 2002). Another common reference is to the observations of OH band intensities by Krassovsky et al. (Planet. Space Sci, Vol. 9, p. 883, 1962). The latter intensities are generally higher than those of Bakanas. The OH band intensities calculated by Llewellyn et al. (Planet. Sp. Sc. Vol. 26, pp. 525-531, 1978) agree quite well with the observations of Bakanas at shorter wavelengths but are higher at longer wavelengths.

In addition to the OH and O_2 emissions there is a continuum that contributes about 1 R/Å up to about 800 nm.

The dominant feature of the night airglow as viewed from space is the (0,0) Atmospheric Band of O_2.

E. Summary of Results

1. Aurora

The following table is for a 1 second exposure in the single pixel mode. The emission rates are given for a 1 kR OI 557.7 nm emission rate. The effective quantum efficiency for a band is defined as Q.E. (effective) $=\Sigma(\text{Emission Rate}_i \times \text{Q.E.}_{.i})/\Sigma(\text{Emission Rate}_i)$ where the subscript refers to each 50 nm interval.

Band	Emission Rate (kR)	Electrons/sec	Effective Q.E.
N_2 1st Positive	6.70	830	0.52
O_2 Atmospheric	13.0	2399	0.78
O_2^+ 1st Negative	0.064	12	0.81
N_2^+ Meinel	3.86	452	0.49
Total	23.6	3693	0.66

In a sentence, 1 kR of OI 557.7 nm auroral emission is equivalent to 23.6 kR auroral emission in the 650-1100 nm spectral region and results in a CCD signal of 3693 electrons/second.

2. Airglow

Total airglow in the spectral region 650-1100 nm: 18.0 kR
O2(0,0) band 4000 R
O2(0,1) band 500 R
OH (650-1000 nm) 12000 R
Continuum (10R/nm from 650 to 800 nm) 1500 R
Estimated total = 18000 R

CCD signal produced by airglow: 1670 electrons/sec

3. Signal-to-Noise Ratio

Based on the above the SNR can be estimated as follows:

SNR= Auroral signal/SQRT(auroral signal + dark signal + airglow + read noise^2)

The following table shows the expected signal and SNR for a range of OI 557.7 nm auroral emission rates.

I(557.7 nm)	**300R**	**500R**	**1 kR**	**5 kR**	**10 kR**	**100kR**
Exposure	0.1 sec	0.1 sec	0.1 sec	0.1 sec	0.1 sec	0.1 sec
Pixels	1	1	1	1	1	1
Electrons (aurora)	111	185	369	1847	3693	36934
Electrons (airglow)	167	167	167	167	167	167
SNR	5.4	8.3	14.2	39.8	58.4	191.4

F. Discussion of Results

1. The auroral emission rate multiplier between OI 557.7 nm and auroral emissions in the spectral range 650-1100 nm is about 23. We can expect a good SNR for IBCI aurora even with an exposure of 0.1 sec. The requirement for the SNR to be >3.0 for an exposure of 0.1 second and an auroral emission rate of 1 kR is easily met if this refers to the equivalence of 1 kR of OI 557.7 nm

2. All the auroral emissions except the O_2 Atmospheric Band come from allowed states and therefore will be prompt. The Einstein transition probability for the O^2 Atmospheric Band is about 0.083 s^{-1} so has a radiative lifetime of about 12 seconds. The effective lifetime is somewhat reduced by the effect of quenching by O_2 (rough estimate, 8 seconds). The consequence of this will be a degree of delay in the response of this band to precipitating electrons. Rapid temporal fluctuations may be more difficult to study than would be the case with all prompt emissions.

March 29, 2005; revised Feb. 26, 2007

2. Background Material for ePOP-FAI Operations Planning

A. Introduction

The purpose of this memo is to provide some calculations that will hopefully be of assistance when planning the science experiments and the operational modes for the Fast Auroral Imager (FAI) on the ePOP satellite. I have used whatever material I could find, but the calculations should still be considered as rather rough estimates. The PDR material produced by Greg Burley and Trond Trondsen were the basis of most of the original choices. Revisions have been made as updated information has become available.

The two cameras are quite different in their application. The FAI-SV camera will be used primarily to measure rather weak 630 nm auroral and airglow emissions of the atomic oxygen. Rapid sampling is not important because the effective lifetime of the excited $O(^1D)$ atom is of the order of 60 s in the upper atmosphere. The FAI-SI camera will image the prompt auroral emissions from molecular species and there is considerable interest in both high temporal and spatial resolution. Viewing the same auroral feature many times during the satellite pass will provide information about the temporal and spatial variation.

In what follows, each camera will be treated separately. What is common is the basic method of calculating the expected signal in data numbers (DN) given the range of emission rates in rayleighs (R), and that will be covered first.

B. Sensitivity Calculations

1. Calculation of irradiance per rayleigh at the CCD:

Irradiance = Em. Rate(R) x 10^{10} x Ω x $\tau/4\pi$ where τ is the optical transmission to the CCD and Ω is the solid angle subtended by a single pixel. The solid angle is defined as the area of the exit aperture, A, divided by the square of the focal length, F. The ratio of $A/F^2 = \pi d^2/4F^2 = \pi/4f^2$ where f is the f-number of the optics. Combining,

Irradiance per rayleigh = 10^{10} x $\tau/16f^2$ photons/m^2 sec

2. Calculation of the signal at the output of the CCD:

Signal/R = Irradiance per rayleigh x QE x A

QE is the quantum efficiency of the CCD at the wavelength of interest, and A is the area of a single pixel in units of m^2. This gives the output in units of electrons/R·second·pixel. This is the calculated **sensitivity** of the CCD for a single pixel. It is the basic signal parameter for the instrument.

For n pixels per superpixel and an exposure time T, the calculated responsivity at the CCD is

Signal/R = Sensitivity for a single pixel x n x T (units of electrons per rayleigh)

The signal electrons are converted to a voltage at the output stage of the CCD. The conversion factor **C** is 1.5μV/electron for the CCD67. The responsivity of the CCD can then be expressed as an output voltage:

CCD Output Voltage/rayleigh = sensitivity for a single pixel x n x T x C

3. The gain of the analog signal chain

The purpose of the analog amplifier is to match the output range of the CCD to the input range of the A/D converter. For the CCD67 the peak signal is given as 600K electrons which corresponds to about C x 600K = 0.9V.

If the input range of the A/D converter is 0 to 5 V, an analog gain **G** of 4.5 is appropriate to match the two ranges. This would result in a conversion factor of 10 electrons/DN.

4. Digital output

The voltage signal at the input of the A/D converter is just the signal at the output of the CCD times the gain G of the analog electronics. At the output of the A/D converter the signal equals the input signal divided by the voltage per DN, i.e. the fixed step size.

The fixed step size can be conveniently chosen to correspond to the readout noise of the CCD. In the case of the CCD67 the readout noise varies from 4 electrons rms at a readout frequency of 20 kHz to 12 electrons rms at a readout frequency of 1MHz. If 10 electrons is used as a typical number, then the readout noise voltage is 10 x C = 15μV which at the input of the A/D converter is G times larger, i.e. 0.07 mV. If this is the step size then 65536 steps (16 bits) correspond to about 5 V at the input of the converter.

The quantity of scientific interest is the number of rayleighs per DN per second. The inverse of this is calculated by multiplying the CCD output (in electrons/rayleigh·sec) by the analog amplifier gain and dividing by the step size (in electrons/DN):

DN/rayleigh·sec = Output of the CCD per rayleigh·sec x G /stepsize

Another way to think about the instrument is to ignore the readout noise and just consider the conversion constant electrons/DN. For example, if 1 electron/DN is chosen, then the maximum output (65536 DN) corresponds to 65536 CCD electrons and the electronic gain is chosen to provide this. In this case it would be about 50. The readout noise of 10 electrons rms would give about 10 DN. For 5 electrons/DN the CCD limit is about 370K electrons corresponding to the saturation of the A/D converter, and the electronic gain is about 10.

The responsivity (in DN/rayleigh·sec) then becomes:

Responsivity = Output of the CCD per rayleigh•sec x stepsize (DN/e^-)

5. The dynamic range

The dynamic range of the CCD can be specified as the peak signal divided by the readout noise when the dark current is negligible. For the case of the CCD67 the dynamic range is therefore about 600K electrons/10 electrons = 60,000. This matches very well the dynamic range of a 16-bit A/D converter for a conversion constant (step size) of 1 electron/DN.

The measurement range of the auroral signal can be estimated using the readout-noise-rayleigh equivalent i.e. the number of rayleighs that correspond to the readout noise. This number varies with the exposure and the number of pixels in a superpixel. For a system in which the readout noise is less than the dark current and/or the background photon noise, the dynamic range is reduced from that calculated from the readout noise alone.

C. Application to FAI-SV

This camera is designed for low light level applications. The 16 bit A/D converter permits a large dynamic range (about 65,000 steps) so it is possible to cover a large range in emission rate. The default repetition rate for images is one per minute.

Relevant data:

- QE of CCD at 630nm = 0.8 (CCD67) (estimated from curve provided by e2v)
- Area of one pixel, A = 26μm x 26μm (CCD67)
- Read noise = 10 electrons rms (not measured)
- Peak signal = 600,000 electrons (single pixel)
- CCD output conversion = 1.5μV/electron
- Transmission, $\tau = \tau_{optics} \times \tau_{taper} \times \tau_{filter}$ = 0.8 x 0.5 x 0.6 = 0.24 (estimated for now)
- f-number of optical system = 0.8 (estimated)
- Choose the step size = 1 DN/electron
- Dark current at 293K = 1000 electrons/second. Dark current at temperature T (in Kelvin) is given by the following expression (from e2v for CCD57 AIMO):

Dark current at temperature T = $122T^3\exp(-6400/T)$ x Dark current at 293K

The variables that remain are the exposure time T and the number of pixels in one superpixel.

The CCD output signal = 0.13 electrons/rayleigh·second·pixel. For exposure T and n pixels per superpixel due to on-chip binning, the total output signal is

Total CCD output signal = 0.13 x T x n (in units of electrons per rayleigh)

Output of the A/D converter in DN/R = 0.13 x T x n x stepsize

Below is a table of some combinations of T and n.

Num. of pixels	Array size	Exposure	CCD electrons/R	DN/R	DN/100R	DN/10kR
4 (2 x 2)	128 x 128	0.5	0.26	0.26	26	2,600
16 (4 x 4)	64 x 64	1.0	2.1	2.1	210	21,000
1	256 x 256	0.5	0.065	.065	6.5	650

Notes regarding this table:

1. The default mode identified in the PDR documentation is the first row. This is suitable for normal operations that require reasonable sensitivity for airglow and weak aurora along with a spatial resolution that matches the image smear due to the satellite motion when the satellite is in nadir mode. The bandwidth requirements are also relatively modest. The sensitivity threshold will likely be determined by the dark current. The dynamic range is limited by the range of the 16-bit A/D converter which corresponds to a photon input rate of about 260 kR.

2. The 4 x 4 binning mode would be used for observations of very weak aurora and airglow. One example is artificial heating experiments of the ionosphere over Alaska and Puerto Rico that are of interest to ePOP experimenters. Other examples are polar patches, detached arcs equatorward of the main auroral oval, sun-aligned arcs and equatorial airglow.

3. The single pixel mode would be useful for observing bright aurora in the oval especially during times of large magnetic disturbances.

4. The single-pixel operation will be useful when the camera is pointed to the star field for test purposes. The satellite should be in an inertial pointing mode for these tests.

5. The above table has been constructed with the data available about the instrument. As tests and characterization proceed it will be important to compile a characterization data base for FAI so that updates and refinements can be made to capability predictions.

6. The repetition rate is not included in this table. The default frame rate is two image per minute.

7. We shall need to be able to change operating parameters in orbit in order to optimize the camera performance relative to a scientific/measurement objective. Some lead time for such commands will obviously be instituted.

Signal-to-Noise Ratio for FAI-SV

The S/N for the FAI-SV camera can be calculated from the expression

$$\frac{S}{N} = \frac{s}{\sqrt{s + d + r^2}}$$ where s is the signal, d is the dark current and r is the read noise

If r is negligible (requires verification) then the dark current is the critical noise component. According to the CCD67 specifications, a dark current of 1000 electrons per second at +20°C degrees is typical for the AIMO version. At a more reasonable temperature like 0^{o}C or -10^{o}C the dark current will be much less. For example, in the default mode of 128 x 128 and 0.5s exposure, for 100R at +20°C the S/N is <1 at the output of the CCD, but for a low temperature the S/N is >1. For typical auroral emission rates of about 1 kR, the S/N is >10 for a CCD temperature less than 0^oC.

It should be noted that if there is non-OI (630nm) emission present, such as scattered light, then the above simple equation is incomplete because the total signal will then have a background and an emission component.

D. Application to FAI-SI

This camera is designed to measure prompt auroral emissions. The emissions cover a large range of wavelengths because the filter blocks short wavelength light but permits long wavelength light (650 nm to 1100 nm)) to be imaged. Before parameters can be finalized, an estimate of the expected total emission rate should be made for various levels of auroral activity. There is also a significant level of airglow emission from OH and O_2 (about 18 kR) that will add an unwanted background component. For now, for purposes of illustration, it is assumed that the aurora will cover the range 0 to 1 megarayleigh (MR).

The default frame rate for images is 1 per second. This allows a single point to be observed 60 times over a period of one minute with the satellite in nadir pointing orientation. Whether this rate can be met depends on the time required to read out the CCD and transmit the image to the DHU over the RS 4.22 serial link. The quality of such images will depend on the auroral brightness at the time of observations.

Input data that differ from that of FAI-SV:

- QE of CCD = 0.66. This value was obtained by calculating the expected signal for the real auroral distribution using the QE curve provided by e2v. Details of the calculation can be found in the document entitled Predicted FAI-SI Response to Aurora.
- Transmission $\tau = \tau_{lens} \times \tau_{taper} \times \tau_{filter} = 0.8 \times 0.5 \times 0.9 = 0.36$ (estimated)
- Choose the stepsize = 1 DN/e^-

The variables that remain are the exposure time T and the number of pixels in one superpixel.

The CCD sensitivity for one pixel = .16 electrons/rayleigh·second·pixel. For exposure T and n pixels per superpixel due to on-chip binning, the output signal per rayleigh = 0 .16 x T x n (in units of electrons per rayleigh)

Output of the A/D converter in DN/R =0 .16 x T x n x stepsize

Below is a table of some combinations of T and n:

Num. of pixels	Array size	Exposure	CCD elec/R	DN/R	DN/kR	DN/MR
1	256 x 256	0.1	0.016	0.016	16	16000
1	256 x 256	0.2	0.032	0.032	32	32000

4(2 x 2)	128 x 128	0.1	0.064	.064	64	64000

Notes:

1. This table refers to auroral emission into the SI passband. The first row is the default settings given in the PDR documentation. At 1 DN per electron, the read noise is about 10 DN which for the default settings is equivalent to about 60 R. The capacity limit of a CCD pixel is 65000 DN/stepsize = 65K electrons. The dynamic range is determined by the airglow: 65K/(18 kR x 16 e^-/kR) ≅ 220.

2. The repetition rate of 1 image per second may not always be achievable because of readout time and telemetry constraints (see below).

3. The third row is a possible mode when the aurora is expected to be weak and a high spatial resolution is not required.

4. The single pixel mode can be used to image the star field during operations.

5. It will be necessary to have a method for changing the parameters during the mission; for example lookup tables that can be modified.

Signal-to-Noise Ratio for FAI-SI

The S/N can be calculated in a similar way as for the visible camera but with the addition of the airglow background signal. It is obvious that the SNR is very low at an auroral emission of 1 kR because the background airglow is about 18 kR. When the auroral emission rate is 1 kR, the expected emission rate of OI 557.7 nm is only about 50R. For IBCI aurora the OI 557.7 nm emission rate is 1 kR and the auroral emission rate in the SI band is about 20 times that (20kR). At 20 kR the SNR is about 14 (see following table) for a 0.1 s exposure in a single pixel. The only reasonable way to interpret the specification of SNR>3 for 1 kR at an exposure of 0.1 s in a single pixel is that the 1 kR refers to the equivalence of 1 kR of auroral emission from the OI 557.7 nm line.

The following table shows the expected signal and SNR for a range of OI 557.7 nm auroral emission rates. Here 1 kR of OI 557.7 nm auroral emission is equivalent to 23.6 kR of auroral emission in the band 650 nm to 1100 nm. The details of this calculation are provided in the document entitled Predicted FAI-SI Response to Aurora.

I(557.7 nm)	300R	500R	1 kR	5 kR	10 kR	100kR
Exposure	0.1 sec	0.1 sec	0.1 sec	0.1 sec	0.1 sec	0.1 sec
Pixels	1	1	1	1	1	1
Electrons (aurora)	111	185	369	1847	3693	36934
Electrons (airglow)	193	193	193	193	193	193
SNR	5.4	8.3	14.2	39.8	58.4	191.4

The above SNR calculations are valid for electrons and for data numbers (DN) if 1 electron equals 1 DN. For the case of 1.7 electrons per DN, the SNR is reduced to about 70% of the table value. (Note added June 26, 2008)

E. Collection of General Questions and Comments

1. How much electronic noise will be produced by the signal chain? Correspondence from Burley Scientific predicts about 1.5 DN. This will be negligible.

2. The cameras will certainly not be operated all the time. Is it realistic to consider “banking” telemetry allocation by being off for some orbits or partial orbits, and then have periods when the FAI telemetry allocation can be very high? Telemetry questions like this should be addressed before detailed operations planning is undertaken. The telemetry allocated to FAI is 1.5 Mbits/second in normal operation. The SI camera alone will require about 1.2 Mbits/s at the default settings.

3. With a 16 bit A/D converter that is sufficient to cover the expected optical input range and with 16 bit data words, compression of data is not necessary.

4. Will there be times when only one camera is operated? Yes: this is allowed for.

5. Although the expected signal-to-noise ratio for a single superpixel as calculated here is helpful when thinking about the design, there are many other factors that will become important to the success of the mission. Most auroral targets have a significant spatial extent which allows for pattern recognition either by machine or by eye even when the statistics for a single pixel are poor. It should also be emphasized that there will be other noise sources to contend with such as background atmosphere radiation, scattered sunlight, ground and cloud albedo, telemetry noise etc.

F. Notes on Experiment Modes

Although imagers are usually regarded as monitoring instruments, the unique features of the SI and SV cameras will open up many possibilities for specific experiments. Here is a sample list of what general types of operations can be anticipated.

a. Both cameras

Observations of auroral substorm phenomena (basic)
Pointing mode: nadir viewing over the high latitude region (>40° lat)
Camera mode: default

Observations of auroral substorm phenomena (special)
Pointing mode: nadir viewing over the high latitude region (>40°lat)
Camera mode: SI in high resolution mode

Observations of polar phenomena
Pointing mode: nadir viewing over the polar regions (>60°lat)
Camera mode: SI in high sensitivity mode; SV in default mode

Altitude distribution of aurora
Pointing mode: horizon viewing
Camera mode: longer exposure is possible without image smear

Extended viewing over a ground location
Pointing mode: slew to target above a ground location for extended viewing
Camera mode: default mode for normal aurora
Note that this mode can also be used during perigee observations of aurora.

Star field viewing for testing/characterization
Pointing mode: inertial pointing at astronomical region
Camera mode: Ideally, single pixel mode

b. FAI-SV only

Observation of polar phenomena
Pointing mode: nadir viewing
Camera mode: depends on target: patches, arcs, polar boundary

Observation of low-latitude phenomena
Pointing mode: nadir viewing
Camera mode: default and possibly reduced resolution configuration to increase the sensitivity to airglow

Extended viewing over a ground location
Pointing mode: slew to target
Camera mode: depends on target: HF heating, equatorial anomaly etc.
Note that this mode can also be used for auroral observations from perigee.

Altitude profile of atomic oxygen emission
Pointing mode: horizon viewing
Camera mode: long exposure time (1.0 seconds or longer) with little binning

G. Disclaimer

The above material was prepared in April 2005 to assist with the process of preparing for the operational phase of ePOP. It is not meant to be in any way used as an authoritative document, but rather an assortment of (hopefully) useful ideas. The included information is all subject to change as design, testing and characterization proceed. There are also obvious gaps in information at present; and there may be misleading oversimplification and even unintentional errors.

April 6, 2005

3. Auroral Tables (650-1100 nm) and CCD Quantum Efficiency

The following charts provide the details of the auroral intensity distribution in the wavelength range 650-1100 nm that form the basis for the calculation of the effective quantum efficiency (QE) for the e2v CCD67. The values of QE were taken from the manufacturer's literature for a typical device. Appendix 1 uses the results presented in these Excel worksheets.

Tau=Tau(lens)xTau(Taper)xTau(filter)=0.8x0.5xTau(filter)
Exposure 0.1 sec
Pixels 1

N2 First Positive Band

Interval (nm)	650-700	700-750	750-800	800-850	850-900	900-950	950-1000	1000-105(	1050-1100
Em. Rate (in R)	669	346	1719	49	2182	238	401	86	1009
Tau(filter)	0.9	0.9	0.9	0.9	0.9	0.9	0.9	0.9	0.9
Tau	0.36	0.36	0.36	0.36	0.36	0.36	0.36	0.36	0.36
Q.E.	0.88	0.81	0.77	0.57	0.46	0.29	0.22	0.1	0.1
Conversion	0.209	0.193	0.183	0.135	0.109	0.069	0.052	0.0238	0.0238
Signal	13.99	6.66	31.46	0.66	23.85	1.64	2.10	0.20	2.40

Tot. Signa 82.97 electrons
Total Int. 6699.00 Rayleighs for 1 kR OI 557.7 nm
Effective quantum efficiency = 0.52 for this band

O_2 Atmospheric Band

Interval (nm)	650-700	700-750	750-800	800-850	850-900	900-950	950-1000	1000-105(	1050-1100
Em. Rate (in R)	42	123	12084	53	649	35	14	7	3
Tau(filter)	0.9	0.9	0.9	0.9	0.9	0.9	0.9	0.9	0.9
Tau	0.36	0.36	0.36	0.36	0.36	0.36	0.36	0.36	0.36
Q.E.	0.87	0.84	0.79	0.65	0.55	0.43	0.15	0.1	0.1
Conversion	0.207	0.200	0.188	0.154	0.131	0.102	0.036	0.024	0.024
Signal	0.87	2.46	226.88	0.82	8.48	0.36	0.05	0.02	0.01

Tot. Signa 239.93 electrons
Tot. Int. 13010.00 Rayleighs for 1 kR OI 557.7 nm
Effective quantum efficiency = 0.78 for this band

First Negative O_2^+ Band

Interval (nm)	650-700	700-750	750-800	800-850	850-900	900-950	950-1000	1000-105(	1050-1100
Em. Rate (in R)	28	18	10	5	2	1	0	0	0
Tau(filter)	0.9	0.9	0.9	0.9	0.9	0.9	0.9	0.9	0.9
Tau	0.36	0.36	0.36	0.36	0.36	0.36	0.36	0.36	0.36
Q.E.	0.88	0.83	0.75	0.64	0.5	0.32	0.15	0.1	0.1
Conversion	0.209	0.197	0.178	0.152	0.119	0.076	0.036	0.024	0.024
Signal	0.59	0.36	0.18	0.08	0.02	0.01	0.00	0.00	0.00

Tot. Signa 1.23 electrons
Tot. Int. 64.00 Rayleighs for 1 kR OI 557.7 nm
Effective quantum efficiency 0.81 for this band

Exposure 0.1 sec
Pixels 1

N_2^+ Meinel Band

Interval (nm)	650-700	700-750	750-800	800-850	850-900	900-950	950-1000	1000-1050	1050-1100
Em. Rate (in R)	153	177	661	499	34	2225	100	4	2
Tau(filter)	0.9	0.9	0.9	0.9	0.9	0.9	0.9	0.9	0.9
Tau	0.36	0.36	0.36	0.36	0.36	0.36	0.36	0.36	0.36
Q.E.	0.88	0.87	0.75	0.68	0.65	0.33	0.22	0.15	0.03
Conversion	0.209	0.207	0.178	0.162	0.154	0.078	0.052	0.036	0.007
Signal	3.20	3.66	11.78	8.06	0.53	17.45	0.52	0.01	0.00

Tot. Signal 45.22 electrons
Total Int. 3855.00 Rayleighs for 1 kR OI 557.7 nm
Effective quantum efficiency = 0.49 for this band

Total auroral emission rate for 1 kR of OI 557.7 nm = 23628.00 Rayleighs of 650-1100 nm emission
Total signal for 1 kR of OI 557.7 nm = 369.34 electrons
Overall effective Q.E. = 0.66 (for aurora only)

4. Effect of Airglow Contribution to the SI Camera Signal

Airglow in the 650-1100 nm spectral region is referred to in Appendix 1 as well as in the discussion of the expected signal-to-noise ratio for aurora. The two main sources of airglow in this region are Atmospheric Band of O_2 and the various bands of OH. The table below provides the intensities used to determine the expected signal from the airglow. In addition, there is a continuum contribution of about 10 R/nm up to about 800 nm, making the total airglow about 18 kR. Airglow is highly variable so the results here are meant only as a rough estimate of what can be expected. The effective quantum efficiency for the airglow contribution is about .39.

Tau=Tau(lens)xTau(Taper)xTau(filter)=0.8x0.5xTau(filter)

Exposure	0.1 sec
Pixels	1

Band	OH(7,2)	OH(8,3)	OH(4,0)	OH(9,4)	OH(5,1)	OH(6,2)	OH(7,3)	OH(8,4)	OH(3,0)	OH(9,5)	OH(4,1)	O2(0,0)	O2(0,1)	Sum
Wavelength (nm)	686.7	728	752.8	775	791.4	835	883	937.8	979.5	995.9	1018.9	761.9	865	
Em. Rate (in R)	120	360	180	470	300	680	880	590	1140	3220	3740	4000	500	18000
Tau(filter)	0.9	0.9	0.9	0.9	0.9	0.9	0.9	0.9	0.9	0.9	0.9	0.9	0.9	0.9
Tau	0.36	0.36	0.36	0.36	0.36	0.36	0.36	0.36	0.36	0.36	0.36	0.36	0.36	0.36
Q.E.	0.87	0.83	0.8	0.75	0.71	0.62	0.46	0.3	0.18	0.15	0.12	0.78	0.53	0.39
Conversion	0.207	0.197	0.190	0.178	0.169	0.147	0.109	0.0713	0.0428	0.0356	0.0285	0.185	0.126	0.093
Signal	2.48	7.10	3.42	8.38	5.06	10.02	9.62	4.21	4.88	11.48	10.67	74.15	6.30	166.83

Total OH	77.31
Total O2	80.45
Tot. Signa	157.76

1 kR of OI 557.7 nm is equivalent to 3240 electrons per second in the SI band
SNR=Auroral signal/SQRT(Auroral signal + Dark signal+Background+Read noise^2)
For 1kR OI 557.7 and CCD at 0C, SNR= 13.3
Total airglow background in R = 16180

I (557.7 nm)	300 R	500R	1 kR	5 kR	10kR	100kR	200R
Electrons (SI band)	97.2	162	324	1620	3240	32400	64.8
Background	157.8	157.8	157.8	157.8	157.8	157.8	157.8
S/N	5.05	7.76	13.3	37.2	54.7	179.2	3.52

Em x QE	104.4	298.8	144	352.5	213	421.6	404.8	177	205.2	483	448.8	3120

Sum (Em x QE)/Sum Em 0.393888

5. Test Sheets from CCD Manufacturer

Spare CCD

e2v technologies

Waterhouse Lane, Chelmsford, Essex CM1 2QU United Kingdom
Telephone: +44 (0) 1245 493493 Facsimile: +44 (0) 1245 492492
Internet: www.e2vtechnologies.com

TITLE: CCD67-00 SLOWSCAN TEST SHEET	10920F
Version: BACK ILLUMINATED (Basic Process), AIMO	Issue 1 (Draft) Sheet 1 of 1

Associated Document:

Device serial number	02272-10-35	Tester (Initials & Clock No.)	Emma
Grade	1	Date	20/3/05
Test data disc number	Disc I	Device Type Number	CCD67-00-*-C97

TEST RESULTS

TEST			RESULT	LIMITS Grade 0	Grade 1	Grade 2	UNITS
GAIN (Amplifier Responsivity)		OSL	1.56	1.0 min., 2.0 max.			μV/e⁻
		OSR	1.59	1.0 min., 2.0 max.			μV/e⁻
NOISE		OSL	4.9	6.0 max.			rms e⁻
		OSR	5.0	6.0 max.			rms e⁻
DEFECTS IN DARKNESS	BRIGHT COLUMNS		0	0	0	1 max.	n/a
	POINT DEFECTS		0	10 max.	20 max.	30 max.	n/a
PHOTO-RESPONSE DEFECTS	TOTAL COLUMNS		0	0	2 max.	8 max.	n/a
	DARK POINT DEFECTS		0	10 max.	20 max.	40 max.	n/a
	TRAPS		0	1 max.	2 max.	5 max.	n/a
MEAN DARK SIGNAL			866	1700 max. at +20°C			e⁻/pix/s
AREA DARK SIGNAL (20 x 20 block)			1293	3400 max. at +20°C			e⁻/pix/s
DNSU (1σ)			152	500 max. at +20°C			e⁻/pix/s

TEST		RESULT	LIMITS for Device Variant -C97 (Mid band)	UNITS
QUANTUM EFFICIENCY	at 350 nm	15.2	10 min.	%
	at 400 nm	41.8	40 min.	%
	at 500 nm	85.8	85 min.	%
	at 650 nm	93.9	85 min.	%
	at 900 nm	37.8	30 min.	%
PHOTO-RESPONSE NON-UNIFORMITY	at 400 nm	1.8	3.0 max.	%
	at 650 nm	1.7	3.0 max.	%
	at 900 nm	1.3	5.0 max.	%

Note (1): minimum separation of adjacent black columns to be 50 pixels

CUSTOM TESTS (if applicable)

OPERATING CONDITIONS

VOLTAGE	VALUE	MIN.	MAX.	UNITS	TEMPERATURE	VALUE	UNITS
VRD	18	15	19	V	For dark signal measurement	0	°C
VSS	7.9	8	11	V			
VOD	29	27	32	V	For Photo-response measurements	-20	°C
Vlφ (high)	12	10	15	V			

NOTES

Results before fitment of fibre optic

SI Camera CCD

e2v technologies

Waterhouse Lane, Chelmsford, Essex CM1 2QU United Kingdom
Telephone: +44 (0) 1245 493493 Facsimile: +44 (0) 1245 492492
Internet: www.e2vtechnologies.com

TITLE: CCD67-00 SLOWSCAN TEST SHEET	10920F
Version: BACK ILLUMINATED (Basic Process), AIMO	Issue 1 (Draft) Sheet 1 of 1

Associated Document:

Device serial number	02272-10-31	Tester (Initials & Clock No.)	Emmc
Grade	1	Date	20/3/05
Test data disc number	Disc I	Device Type Number	CCD67-00-*-C97

TEST RESULTS

TEST			RESULT	LIMITS			UNITS
				Grade 0	Grade 1	Grade 2	
GAIN (Amplifier Responsivity)		OSL	1.52	1.0 min., 2.0 max.			μV/e⁻
		OSR	1.56	1.0 min., 2.0 max.			μV/e⁻
NOISE		OSL	4.8	6.0 max.			rms e⁻
		OSR	5.0	6.0 max.			rms e⁻
DEFECTS IN DARKNESS	BRIGHT COLUMNS		0	0	0	1 max.	n/a
	POINT DEFECTS		0	10 max.	20 max.	30 max.	n/a
PHOTO-RESPONSE DEFECTS	TOTAL COLUMNS		0	0	2 max.	8 max.	n/a
	DARK POINT DEFECTS		0	10 max.	20 max.	40 max.	n/a
	TRAPS		1	1 max.	2 max.	5 max.	n/a
MEAN DARK SIGNAL			529	1700 max. at +20°C			e⁻/pix/s
AREA DARK SIGNAL (20 x 20 block)			747	3400 max. at +20°C			e⁻/pix/s
DNSU (1σ)			114	500 max. at +20°C			e⁻/pix/s

TEST		RESULT	LIMITS for Device Variant -C97 (Mid band)	UNITS
QUANTUM EFFICIENCY	at 350 nm	17.4	10 min.	%
	at 400 nm	42.1	40 min.	%
	at 500 nm	86.5	85 min.	%
	at 650 nm	94.1	85 min.	%
	at 900 nm	38.9	30 min.	%
PHOTO-RESPONSE NON-UNIFORMITY	at 400 nm	1.6	3.0 max.	%
	at 650 nm	1.7	3.0 max.	%
	at 900 nm	1.0	5.0 max.	%

Note (1): minimum separation of adjacent black columns to be 50 pixels

CUSTOM TESTS (if applicable)

OPERATING CONDITIONS

VOLTAGE	VALUE	MIN.	MAX.	UNITS
VRD	18	15	19	V
VSS	7.9	8	11	V
VOD	29	27	32	V
VIφ (high)	12	10	15	V

TEMPERATURE	VALUE	UNITS
For dark signal measurement	0	°C
For Photo-response measurements	-20	°C

NOTES

Results before fitment of fibre optic.

SV Camera CCD

e2v technologies

Waterhouse Lane, Chelmsford, Essex CM1 2QU United Kingdom
Telephone: +44 (0) 1245 493493 Facsimile: +44 (0) 1245 492492
Internet: www.e2vtechnologies.com

TITLE: CCD67-00 SLOWSCAN TEST SHEET	10920F
Version: BACK ILLUMINATED (Basic Process), AIMO	Issue 1 (Draft) Sheet 1 of 1

Associated Document:

Device serial number	02272-10-33	Tester (Initials & Clock No.)	Emma
Grade	1	Date	20/3/05
Test data disc number	Disc I	Device Type Number	CCD67-00-*- C97

TEST RESULTS

TEST		RESULT	LIMITS Grade 0	Grade 1	Grade 2	UNITS
GAIN (Amplifier Responsivity)	OSL	1.61	1.0 min., 2.0 max.			μV/e⁻
	OSR	1.57	1.0 min., 2.0 max.			μV/e⁻
NOISE	OSL	4.9	6.0 max.			rms e⁻
	OSR	4.8	6.0 max.			rms e⁻
DEFECTS IN DARKNESS	BRIGHT COLUMNS	0	0	0	1 max.	n/a
	POINT DEFECTS	0	10 max.	20 max.	30 max.	n/a
PHOTO-RESPONSE DEFECTS	TOTAL COLUMNS	0	0	2 max.	8 max.	n/a
	DARK POINT DEFECTS	0	10 max.	20 max.	40 max.	n/a
	TRAPS	1	1 max.	2 max.	5 max.	n/a
MEAN DARK SIGNAL		498	1700 max. at +20°C			e⁻/pix/s
AREA DARK SIGNAL (20 x 20 block)		780	3400 max. at +20°C			e⁻/pix/s
DNSU (1σ)		104	500 max. at +20°C			e⁻/pix/s

TEST		RESULT	LIMITS for Device Variant -C97 (Mid band)	UNITS
QUANTUM EFFICIENCY	at 350 nm	15.8	10 min.	%
	at 400 nm	43.7	40 min.	%
	at 500 nm	85.5	85 min.	%
	at 650 nm	92.6	85 min.	%
	at 900 nm	40.1	30 min.	%
PHOTO-RESPONSE NON-UNIFORMITY	at 400 nm	1.5	3.0 max.	%
	at 650 nm	1.7	3.0 max.	%
	at 900 nm	1.3	5.0 max.	%

Note (1): minimum separation of adjacent black columns to be 50 pixels

CUSTOM TESTS (if applicable)

OPERATING CONDITIONS

VOLTAGE	VALUE	MIN.	MAX.	UNITS
VRD	18	15	19	V
VSS	7.9	8	11	V
VOD	29	27	32	V
VIφ (high)	12	10	15	V

TEMPERATURE	VALUE	UNITS
For dark signal measurement	0	°C
For Photo-response measurements	-20	°C

NOTES

Results before fitment of Fibre Optic

6. FAI Data Processing Outline

A. Level 0 data are stored by eSOC as one file per raw image containing a header, a trailer, and 16-bit image data. Quicklook products will be generated utilizing Level 0 data.

B. Level 1 processing tasks

Step 1: Remove the electronic offset by subtracting the average signal in the last six offset columns (i.e. CCD cols. 273 to 279 in the image).
Step 2: Remove the dark current for each pixel using the measured CCD temperature and the library of coefficients
Step 3: Remove the hot columns using the hot column coefficients for each pixel
Step 4: Remove the dark current that was generated during the image readout
Step 5: Apply the correction for non-uniform response using the library of coefficients
Step 6: Apply the correction for image distortion
Step 7: Insert satellite position/attitude information into header
Step 8: Rename and save the corrected image as Level 1 data.
It is planned to generate Summary Plots for distribution utilizing Level 1 data.

C. Level 2 processing tasks

Step 1: Insert ancillary useful information such as the locations of the centres and/or corners of the image in geographic and geomagnetic coordinates, solar depression angle, MLT, etc. There is room for these in the image header.
Step 2: Rename and save the images as Level 2 data.
Most scientific studies will utilize Level 2 data.

D. Level 3 processing tasks

No routine tasks are anticipated for Level 3. Applying the absolute calibration is fraught with pitfalls and cannot be achieved on a routine basis. We shall have to remove the non-auroral background, perhaps correct for viewing angle, albedo etc. Considerable time and effort will be required to produce a selected few fully-corrected images on a case-by-case basis.